THE ROLE OF TRIM58 IN ERYTHROPOIESIS

Christopher S Thom

A DISSERTATION

in

Cell and Molecular Biology

Presented to the Faculties of the University of Pennsylvania

in

Partial Fulfillment of the Requirements for the

Degree of Doctor of Philosophy

2014

Supervisor of Dissertation

_____

Mitchell J Weiss, MD, PhD, Professor of Pediatrics

Graduate Group Chairperson

_____

Daniel S Kessler, PhD, Associate Professor of Cell and Developmental Biology

Dissertation Committee

Roger A Greenberg, MD, PhD, Associate Professor of Cancer Biology (Chair)

Mark L Kahn, MD, Professor of Medicine

Stephen A Liebhaber, MD, Professor of Genetics

Serge Y Fuchs, MD, PhD, Professor of Cell Biology

Michael Lampson, PhD, Associate Professor of Biology

Erika L Holzbaur, PhD, Professor of Physiology

THE ROLE OF TRIM58 IN ERYTHROPOIESIS

DEDICATION

I dedicate this thesis to

my daughter Madeline and wife Colleen;

my father Stephen, mother Linda, brother Matthew, and sister Megan;

my scientific mentors Charles Lovett, Charles Roberts, and Mitchell Weiss.

ACKNOWLEDGMENTS

I am extremely grateful for the guidance and mentorship that I have received from Mitch Weiss over the course of my thesis work. He has been a role model as a physician-scientist in conducting interesting and important work, as well as everything else that comes with being an Investigator. He has supported me through the ups and downs of this project, through several “life events” during the course of my graduate studies, and has helped me to grow as a scientist.

I am fortunate to have collaborated closely with unbelievably talented MD/PhD students during my time in the Weiss Lab. Eugene Khandros literally showed me where everything was in the lab and how to technically accomplish a variety of experiments. He is directly responsible for much of the success I have had during my graduate studies. On my first day in the lab, we pored over a list of proteins that Eugene identified in a screen. The number one hit was Trim58, which we thought might be interesting to study. For this and many other reasons, I am lucky to have followed in his footsteps. Elizabeth Traxler, another MD/PhD student, will continue work on Trim58 after my graduation. She has already made valuable contributions to our understanding of Trim58 biology, and I am sure she will do great things in the future. I appreciate all that she has taught me and I wish her all the success in the world.

Yu Yao and Jenna Nickas provided technical assistance throughout the course of my thesis work. Their work was instrumental to the success of my projects, and it was a pleasure to work with both of them.

Without my family and friends, I would not be in this position today. My father Stephen is physician-scientist who has provided fatherly advice, scientific mentorship, and even specific suggestions related to my thesis projects. I am incredibly lucky to have him in my life as a devoted father and scientific role model. I am also grateful for support from my mother Linda, brother Matt, and sister Megan throughout all these years of higher education. I also thank my family members-in-law Angela, James Sr., Kathleen, James Jr., Mariela, and Isabella, and too many friends to specifically name here, for putting up with me and supporting me through good times and bad.

Finally, and most importantly, to my daughter Madeline and wife Colleen: You make me the happiest person in the world. Your strength and determination inspire me to be a better person.

I am also grateful to the following people for scientific support and helpful discussions:

Weiss Lab
Vikram Paralkar
Orna Steinberg-Shemer
Olivia Y Zhou
Dolly Prabhu
Duonan Yu
Guowei Zhao
Jiyoon Noh
Maxim Pimkin
Janine D'Souza

Blobel Lab
Gerd Blobel
Stephan Kadauke
Amy Campbell
Rena Zheng

Holzbaur Lab
Jacob E Lazarus
Meredith H Wilson
Swathi Ayloo
Mariko Tokito

Kahn Lab
David Rawnsley
David Enis
Patricia Mericko-Ishizuka

Thesis Committee
Roger A Greenberg
Mark L Kahn
Stephen A Liebhaber
Serge Y Fuchs
Erika L Holzbaur
Michael A Lampson

Collaborators
Ana PG Silva and Joel P Mackay, University of Sydney
Kazuhiko Adachi, Children's Hospital of Philadelphia

Medical Scientist Training Program Administration
Lawrence F Brass
Maggie Krall
Maureen Kirsch

Other individuals who supported the work presented in Chapter 3
Drs. Katherine S Ullman (University of Utah) and Laura Gutiérrez (Erasmus MC, Netherlands) provided helpful conversations, protocols and reagents.

Dr. Min Min Lu and the University of Pennsylvania Molecular Cardiology Research Center Histology and Gene Expression Core assisted with radioactive *in situ* hybridization experiments.

Dr. Andrea Stout and the University of Pennsylvania Cell and Developmental Biology Microscopy Core assisted with imaging.

ABSTRACT

THE ROLE OF TRIM58 IN ERYTHROPOIESIS

Christopher S Thom

Mitchell J Weiss, MD, PhD

Red blood cells (erythrocytes) deliver oxygen to all tissues of the body. Defects in red blood cell production (erythropoiesis) can cause disease. Mammalian erythropoiesis culminates in enucleation, an incompletely understood process that entails the physical separation of the nucleus and cytoplasm. The work in this thesis investigated the role of a previously uncharacterized protein named Trim58 in erythropoiesis.

Human genetic studies suggested that *TRIM58* played an important role in erythroid development. In humans and mice, *Trim58* expression was found to be restricted to red blood cell precursors during late stage maturation. In fact, murine Trim58 was upregulated just prior to enucleation. Using short hairpin RNAs, *Trim58* expression was inhibited in cultured murine erythroblasts. Through a variety of analyses, it was demonstrated that Trim58 is dispensable for early erythroid maturation. However, *Trim58* knockdown impaired movement of the nucleus, thereby inhibiting enucleation.

Trim58 is a member of the tripartite motif-containing family of proteins, many of which function as E3 ubiquitin ligases that can facilitate protein degradation. Protein interaction studies demonstrated that Trim58 bound directly to the molecular motor protein complex dynein. Consistent with its putative role as an E3 ubiquitin ligase, ectopic Trim58 expression in HeLa cells caused dynein degradation in a proteasome-

dependent fashion. Furthermore, dynein loss and efficient enucleation were coincident and dependent upon Trim58 induction during erythroid culture maturation.

Dynein mediates unidirectional nuclear movement toward the microtubule organizing center. Erythroid enucleation requires nuclear movement in the opposite direction. Hence, Trim58-mediated dynein degradation may be responsible for nuclear movement during enucleation. Our findings identify Trim58 as the first erythroid-specific protein that regulates this process. More broadly, regulated proteolysis represents a previously unappreciated mode of regulation for dynein, which is critical for many cellular processes.

TABLE OF CONTENTS

LIST OF TABLES

LIST OF FIGURES

Figure Page

CHAPTER 1: INTRODUCTION

Red blood cell development is a complex process, with some aspects that are rare or unique within the realm of cell biology. For example, late in their development, mammalian erythroblasts expel their nucleus. The genes and processes that facilitate enucleation are not well understood, and I investigated this interesting process during the course of my graduate work. Genetic tools led us to identify *Trim58* as a relatively erythroid-specific gene that we functionally linked with enucleation.

This introduction aims to concisely describe prior work that informed our studies. A basic appreciation of several biological processes is necessary to understand our hypotheses and our investigation. These topics include red blood cell development, and in particular enucleation; how microtubule molecular motors, like dynein, facilitate nuclear movement; and how proteins are degraded via the ubiquitin-proteasome system. Red blood cell development, molecular motor activities, and protein degradation are all complex and intensively studied areas of biology. For general overviews of these subjects, the reader is referred to excellent review articles that are referenced in the appropriate sections.

Chapter Two includes a description of the Materials and Methods used in our investigation, while Chapter Three details our findings with regard to the role of Trim58 in erythropoiesis. Chapter Four summarizes our findings and proposes experiments for to continue our investigation of Trim58 biology.

An overview of the importance of erythropoiesis

The importance of red blood cell function

Mature red blood cells (erythrocytes) contain an incredibly high concentration (~340 mg/ml, ~5.2 mM) of the heterotetrameric protein hemoglobin (Hb). Hb is directly responsible for binding oxygen (O_2), so abundant Hb enables erythrocytes to perform their main function; efficiently delivering O_2 to tissues throughout the body. Vertebrate cells rely on large quantities of O_2 to generate energy in the form of adenosine triphosphate (ATP), thus permitting optimal aerobic tissue function.

But why do we need erythrocytes to carry and deliver O_2? The solubility of O_2 in water is only ~0.3 mM at 20 ˚C and 1 atmosphere pressure. Without erythrocytes, the quantity of O_2 dissolved in plasma would never be high enough to fully oxygenate tissues. Consequently, almost all vertebrates (with the exception of certain arctic fishes (Ruud, 1954)) have evolved heme-based O_2 transport systems to raise the concentration of O_2 in blood. Heme is a heterocyclic porphyrin molecule that directly coordinates iron, which in turn provides a docking site for an O_2 molecule. Left in isolation, however, an oxygenated heme moiety is prone to chemical oxidation that produces harmful reactive O_2 species. Globin proteins protect the heme iron moiety from chemical perturbations. Globins also augment O_2 delivery by making the heme-O_2 interaction reversible through allosteric regulatory mechanisms. We have recently reviewed the biochemical structure and function of normal and variant Hb molecules (Thom et al., 2013). Interestingly, free Hb normally degrades nitric oxide in the bloodstream to regulate vascular contractility (Straub et al., 2012). During hemolysis, however, too much free Hb can alter blood pressure control. Thus, erythrocytes sequester Hb to prevent this from happening.

Hb is composed of two α- and two β-like subunits (i.e., $\alpha_2\beta_2$), each coordinated to a heme. Each heme binds one O_2 molecule, so each Hb tetramer can bind up to four. The high concentration of Hb in blood (~5.2 mM Hb tetramer, thus ~21 mM heme), and the fact that red cells account for ~45% of total blood volume (~5 million erythrocytes per mL (Dzierzak and Philipsen, 2013)), gives a theoretical blood O_2 concentration of ~9 mM. This is roughly equivalent to the levels of O_2 in the air we breathe.

The importance of red blood cell shape and size

Erythroid development is incredibly specialized to meet the unique demands and functions of erythrocytes. In order to physically deliver O_2 to tissues, erythrocytes must be durable and distensible enough to withstand shear stress in the bloodstream and repeated passages through tiny capillaries, which can be about half the size of a mature erythrocyte (Keerthivasan et al., 2011). Evolutionary adaptations have augmented the ability of red cells to make such repeated journeys through the microvasculature by enhancing their durability and reducing their size (Boylan et al., 1991; Gaehtgens et al., 1981a; Gaehtgens et al., 1981b; Hawkey et al., 1991).

The durability of red cells is dependent on a complex array of specialized cytoskeletal membrane proteins that includes a Spectrin-based lattice structure as well as Actin, Adducin, and other proteins (Da Costa et al., 2013; Nans et al., 2011). Mutations in erythrocyte membrane proteins alter their mechanical stability, leading to hemolysis and anemia. Common examples of such disorders include hereditary spherocytosis and hereditary elliptocytosis, named for the abnormal shapes of the patient's erythrocytes (Da Costa et al., 2013). These have been linked with mutations in several important erythrocyte cytoskeletal components (Da Costa et al., 2013).

Many species' erythrocytes also have a circumferential "marginal band" of bundled microtubules that helps to maintain their shape and stability (Monaco et al., 1982; Trinczek et al., 1993), particularly under osmotic stress (Joseph-Silverstein and Cohen, 1984). Interestingly, adult mammalian erythrocytes do not have marginal bands (van Deurs and Behnke, 1973), although camels provide an exception to this statement (Long, 2007). Marginal bands in Camelidae erythrocytes have been hypothesized to be beneficial since ellipsoid erythrocytes are able to move through thick blood encountered in these species during dehydration[i] (Long, 2007).

Decreased erythrocyte size can also enhance tissue O_2 delivery, since small erythrocytes are better able to navigate our microvasculature. Small erythrocytes also have an increased surface area-to-volume ratio, which increases the theoretical O_2 exchange capacity of the blood. Perhaps for these reasons, there seems to have been evolutionary selection for organisms to have large numbers of tiny erythrocytes (Hawkey et al., 1991). In a survey of 441 species, mammals and birds had roughly equivalent amounts of hemoglobin and packed red cell volumes in their blood (Hawkey et al., 1991). The mean corpuscular hemoglobin concentration for mammals was 34.7±2.8 g/dL versus 33.5±2.5 g/dL for birds. However, there were stark differences in the sizes and numbers of erythrocytes. The average size of a mammalian erythrocyte was about one third the size of an average bird erythrocyte (62.1±22.2 fL compared to 168.9±28.5 fL for birds), and mammalian erythrocyte counts were three times that of birds

[i] There is a common misconception that camel erythrocytes are nucleated. They are indeed anucleate, but *different* from other mammalian erythrocytes in that some of their erythrocytes (~3%) retain a marginal band and, perhaps as a result, are ellipsoid in shape (Cohen, W.D., and Terwilliger, N.B. (1979). Marginal bands in camel erythrocytes. J Cell Sci *36*, 97-107.)

(7.77±2.86 x10^{12} cells/L versus 2.79±0.53 x10^{12} cells/L for birds). An inverse relationship between red cell size and volume was also evident within animal classes, presumably to keep total Hb content consistent (Boylan et al., 1991; Hawkey et al., 1991). Altered cell morphology (i.e., cell shrinkage) and enucleation are two ways that mammalian erythrocytes can become so small (see Section entitled Erythroid maturation).

The importance of studying red blood cell development

The genes and biochemical processes that govern erythropoiesis are of considerable medical interest. Defective red blood cell formation or function can cause anemia, a condition that affects an estimated one-quarter of the world's population with huge ramifications on health and economic interests (Balarajan et al., 2011). The causes of anemia are multifactorial, including socioeconomic factors leading to dietary iron deficiency (Balarajan et al., 2011). This limits erythropoiesis since large amounts of iron are required to support normal erythrocyte production.

Several heritable anemias have also been described, such as the congenital dyserythropoietic anemias (CDA). CDA disorders are characterized by varying degrees of anemia and morphological identification of multinucleated erythroblasts in the bone marrow (Iolascon et al., 2012; Iolascon et al., 2011). Nucleated and/or multinucleated erythroblasts can also be observed in circulation. CDA pathology is linked with iron overload, as iron intake is increased due to inappropriate suppression of hepcidin, a hormone that normally suppresses iron absorption (Tamary et al., 2008). Currently, treatment for these disorders consists of blood transfusions, iron chelation, hematopoietic stem cell transplant or, in the case of CDA type I, interferon therapy (Renella and Wood, 2009). Novel therapeutics would greatly reduce the toxicity

associated with these therapeutic modalities. Causative genes have been linked with all classical variants of this disease, including Codanin I for CDA type I (Dgany et al., 2002), SEC23B for CDA type II (Schwarz et al., 2009), MKLP1/KIF23 for CDA type III (Liljeholm et al., 2013b), and GATA1 (Nichols et al., 2000) and KLF1 (Arnaud et al., 2010) for "variant type" CDA. The mechanistic basis for these diseases remains unclear, although KIF23 regulates mitosis through its activity within the centralspindlin complex (White and Glotzer, 2012). This suggests that defective cell division could play some role in CDA III pathogenesis (Traxler and Weiss, 2013).

Ultimately, the pathogenesis of anemia involves decreased erythrocyte production relative to destruction. A better understanding of normal and diseased erythrocyte development might improve treatment or facilitate discovery of novel therapeutics for these conditions.

Mammalian erythrocytes are anucleate. Investigations specifically aimed to better understand the process by which mammalian erythroblasts eliminate their nuclei have important technical and medical applications. There is a chronic shortage of transfusable packed red blood cells in many parts of the world (Anstee et al., 2012; Migliaccio et al., 2012). The generation of erythrocytes *in vitro* holds promise for vastly increasing the supply of transfusable blood, but these efforts are hindered by inefficient enucleation in culture (Lapillonne et al.; Peyrard et al., 2011). Novel insights into erythroid enucleation will be necessary to overcome this obstacle. Recent technological advances in cultured primary murine erythroblasts have allowed groups to study enucleation under experimentally controlled conditions (Koury et al., 1988; Yoshida et al., 2005; Zhang et al., 2003). This has enabled the identification of numerous genes and processes that

contribute to enucleation (see Subsection entitled Enucleation), including the work presented in this thesis.

An overview of erythropoiesis

Ontogeny of erythropoiesis

The morphology and globin gene expression profile of a given erythrocyte depends on the timing and location of its development. There are, in fact, two types of erythropoiesis that share many aspects of development but can be delineated based on morphology (essentially, differences in erythrocyte size) and by the type of Hb they contain.

"Primitive" erythropoiesis occurs *in utero* and yields macrocytic, nucleated (or sometimes anucleate (Fraser et al., 2007)) red cells that express embryonic globin genes and contain Hbs Gower 1 ($\zeta_2\varepsilon_2$), Gower 2 ($\alpha_2\varepsilon_2$), Portland 1 ($\zeta_2\gamma_2$), and Portland 2 ($\zeta_2\beta_2$). "Definitive" erythropoiesis begins at mid-gestation and continues post-natally, yielding small, anucleate erythrocytes. Definitive erythrocytes initially contain high levels of fetal Hb ($\alpha_2\gamma_2$, HbF) in late gestation through birth. HbF levels gradually decline to ~1% after the first six months of life in favor of HbA ($\alpha_2\beta_2$, 97%) and a small amount of HbA_2 ($\alpha_2\delta_2$, 2%). The purposes for globin gene "switching" from HbF to HbA likely include, but are not limited to, *in utero* exchange of O_2 with maternal blood (Bard et al., 1998). HbF has higher O_2 affinity than HbA. This thesis investigated definitive erythroid maturation.

The anatomical site of erythropoiesis changes throughout development in a sequential fashion from the yolk sac to the fetal liver, and ultimately the bone marrow (reviewed in (McGrath and Palis, 2008)). Under normal circumstances, the bone marrow is the site of all erythropoiesis *ex utero*, although the liver and spleen can serve as extramedullary erythropoietic organs in stress situations. Definitive erythropoiesis begins in the fetal liver around mid-gestation. In a mouse, this occurs ~12 days post-conception (McGrath and Palis, 2008).

In adult bone marrow, erythroblasts mature in “erythroblast islands” surrounding a central macrophage (Billat, 1974; Sjogren and Brandt, 1974). Specialized interactions between developing erythroblasts and macrophages facilitate erythroblast proliferation, differentiation, and enucleation (Hanspal and Hanspal, 1994; Hanspal et al., 1998; Lee et al., 2003; Mankelow et al., 2004; Sadahira et al., 1995; Soni et al., 2006; Yoshida et al., 2005). Macrophages phagocytose expelled nuclei and use DNase II activity to degrade them (Kawane, 2001; Socolovsky, 2013; Soni et al., 2006). For some time, it was thought that erythroblast-macrophage interactions, or at least interactions with stromal factors like fibronectin, were necessary to promote enucleation (Patel and Lodish, 1987). However, the achievement of enucleation of macrophage- and stroma-free systems has revised this view (Yoshida et al., 2005; Zhang et al., 2003). I used cultured definitive erythroblasts from murine fetal livers to model erythropoiesis in stroma-free conditions during the course of this thesis.

Erythroid maturation

All definitive erythroid cells are derived from hematopoietic stem cells (HSCs) (Dzierzak and Philipsen, 2013). HSCs proliferate and differentiate to give rise to all the

blood lineages (see for example (Orkin and Zon, 2002)), including the erythroid lineage (Koury et al., 2002). The process of lineage commitment remains controversial and multiple models exist, but the process by which committed erythroid progenitor cells mature into erythrocytes has been confirmed in remarkable detail (summarized in (Dzierzak and Philipsen, 2013; McGrath and Palis, 2008)).

Once differentiated and committed to the erythroid lineage, so called "burst-forming unit" (BFU-Es) precursors begin to express erythropoietin receptor (EpoR) and reach maximal EpoR expression by the time they become "colony-forming units" (CFU-Es) (Sawada et al., 1990), which are dependent on erythropoietin signaling for survival (Wu et al., 1995). The name "burst forming unit" derives from the large colonies, containing several thousand hemoglobinized cells, that "burst" from these immature, motile precursor cells when cultured on methylcellulose (Dzierzak and Philipsen, 2013). CFU-Es, which are slightly more mature, yield smaller colonies of 16-125 cells.

These committed erythroblast precursors then undergo the dramatic alterations in gene expression and morphology described below as they develop further into mature, O_2-carrying erythrocytes.

Altered gene expression

The "master" erythroid transcriptional regulators GATA1 and SCL/TAL1 direct erythroid maturation through transcriptional induction of erythroid lineage-specific genes and repression of alternate lineage genes (Cheng et al., 2009; Kingsley et al., 2013; Welch et al., 2004). The erythroid lineage-specific set of genes are largely established early in development (Kingsley et al., 2013), and maintained through subsequent cell divisions in part through GATA1-mediated mitotic bookmarking (Kadauke et al., 2012).

Global DNA demethylation occurs at the onset of erythroid maturation and may provide a “blank slate” upon which to direct transcription of erythroid-specific genes (Shearstone et al., 2011). The erythroid transcriptional program includes globin genes. General paradigms for long-range cis-regulatory chromatin interactions, including “chromatin looping,” have been established through the study of the well-characterized β globin locus and enhancer regions (Deng et al., 2012).

Publicly available microarray gene expression databases from human (Merryweather-Clarke et al., 2011) and murine erythroblasts (Kingsley et al., 2013) that were FACS-purified at different developmental stages based on cell surface markers, provide valuable resources to characterize transcriptional patterns for genes of interest in multiple species.

Altered cell cycles and cell morphology

Dramatic changes in appearance enable stratification of erythroid precursors into discrete stages of development. From the CFU-E stage, cells undergo 4-5 cell divisions that sequentially yield morphologically distinct basophilic erythroblasts, polychromatic erythroblasts, orthochromatic erythroblasts, and ultimately anucleate reticulocytes (Dzierzak and Philipsen, 2013; Keerthivasan et al., 2011). Basophilia correlates with the presence of abundant cytoplasmic ribosomes, which stain purple by Giemsa stain. These ribosomes are used to translate large amounts of globin (and other proteins), which yields the pink or gray cytoplasmic coloration seen by May Grunwald-Giemsa staining in later stage polychromatic and orthochromatic erythroblasts. These morphologic changes can be viewed as preparation for enucleation and ultimately erythrocyte functionality.

Each cell division during erythroid maturation yields two cells with decreased size as a result of specialized cell cycles (Keerthivasan et al., 2011; Koury et al., 1988). Shortened G1 phases allow maturing erythroblasts to physically shrink with each division, since they do not have opportunity to double in size prior to dividing (Dolznig et al., 1995; Grebien et al., 2005). Cyclin D3, one of three D-type cyclins that regulate G1-S progression (Malumbres and Barbacid, 2009; Sherr and Roberts, 2004), regulates these specialized cell divisions (Sankaran et al., 2012). Cultured erythroblasts treated with Cyclin D3-directed shRNAs demonstrated reduced numbers of divisions during development. Without the opportunity to divide and shrink, mature erythrocytes were macrocytic and reduced in number. Indeed, Cyclin D3 knockout mice have macrocytic erythrocytes, and humans that inherit genetic polymorphisms that diminish activity at the Cyclin D3 promoter demonstrate altered erythrocyte size and number (Ganesh et al., 2009; Soranzo et al., 2009).

Recently, erythroblast cell cycle progression was linked with transcription factor activities and lineage-specific gene expression, forming a “synchromesh” to coordinate erythroid maturation events with the cell cycle clock (Pop et al., 2010). The need for such a mechanism highlights the dramatic transcriptional and morphologic changes that must occur simultaneously within rapid cell divisions during erythroid maturation.

Following these specialized cell divisions, orthochromatic erythroblasts undergo Retinoblastoma (Rb)-, E2F-, and cyclin dependent kinase inhibitor (CDK inhibitor)-dependent cell cycle exit (Dirlam et al., 2007; Pop et al., 2010; Sankaran et al., 2008; Zhu and Skoultchi, 2001). Thus, further maturation events, including enucleation, occur in post-mitotic orthochromatic erythroblasts.

Nuclear condensation

During late erythroid maturation, large, active nuclei are transformed into condensed, transcriptionally attenuated “viscoelastic balls” (Dr. Harvey Lodish, Whitehead Institute, personal communication). Defective chromatin condensation inhibits enucleation (Ji et al., 2010; Popova et al., 2009), suggesting that an orthochromatic erythroblast is only able to efficiently expel a small, condensed nucleus. Chromatin condensation and nuclear shrinkage are facilitated by large-scale epigenetic changes, including histone deacetylase 2 (HDAC2)-mediated histone deacetylation (Ji et al., 2010; Popova et al., 2009). Downregulation of c-Myc is also necessary for this process. Enforced Myc expression prevented histone deacetylation and condensation during erythropoiesis (Jayapal et al., 2010), and the c-Myc antagonist Mxi1 (MAX-interacting protein 1) is induced during erythroid development (Zhang et al., 2011). Mxi1 is a target for miR-191; silencing of this microRNA during late erythropoiesis upregulates Mxi1 (as well as an atypical protein kinase RIO kinase 3 (Riok3)) to facilitate nuclear condensation (Zhang et al., 2011).

Some of the proteins that enact chromatin condensation are present in virtually all cell types, whereas others are erythroid-specific. The latter include Mature Erythrocyte Nuclear Termination (MENT) stage specific protein, which regulates chromatin condensation and nuclear collapse in chicken erythroblasts (Grigoryev et al., 1992), as well as Mxi1 and Riok3, which are enriched in late stage mammalian erythroblasts (Wu et al., 2009; Zhang et al., 2011). There likely remain unidentified erythroid-specific factors that facilitate erythroblast nuclear condensation as well.

Enucleation

Following the maturation processes described above, mammalian orthochromatic erythroblasts undergo separation of the condensed nucleus and cytoplasm in a process called enucleation[ii]. The expelled nucleus, ensheathed in a thin rim of cytoplasm, is called a pyrenocyte (McGrath et al., 2008). Pyrenocytes are rapidly degraded within macrophages in the bone marrow following their formation (Soni et al., 2006). Meanwhile, the cytoplasm from the orthochromatic erythroblast becomes the nascent reticulocyte, which is released from the bone marrow and ultimately becomes a mature erythrocyte.

Erythroid enucleation theoretically provides several evolutionary benefits. Enucleation is thought to enhance erythrocyte transit through small capillaries since anucleate erythrocytes are smaller (Gaehtgens et al., 1981a; Gaehtgens et al., 1981b). As previously described, having many small erythrocytes also increases the overall surface area available for O_2 transfer (Gaehtgens et al., 1981a; Gaehtgens et al., 1981b; Hawkey et al., 1991). An additional benefit may be that anucleate erythrocytes cannot undergo malignant transformation (Ney, 2011).

For some time, the process by which erythroblasts enucleate has been controversial. Apoptosis-like processes facilitate enucleation in epithelial cells from the ocular lens and skin keratinocytes (Ishizaki et al., 1998; Nagata, 2002). These

[ii] Although typically thought of as a mammalian-specific phenomenon, sparse examples of non-mammalian species with anucleate erythrocytes exist as well. For instance, five clades within the Plethodontae family of salamanders have anucleate erythrocytes. This seems to correlate with small body forms and large genome size (Mueller, R.L., Gregory, T.R., Gregory, S.M., Hsieh, A., and Boore, J.L. (2008). Genome size, cell size, and the evolution of enucleated erythrocytes in attenuate salamanders. Zoology (Jena) *111*, 218-230.). These observations suggest that while we have good theoretical reasons for why mammalian erythroblasts enucleate, we may not yet comprehend the whole purpose for this phenomenon.

observations led to the hypothesis that similar mechanisms could regulate erythroblasts enucleation. However, caspase-mediated apoptosis does not regulate enucleation (Carlile et al., 2004; Krauss et al., 2005; Yoshida et al., 2005), although non-apoptotic caspase-3 activities are required for other aspects of terminal erythropoiesis (Boehm et al., 2013; De Maria et al., 1999; Ribeil et al., 2007; Sztiller-Sikorska et al., 2009; Zeuner et al., 2003). Instead, the currently prevailing model for erythroblast enucleation involves a specialized asymmetric cell division. This is supported through the observations detailed below.

The physical events that occur during enucleation were described through electron microscopic studies dating back to the 1960s (Eitan et al., 1976; Repasky and Eckert, 1981; Simpson and Kling, 1967; Skutelsky and Danon, 1970). Evident physical processes from published images included nuclear condensation, polarized movement of the condensed nucleus toward the side of the cell, extrusion of the nucleus from the spherical boundaries of the cytoplasm, cleavage furrow-like cell membrane contraction at the boundary between the polarized nucleus and cytoplasm, and vesicle deposition at this boundary that seems to coincide with separation of the two (Figure 1.1A).

These enucleation events largely parallel those that occur during normal mitotic cell division from anaphase through cytokinesis (Figure 1.1B) (Barr and Gruneberg, 2007; Eggert et al., 2006; Fededa and Gerlich, 2012). Successful cell division requires sequential microtubule-dependent chromosome movement during anaphase, followed by GTPase-dependent contractile actomyosin ring (CAR) formation, cleavage furrow ingression, and lipid-containing vesicle deposition within the midbody during telophase to facilitate daughter cell separation. The observation that pyrenocytes contain a thin rim of cytoplasm is consistent with this cytokinesis-like model for enucleation (Keerthivasan et

al., 2011). However, one notable difference is that mitotic cells undergo nuclear envelope breakdown and reformation, whereas condensed erythroid nuclei remain intact throughout the process. The studies described below used *in vitro* erythroblast culture and *in vivo* mouse models to demonstrate that mitosis-related proteins and processes contribute to enucleation.

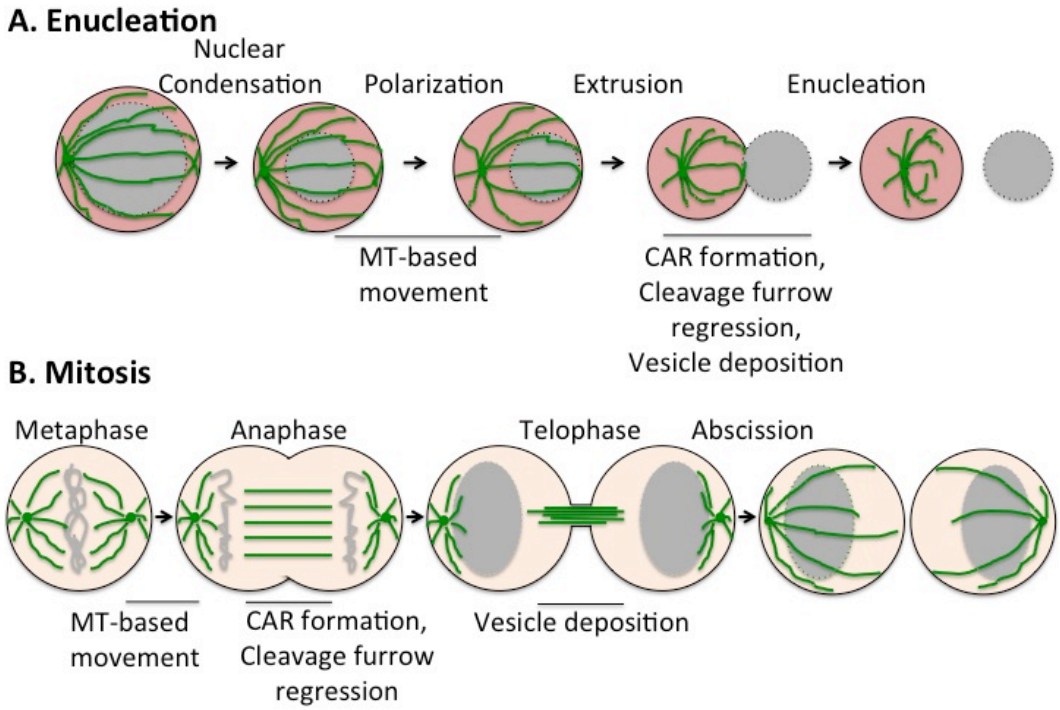

Figure 1.1. Many events during enucleation parallel those that occur during mitosis. (A) During erythroblast enucleation, nuclei (gray) are sequentially condensed, polarized, and extruded in preparation for enucleation from the hemoglobinized cytoplasm (red). Nuclear polarization is dependent on microtubule (MT)-based movement (Konstantinidis et al., 2012b; Wang et al., 2012). Microtubules, shown in green, emanate from the MTOC (green dot). Nuclear extrusion depends on formation of a contractile actomyosin ring (CAR) and actomyosin-based cleave furrow ingression (Ji et al., 2008; Konstantinidis et al., 2012b). Vesicle deposition at the boundary between nucleus and cytoplasm facilitates separation (Keerthivasan et al., 2010). (B) During mitosis, microtubules (green) facilitate condensed chromosome (gray) alignment at metaphase and chromosome separation at anaphase (reviewed in (Fededa and Gerlich, 2012)). CAR formation and actomyosin-based cleavage furrow ingression generate a midbody, containing bundled bipolar microtubules, at telophase. Nuclear envelopes, which are disassembled during prophase, are reformed at this stage. Vesicle deposition at the midbody facilitates abscission between daughter cells. Note that cell sizes are not drawn to scale.

One of the first obvious commitments of an erythroblast to enucleation is the polarized movement of a condensed nucleus toward the side of the cell. At this stage of enucleation, the cell remains spherical. Erythroblasts treated with colchicine or nocodazole to depolymerize microtubules show reduced polarization (Konstantinidis et al., 2012b; Wang et al., 2012). Sustained microtubule polymerization with taxol resulted in thickened microtubule bundles around the nucleus, although polarization was not measured (Konstantinidis et al., 2012b; Koury et al., 1989). Enucleation was inhibited in response to microtubule polymerization or depolymerization. Together, these findings implicate dynamic microtubule-based activities in nuclear polarization and enucleation (see Section entitled Microtubules, molecular motor proteins, and nuclear movement).

Microtubule-based activities function at least in part by regulating PI3K signaling in enucleating erythroblasts. PI3K normally regulates cell polarization in migrating cells, and direct chemical PI3K suppression using the compound LY294002 inhibited polarization (Wang et al., 2012). Nocodazole treatment also inhibited PI3K signaling (and nuclear polarization), as evidenced by the improper localization of downstream PI3K targets (Wang et al., 2012).

The next phase of enucleation involves nuclear extrusion from the spherical confines of the cytoplasm. Nuclear extrusion results from CAR-mediated cleavage furrow-like ingression at the pyrenocyte-reticulocyte boundary (Ji et al., 2008; Koury et al., 1989; Repasky and Eckert, 1981; Skutelsky and Danon, 1970). Similar to mitosis, the CAR is set up through the actions of Rac GTPases (Ji et al., 2008; Konstantinidis et al., 2010; Konstantinidis et al., 2012b) and the GTPase effector protein mDia2 (Diaphanous-related formin), which nucleates unbranched actin filaments (Ji et al.,

2008). Actin can be visualized at the point of ingression (Ji et al., 2008; Koury et al., 1989; Wickrema et al., 1994; Xue et al., 1997). Time-lapse microscopy indicates that CAR-mediated contraction is responsible for extrusion of the polarized nucleus (Ji et al., 2008; Wang et al., 2012). Inhibition of actomyosin contraction with the small molecule blebbistatin inhibits nuclear extrusion (Wang et al., 2012).

During extrusion, the distance between the nucleus and centrosome/microtubule organizing center (MTOC) increases (Wang et al., 2012). This suggests that the nucleus is not tethered to the MTOC, but instead might be “pushed” away from the MTOC at this stage of enucleation (see Section entitled Microtubules, molecular motor proteins, and nuclear movement).

Abscission, or separation, of the pyrenocyte and reticulocyte is then achieved through the trafficking and deposition of lipid raft-containing vesicles. During normal cell division, such vesicles are thought to provide additional membrane at the site of daughter cell separation (Fededa and Gerlich, 2012). Clathrin facilitates normal cell division in multiple ways, including vesicle generation via endocytosis (Smith and Chircop, 2012). Erythroblasts treated with clathrin-targeted siRNAs or small molecules that inhibit vesicle trafficking showed inhibited enucleation (Keerthivasan et al., 2010).

While multiple aspects of enucleation parallel cytokinesis, some studies have called into question how closely these processes are associated. CAR-based activities have been one point of contention. In one study, treatment of late stage, post-mitotic erythroblasts with the myosin inhibitor blebbistatin did not inhibit enucleation, as one might expect if constriction between cytoplasm and pyrenocyte were actomyosin-based (Keerthivasan et al., 2010). However, this is in direct conflict with more recent studies showing inhibited enucleation following blebbistatin treatment (Wang et al., 2012). The

reason for this discrepancy may be that cells were treated at different maturation stages in these studies.

Additionally, the roles of GTPases remain unclear. Rac and Rho GTPases regulate cytokinesis, cell cycle progression, and actin cytoskeletal functions (Schwartz, 2004). The downstream RhoA target ROCK phosphorylates myosin regulatory light chain (MRLC) to stimulate actomyosin contractility. MRLC exhibits a striking localization at the “back end” of polarized erythroblasts during enucleation (Wang et al., 2012). Although data presented in abstract form suggest that RhoA activity may be required for some aspect(s) of this process (Konstantinidis et al., 2012a), several previous studies did not identify a role for RhoA or its downstream targets in enucleation (Bement et al., 2005; D'Avino et al., 2005; Glotzer, 2005; Wadsworth, 2005).

Other normal mitotic processes seem to be absent during erythroblast enucleation, or at least have not yet been elucidated. Although the chromosomal passenger complex (CPC) protein Survivin is important for enucleation, it did not coimmunoprecipitate with other CPC proteins, like Aurora B, in enucleating erythroblasts (Keerthivasan et al., 2012). Instead, it co-localized with epidermal growth factor receptor substrate 15 and clathrin, presumably to mediate endocytic vesicle trafficking. This suggests that some normal mitotic processes and some erythroid-specific alterations to normal mitotic machinery are required for enucleation. Finally, there has not yet been a report detailing a midbody-like structure in enucleating erythroblasts, which would be expected if enucleation proceeds through a telophase-like state prior to enucleation. Electron micrographs do, however, hint at the presence of such a structure (Skutelsky and Danon, 1970).

Overall, recent studies of erythroid enucleation have elucidated roles for several molecules that facilitate mitosis and/or cytokinesis in most cell types. Parallels with normal cell division are certainly warranted, and the inconsistencies noted above may indicate specialized erythroid adaptations of cytokinetic machinery. Specialized mitoses late in erythroid development may underlie the pathology seen in some erythroid-specific diseases, such as CDA. Our laboratory and others have used genetic tools to identify erythroid-specific factors that regulate enucleation (see Section entitled Genetic tools can identify novel regulators of erythropoiesis & enucleation).

Reticulocyte maturation

Following enucleation, reticulocytes leave the bone marrow and enter the peripheral circulation, where they undergo substantial remodeling in order to achieve a characteristic biconcave shape (Coulombel et al., 1979; Mel et al., 1977). Reticulocyte maturation involves autophagic degradation of all remaining ribosomes, mitochondria, and other membrane-bound organelles, as well as exocytosis of substantial amounts of lipid and membrane (reviewed in (Ney, 2011)). These morphologic changes are important for erythrocyte functionality. Several canonical autophagy components are induced during erythropoiesis (Kang et al., 2012), and autophagic machinery is retained in reticulocytes to facilitate remodeling. Erythroid-specific autophagy factors also participate reticulocyte maturation, including the BCL2-related protein Nix that regulates mitochondria autophagy (“mitophagy”) (Schweers et al., 2007).

Microtubules, molecular motor proteins, and nuclear movement

Microtubules are cylindrical filaments composed of polymerized heterodimeric α- and β-tubulin subunits that form a cytoskeletal network within cells (Mandelkow and Mandelkow, 1989). Microtubules are polarized structures that extend from a "minus end" toward a dynamically growing or shrinking "plus end". In interphase cells, the minus ends of microtubules typically reside at the perinuclear centrosome, or microtubule-organizing center (MTOC), while plus ends often extend peripherally to the cell membrane.

The polarized structure of microtubules facilitates directional intracellular transport. Dynein and kinesin family motors are generally thought to facilitate unidirectional minus end- or plus end-directed movements, respectively. These molecular motors facilitate many biological processes through transport of vesicles (Hendricks et al., 2010), autophagosomes (Maday et al., 2012), mitochondria (Tanaka et al., 1998), and other membrane-bound compartments and organelles (Hirokawa, 1998; Moughamian et al., 2013).

Microtubule-based activities have been specifically implicated in nuclear polarization (Konstantinidis et al., 2012b; Wang et al., 2012) and perhaps nuclear extrusion (see Subsection entitled Enucleation) (Wang et al., 2012). These findings indirectly implicate microtubule motor proteins in enucleation, although prior to our work the roles of dynein or kinesins had never been investigated in enucleating erythroblasts. However, dynein and kinesins regulate nuclear movement in many cell types (Fridolfsson and Starr, 2010; Splinter et al., 2010; Tsai et al., 2007; Tsai et al., 2005; Tsai et al., 2010; Wilson and Holzbaur, 2012).

In fact, nuclear movement and asymmetric positioning are seen in many organisms and tissues (Gundersen and Worman, 2013). One commonly studied

example is the neuroepithelial cell nucleus, which undergoes “interkinetic nuclear migration” (i.e., altered nuclear positioning) as a function of the cell cycle (Spear and Erickson, 2012a, b). Nuclei in these cells are typically found in a polarized position toward the basal side of the cell at interphase, but undergo mitosis at the apical side near the centrosome/MTOC. Dynein recruitment to the nuclear pores directs apical transport and promotes cell cycle progression (Hu et al., 2013). Although the true purpose for this phenomenon is unclear, it may augment progenitor cell packing in the limited space available at the luminal (apical) border, since most nuclei are displaced basally (Spear and Erickson, 2012a, b).

Dynein

Dynein is the predominant minus end-directed microtubule motor protein eukaryotes (Holzbaur and Vallee, 1994). In interphase cells, dynein carries cargo toward the MTOC that normally resides near the center of the cell. Dynein cargoes include several cytoplasmic organelles, including endosomes, lysosomes, phagosomes, and Golgi bodies (Hirokawa, 1998; Hirokawa et al., 1998). It is responsible for many critical processes, including vesicle transport, cell migration, and multiple aspects of mitosis, including nuclear envelope breakdown, mitotic spindle assembly and orientation, and chromosome dynamics (Collins et al., 2012; Howell et al., 2001; Tanenbaum et al., 2010; Vallee et al., 2012). Given these varied and important functions, it is not surprising that dynein perturbations cause disease. Dynein mutations commonly manifest as defective neuronal development (Harms et al., 2012; Ori-McKenney and Vallee, 2011; Poirier et al., 2013).

Dynein was initially discovered in *Tetrahymena pyriformis* as a protein with ATPase activity that was required for ciliary motility (Gibbons and Rowe, 1965). This was a relatively easily purified “axonemal” dynein. A cytoplasmic version of dynein, discovered later, demonstrated similar activity as it facilitated retrograde microtubule-based organelle transport in neurons (Paschal and Vallee, 1987). This thesis studied cytoplasmic dynein-1, heretofore referred to only as dynein, although other family members for this protein include axonemal (ciliary or flagellar) motors and cytoplasmic dynein-2, which helps assemble the axoneme and participates in intraflagellar transport (Allan, 2011).

Structurally, dynein is a 1.2 MD complex composed of paired heavy chains (DHC), intermediate chains (DIC), light intermediate chains (DLIC), and several light chains. Whereas DHC genes are evolutionarily conserved from algae to man (Kikkawa, 2013), the number and identities of the associated subunits vary considerably in different organisms (Holzbaur and Vallee, 1994).

DHC is an AAA+ (ATPase Associated with diverse cellular Activities) molecular motor that converts energy from ATP hydrolysis into microtubule-based processive locomotor activity. Structural studies were initially complicated by the large size (>500 kD), but DHC crystal structures from several organisms have now been solved (Carter et al., 2011; Kon et al., 2012; Kon et al., 2011; Schmidt et al., 2012). The DHC protein consists of stalk, loop, linker and tail domains (Figure 1.2) (Cho and Vale, 2012). The stalk is a ~15 nm coiled coil domain with a microtubule binding domain at its tip (Gee et al., 1997) and protrudes from a six-membered loop structure comprised of tandem AAA (ATPase) domains (Burgess et al., 2004; Samso et al., 1998). The linker domain dynamically associates with the loop (Roberts et al., 2012; Roberts et al., 2009) and

functions as a force-producing motile element similar to a mechanical “lever arm” (Burgess et al., 2003; Kon et al., 2005; Shima et al., 2006; Vale and Milligan, 2000). The stalk, loop, and linker domains participate in the ATP hydrolysis-dependent “powerstroke” that facilitates motility (Carter, 2013). The amino-terminal tail is the most evolutionarily divergent domain (Holzbaur and Vallee, 1994). It facilitates DHC dimerization and also interacts with dynein intermediate and light intermediate chains, which bind other subunits and link DHC to cargo (Carter, 2013).

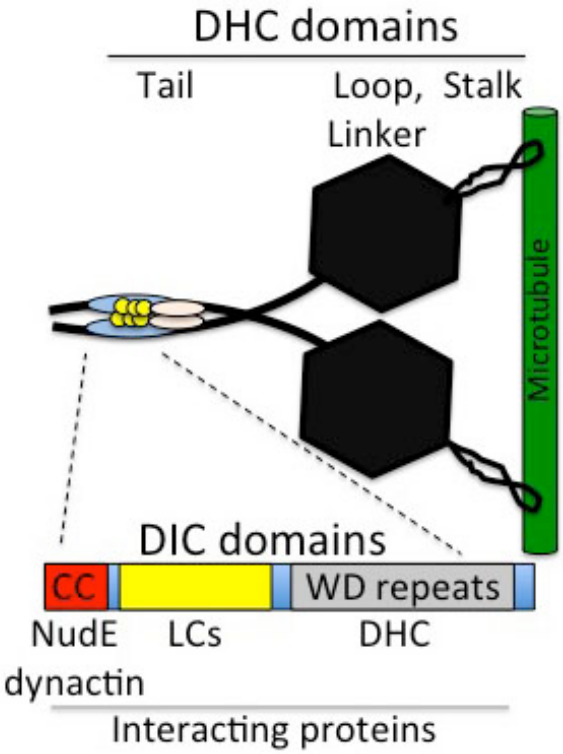

Figure 1.2. Dynein structure and protein interactions. Dynein heavy chain (DHC, black) contains stalk, loop, and linker domains that regulate ATP-dependent processive motility along microtubules (green) (reviewed in (Carter, 2013)). The DHC amino-terminal tail domain interacts with dynein intermediate (DIC, blue) and light intermediate chain (pink) subunits. DIC carboxy-terminal WD repeats (gray) bind DHC (Ma et al., 1999). The DIC amino terminus contains a coiled coil (CC) domain (red) that interacts with NudE and dynactin (McKenney et al., 2011; Zimmet and Ravid, 2000), as well a region depicted in yellow that interacts with several dynein light chains (LCs) (Carter, 2013). Note that protein sizes are not drawn to scale.

DIC, through several carboxy terminal tryptophan-aspartic acid (WD) repeats motifs, interacts with the DHC amino terminal tail domain (Figure 1.2) (Ma et al., 1999). At the same time, DIC interacts with dynein light chain subunits and other regulatory factors through its amino terminus (Ma et al., 1999; Vallee et al., 2012). Free DIC is a disordered polypeptide, but rapidly adopts its structure and assembles into a dimer following dynein light chain binding (Asthana et al., 2012; Makokha et al., 2002; Mok et al., 2001; Nyarko and Barbar, 2011; Nyarko et al., 2004). DIC recruits a number of factors that regulate holodynein activities in important ways, including dynactin, NudE (nuclear distribution protein E), NudEL (NudE-like), and Lis1 (lissencephaly 1 protein) (Vallee et al., 2012). Interestingly, NudE and dynactin were recently shown to competitively bind to the same location on DIC, perhaps ensuring that dynein can only be regulated by one factor at a time (McKenney et al., 2011).

Dynein light intermediate (LIC) and light chains (LC) functions are, in many cases, not well understood. Recent studies have shown that LIC1 and LIC2 regulate mitosis through localization at the mitotic spindle and midbody, or spindle poles, respectively (Horgan et al., 2011). These may recruit dynein to these sites during mitosis, but the separate localizations for these LIC subunits suggest that they may have distinct functions. In *D. melanogaster*, LIC regulates several dynein functions, including holodynein-mediated spindle checkpoint inactivation (Mische et al., 2008). LC subunits also regulate mitotic spindle assembly and progression (Asthana et al., 2012; Stuchell-Brereton et al., 2011). Some LC functions, such as Tctex-1-mediated RhoGEF inhibition, are dependent on interactions with the holodynein complex (Meiri et al., 2012). Other LC functions are holodynein-independent. For example, ectopic expression of the Tctex-1 subunit causes defective neurite extension in a dynein-independent fashion (Chuang

et al., 2005). Further studies are necessary to clarify the binding partners and functions of LIC and LC subunits.

Several important regulatory accessory proteins influence dynein functions. The multi-subunit complex dynactin stimulates dynein processivity along microtubules (McGrail et al., 1995), acts as an adapter protein between dynein and cargo (Hammesfahr and Kollmar, 2012), and inhibits microtubule catastrophe through actions at the plus ends of neuronal microtubules (Lazarus et al., 2013). Dynactin regulates dynein functions during mitosis (Quintyne et al., 1999) and organelle transport (Moughamian et al., 2013). Given these important functions, it is not surprising that dynactin mutations cause disease, including disrupted motor neuron development (Puls et al., 2003) and neurodegeneration (Moughamian and Holzbaur, 2012).

Dynactin contains a coiled coil domain that directly interacts with the DIC amino terminal coiled coil motif (Figure 1.2) (Ma et al., 1999). DIC phosphorylation inhibits this interaction (Vaughan and Vallee, 1995). Ectopic expression of this domain, called CC1, is thought to competitively inhibit normal DIC-dynactin interactions and thereby perturb normal dynein functions (Quintyne et al., 1999).

NudE/NudEL and Lis1 also regulate dynein functions. These proteins regulate dynein-dependent nuclear positioning (Hu et al., 2013; Shu et al., 2004; Tsai et al., 2007), cell migration (Dujardin et al., 2003; Shen et al., 2008), chromosome alignment and mitotic spindle assembly (Faulkner et al., 2000; Liang et al., 2007; Siller and Doe, 2009; Siller et al., 2005; Stehman et al., 2007; Vergnolle and Taylor, 2007). Mutations in these genes cause neurological diseases including congenital Lissencephaly (Alkuraya et al., 2011; Reiner et al., 1993). NudE binds the DIC amino terminus (Figure 1.2)

(McKenney et al., 2011) and Lis1 binds to the DHC motor domain loop during the pre-powerstroke stage (Sasaki et al., 2000).

As mentioned in the preceding paragraphs, several studies have directly implicated dynein in nuclear movement. In fact, defects in nuclear movement and mitotic spindle positioning were the first phenotypes associated with dynein deficiency in *S. cerevisiae* (Eshel et al., 1993; Li et al., 1993). Time lapse imaging of *C. elegans* suggested that dynein minus end-directed nuclear movement was necessary to bypass intracellular “roadblocks” on microtubules (Fridolfsson and Starr, 2010). The same is true in primary myoblasts, which form syncytia through nuclear migration (Wilson and Holzbaur, 2012). Dynein also facilitates nuclear movement toward the MTOC in U2OS cells. Treatment with DHC-targeted siRNA or injection of anti-DIC antibody caused increased distance between the nucleus and MTOC at G2/prophase, when dynein is recruited to the nuclear envelope (Splinter et al., 2010). In fact, dynein interactions at the nuclear envelope during G2 are required for cell cycle progression in neurons (Hu et al., 2013).

Regulatory proteins are important for dynein-mediated nuclear migration. NudE, Lis1, and dynein colocalize at the nuclear envelope (Bolhy et al., 2011; Hebbar et al., 2008) and control neuronal nuclear movement via a microtubule cage-like structure that pulls nuclei toward the centrosome (Shu et al., 2004; Tsai et al., 2007; Xie et al., 2003). Concurrent binding of NudE and Lis1 induce dynein into a persistent force-producing state, which is important for moving large cargo like the nucleus (McKenney et al., 2010). Dynactin, Ranbp2 (Ran binding protein 2)-Bicd2 (Bicaudal D2), Nup133 (Nucleoporin 133)-CENPF (Centromere protein F), SUN/KASH (Sad1p, UNC-84/Klarsicht, ANC-1, Syne Homology) domain-containing proteins, and Nesprins

(Nuclear envelope spectrin repeat proteins) are also involved in dynein recruitment to the nuclear envelope (reviewed in (Vallee et al., 2012)).

Dynein also regulates important cellular functions through localization at the cell cortex. NudE/Lis1, dynactin, and other regulators like NuMA (Nuclear mitotic apparatus protein) colocalize with dynein at the cell cortex (Kotak et al., 2013; Moore and Cooper, 2010; Shen et al., 2008). Its cortical positioning regulates cell migration, cell polarity, morphogenesis, and mitosis (Kirschner and Mitchison, 1986; Kotak et al., 2013; Moore and Cooper, 2010; Shen et al., 2008). Cortical dynein also stabilizes microtubule plus ends and prevents microtubule depolymerization (i.e., “catastrophe”) (Hendricks et al., 2012).

Kinesins

Kinesin proteins are microtubule plus end-directed motors that carry cargo in the opposite direction to dynein; typically toward the cell periphery in interphase cells (Verhey et al., 2011). Standardized nomenclature delineates 14 families of kinesin molecules, with varied forms and functions (Lawrence et al., 2004). Abnormalities in kinesin-mediated transport have been linked to neurodegenerative diseases, polycystic kidney disease, and cancer (Gerdes et al., 2009; Salinas et al., 2008; Yu and Feng, 2010).

Structurally, all kinesins have head, neck, and tail domains. The amino-terminal motor head domain binds microtubules and facilitates processivity (Verhey et al., 2011). The neck domain includes linker and coil regions that mediate processivity and kinesin oligomerization. The tail domain binds kinesin light chain (KLC) proteins, which mediate attachment to substrates or regulatory proteins but are not necessary for kinesin motor

activity. In fact, the tail domain can interact with some kinesin motor domains to facilitate autoinhibition in the absence of cargo. In contrast to the multi-subunit holodynein complex, kinesins transport cargo as single proteins or homomultimers without adapter proteins, although kinesin light chains can provide adapter function in some circumstances (Verhey et al., 2011).

Kinesin-1 proteins, otherwise known as the canonical kinesin heavy chains (KHC), are perhaps the most well understood kinesin family members. In mammals, the *KIF5A*, *KIF5B*, and *KIF5C* genes encode KHC proteins. Whereas KIF5A and KIF5C are restricted to neuronal cells, KIF5B expression is relatively ubiquitous (Xia et al., 1998). A KIF5B knockout mouse is embryonic lethal, but work with KIF5B$^{-/-}$ murine embryonic fibroblasts showed that KIF5B was necessary for mitochondria distribution toward the cell periphery (Tanaka et al., 1998).

Plus end-directed nuclear movements were mediated by KHC in several of the studies (Fridolfsson and Starr, 2010; Splinter et al., 2010; Wilson and Holzbaur, 2012). In fact, dynein and kinesin-1 physically interact to co-regulate motor activity and mediate bidirectional transport (Ligon et al., 2004). However, kinesin-3 (KIF1A), which has similar processivity properties as kinesin-1 (Hammond et al., 2009), has also been shown to facilitate nuclear movement in neuronal progenitor cells (Tsai et al., 2010). It is possible that other kinesins can promote nuclear transport as well.

Other kinesin proteins have varied mechanisms that extend beyond simple cargo transport. For instance, Kif23/Mklp-1 (Mitotic kinesin-like protein 1) regulates Rho GTPase activation, mitotic spindle compaction, and formation of bipolar microtubule arrays during telophase as part of the centralspindlin complex (White and Glotzer, 2012). Mutations in Kif23 cause CDA type III and result in multinucleated erythroid precursors,

presumably through failed cytokinesis during erythroid maturation (Liljeholm et al., 2013a; Traxler and Weiss, 2013). Kif20a/MKLP-2 also regulates cell division through its localization at mitotic spindles, which facilitates recruitment of the chromosomal passenger complex (Hummer and Mayer, 2009). Kif20a also regulates vesicular trafficking through Golgi bodies through association with Rab6 (Duden, 2001; Echard et al., 1998). Kif2a, another kinesin family protein, depolymerizes microtubules. Kif2a knockout mice show aberrant axonal branching from over-extended microtubules, which results in neurological dysfunction (Homma et al., 2003). Kif2a also regulates the length of the central spindle during mitosis by depolymerizing the distal ends of microtubules (Uehara et al., 2013).

An overview of the ubiquitin-proteasome system

The ubiquitin-proteasome system (UPS) utilizes a cascade of E1 ubiquitin-activating, E2 ubiquitin-conjugating, and E3 ubiquitin-ligating enzymes to covalently link the small (76 amino acids, ~8.5 kD) polypeptide ubiquitin to substrates (Figure 1.3) (Deshaies and Joazeiro, 2009; Dikic and Robertson, 2012). Polyubiquitin chains are then created by covalent linkage of ubiquitin monomers through one of seven lysine residues (Komander, 2009). Substrate ubiquitylation can alter intracellular signaling, protein interactions, or allosteric regulation, or lead to degradation by the lysosome or 26S proteasome (Deshaies and Joazeiro, 2009; Komander, 2009). Initially regarded as a housekeeping mechanism to destroy and recycle amino acids from damaged proteins, the UPS has now been centrally implicated in cell cycle regulation, intracellular transport, cell signaling, transcription, translation, and DNA repair (Dikic and Robertson, 2012; Komander, 2009; Messick and Greenberg, 2009; Pickart, 2004).

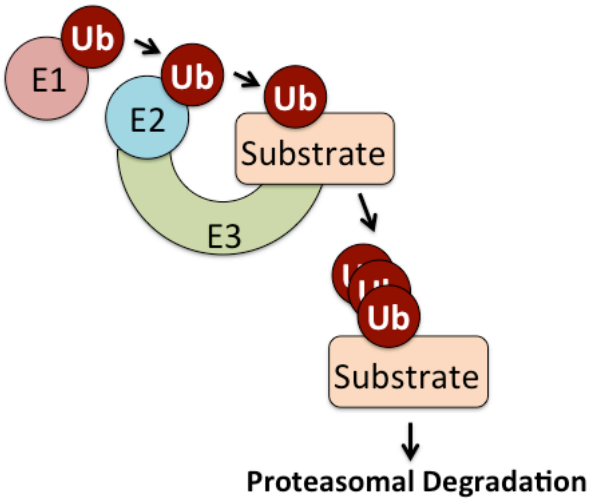

Figure 1.3. Schematic depiction of ubiquitin proteasome system activity. The ubiquitin-proteasome system covalently attaches the small polypeptide ubiquitin (Ub) to substrates through sequential actions of E1, E2, and E3 enzymes. E1 activating enzymes catalyze ATP-dependent chemical activation of ubiquitin, which is subsequently transferred to E2 conjugases via transthioesterification. RING-containing E3 ligases simultaneously recruit E2 conjugases, carrying activated Ub, and substrates through direct interactions. Ubiquitylation frequently targets substrates for proteasomal degradation.

E3 ubiquitin ligases confer UPS target specificity by virtue of direct interactions with substrates. Whereas there are ~7 E1 ubiquitin activating enzymes and ~40 E2 ubiquitin conjugases, more than 600 human E3 ubiquitin ligases exist (Deshaies and Joazeiro, 2009; Metzger et al., 2012). By comparison, there are only 518 known protein kinase genes, lending some idea of the prevalence of protein ubiquitylation as a post-translational mechanism in cell biology.

E3 ligases can function through one of two biochemical mechanisms, depending on whether they contain a HECT (Homologous to E6-AP Carboxyl Terminus) or a RING (Really Interesting New Gene) domain. HECT-containing E3 ligases carry activated ubiquitin and mediate attachment directly to substrates. In contrast, RING-containing E3 ligases simultaneously recruit E2 conjugases (carrying activated ubiquitin) and substrates, facilitating ubiquitin transfer by proximity (Figure 1.3).

The vast majority of E3 ligases contain RING or RING-like (i.e. Plant homeodomain, PHD; Leukemia associated protein, LAP; or U-box) domains (Deshaies and Joazeiro, 2009; Metzger et al., 2012). Indeed, the mammalian genome encodes more than 600 putative RING E3 ligases (Li et al., 2008). The identities of both the E2 and substrate are important when considering the function(s) of a RING E3 ligase, since the recruited E2 conjugase directs both the type of polyubiquitin linkage (Deshaies and Joazeiro, 2009; Metzger et al., 2012) and can alternatively carry activated ubiquitin-like SUMO, Nedd, or ISG moieties (Dikic and Robertson, 2012; Metzger et al., 2012; Napolitano and Meroni, 2012).

Tripartite motif-containing proteins are putative RING E3 ubiquitin ligases

The Trim (Tripartite motif-containing) proteins comprise the largest family of RING-containing putative E3 ligases (Marco Sardiello, 2008; Meroni and Diez-Roux, 2005; Napolitano et al., 2011; Napolitano and Meroni, 2012), with more than 65 members identified in human cells (Meroni and Diez-Roux, 2005; Versteeg et al., 2013). Trim proteins function broadly in physiology and disease states (Napolitano and Meroni, 2012). Their prominent roles in developmental biology (Petrera and Meroni, 2012), oncogenesis (Hatakeyama, 2011), transcriptional regulation (Cammas et al., 2012), innate immunity (Ozato et al., 2008; Rhodes et al., 2005), and viral infection responses (Nisole et al., 2005) have been the subjects of recent review articles.

By definition, Trim proteins contain a tripartite motif composed of a RING domain, one or two B-box domains, and a coiled-coil (CC) region (Figure 1.4). The presence of all three domains within the tripartite motif is generally thought to allow proper function,

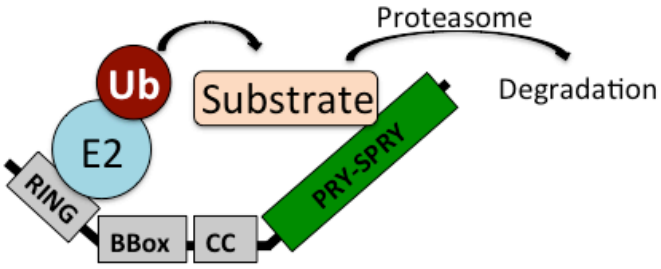

Figure 1.4. Structure and function for common Trim protein domains. Trim proteins contain a tripartite RING-BBox-Coiled Coil (CC) motif (gray) linked with a carboxy-terminal substrate-binding domain which, in more than half of mammalian Trim proteins, is an immunoglobulin-like PRY-SPRY domain (green). Concomitant RING-dependent E2 conjugase/activated ubiquitin (Ub) recruitment and PRY-SPRY-mediated substrate binding can target substrates for proteasomal degradation.

although this has not been tested on all Trim proteins and splice variants are known to exist (Napolitano and Meroni, 2012). The RING and BBox domains coordinate zinc ions through conserved cysteine and/or histidine residues. Whereas RING domains function to recruit E2 conjugases, the biological roles of the BBox domain(s) are significantly less well understood. The BBox may augment the E3 ligase activity of the RING domain (i.e., as an “E4” enzyme) (Kuhlbrodt et al., 2005; Massiah et al., 2006) or recruit substrates. For example, the Trim18/MID1 BBox domain binds and ubiquitylates the protein phosphatase 2A (PP2A) α4 subunit to promote its degradation (Liu et al., 2001; Short et al., 2002; Trockenbacher et al., 2001).

Trim protein CC domains facilitate homo- or hetero-oligomerization of Trim proteins, which is generally considered necessary for proper function (Meroni and Diez-Roux, 2005; Napolitano and Meroni, 2012). Deletion of the CC abrogates activity for Trim5α (Javanbakht et al., 2006) and alters binding properties for several Trim proteins

(Reymond, 2001). CC-mediated multimerization significantly increases the activity of several Trim proteins *in vitro* (Streich et al., 2013).

The tripartite motif is typically linked with a carboxyl-terminal domain that recruits substrates or determines subcellular localization (Meroni and Diez-Roux, 2005; Napolitano and Meroni, 2012). Although the identity of the carboxy-terminal domain varies among Trim proteins, more than half of mammalian Trim proteins contain an immunoglobulin-like PRY-SPRY (Sp1a and Ryanodine Receptor) domain that typically facilitates protein interaction(s) (Rhodes et al., 2005). This domain has historically been referred to as a B30.2 domain or an Rfp-like (Ret finger protein-like) domain (Meroni and Diez-Roux, 2005; Napolitano and Meroni, 2012). Some PRY-SPRY domains recruit substrates for ubiquitylation and proteasomal degradation (see for example (Zhang et al., 2012a; Zhang et al., 2012b; Zhao et al., 2012)). While other carboxy-terminal domain types are functionally important for certain Trim proteins, this thesis will focus on the PRY-SPRY since Trim58 contains one such domain.

The PRY-SPRY domain is evolutionarily restricted to vertebrates with an adaptive immune system (Rhodes et al., 2005). It is found in ~700 proteins, including ~150 mammalian proteins across 11 different protein families (Rhodes et al., 2005; Woo et al., 2006a). For example, in addition to Trim proteins, the PRY-SPRY domain is also found in butyrophilin family proteins, which are immunoglobulin-like cell surface receptor glycoproteins (Rhodes et al., 2005).

The PRY and SPRY subdomains are co-dependent for stability and function (D'Cruz et al., 2013). Crystallization studies show that PRY-SPRY domains contain eight variable loops, designated A-F, which form a substrate binding pocket with a single two-layered β-sandwich fold at its core (see for example (D'Cruz et al., 2013; Rhodes and

Trowsdale, 2007; Woo et al., 2006a; Woo et al., 2006b)). The composition of these variable loops determines substrate identity. Structural studies demonstrated that the loops mediate interaction with short (<20 amino acids) sequence motifs, suggesting that each PRY-SPRY domain can bind multiple target substrates (Woo et al., 2006a; Woo et al., 2006b).

Human pathophysiology is associated with PRY-SPRY dysfunction. For example, point mutations in the PRY-SPRY domains of TRIM20/Pyrin cause Familial Mediterranean Fever (Bakkaloglu, 2003). This autoimmune disorder is marked by recurrent episodes of joint and organ inflammation, most seriously affecting the kidneys and leading to renal failure (Shohat and Halpern, 2011). Pyrin protein normally inhibits inflammasome activation (Xu et al., 2013a). Defective Pyrin function causes disease via aberrant inflammatory pathway activation in immune cells.

The role of the ubiquitin proteasome system in erythropoiesis

The UPS serves integral functions during erythroid maturation, including the ubiquitylation and degradation of important erythroid proteins. In fact, the UPS was initially characterized in Nobel prize-winning work using rabbit reticulocyte lysate (Ciechanover et al., 1978; Etlinger and Goldberg, 1977; Hershko et al., 1983). During erythroid maturation, cells degrade much of their proteome and synthesize large amounts of Hb. Robust UPS activity is necessary both to degrade normal but unnecessary proteins, as well as misfolded or aggregated Hb subunits (Khandros et al., 2012; Khandros and Weiss, 2010). Other UPS targets in erythroid cells include activated erythropoietin receptor (Walrafen et al., 2005) and cytoskeletal proteins such as actin and tubulin (Liu et al., 2010). Many E2 and E3 enzymes are induced during

erythropoiesis ((Lausen et al., 2010; Wefes et al., 1995) and our unpublished observations). In fact, pathway analysis of the human erythrocyte proteome identifies a large number of UPS-related molecules (~35% of all protein ubiquitylation pathway molecules as defined by Ingenuity Systems (Roux-Dalvai et al., 2008)).

Given the important roles of the UPS in cell biology and the abundance of UPS-related proteins in erythropoiesis, it is likely that much can be learned about erythroid biology by studying UPS activity in this lineage. For example, general UPS inhibition with the proteasome inhibitor MG132 reduces enucleation efficiency in cultured erythroblasts (Chen et al., 2002). However, few E3 ligases have been shown to regulate erythroid development. Mdm2 and Mdm4 inhibit p53 (Maetens et al., 2007), Cul4A targets the cell cycle inhibitor p27 (Li et al., 2006), and Fbw7-mediated cyclin E degradation (Xu et al., 2013b) all help to control cell cycle progression during terminal erythroid maturation. These E3 ligases are expressed in many tissues. To our knowledge, the work presented in this thesis is the first illustration of a putative erythroid-specific E3 ligase that regulates terminal erythropoiesis through UPS activity.

Genetic tools can identify novel regulators of erythropoiesis & enucleation

The Weiss lab has previously used genetic tools to identify novel regulators of erythropoiesis, such as alpha hemoglobin stabilizing protein (AHSP) (Kihm et al., 2002) and microRNA 144/451 (Yu et al., 2010). Microarray analyses indicated that these genes were transcriptionally induced during erythroid development through the actions of important transcription factors, including Gata1 and SCL/Tal1 (Cheng et al., 2009; Welch et al., 2004). Through gene expression analysis of fluorescence-activated cell sorting (FACS)-purified primary murine erythroblasts, we identified *Trim58* as a gene that is also

transcriptionally induced during late erythroid maturation. Gata1 and SCL/Tal1 activities are likely to facilitate *Trim58* induction (see Chapter 3).

Genome wide association studies (GWAS) aim to link single nucleotide polymorphisms (SNPs) with important human health traits. Recent GWAS have associated many understudied genes with altered erythrocyte size and/or count (Kamatani et al., 2010; Nuinoon et al., 2009; Soranzo et al., 2009; van der Harst et al., 2012). Each of these genes potentially regulates important aspects of normal human red cell development. Putative and validated E3 ubiquitin ligases, including *TRIM58,* were among the genes identified. SNPs linked with *TRIM58* were statistically significantly associated with altered red blood cell size and/or count in two GWAS (Kamatani et al., 2010; van der Harst et al., 2012). In addition to our identification of *Trim58* as an erythroid-regulated gene, these findings compelled us to investigate the functions of the previously uncharacterized Trim58 protein.

CHAPTER 2: MATERIALS AND METHODS

A. Trim58 cloning

The full length Trim58 gene, including 5' and 3' untranslated regions (UTR), was initially TOPO cloned into pCRII-Dual vector (Invitrogen) from murine fetal liver erythroblast cDNA using the following primers (Forward: GCCATGGCCACGGCACCCGGGG, Reverse: CAGCACTTCTGGATGGGTTT). Full length (wild type) Trim58 was subcloned from pCRII-Dual-Trim58 into retroviral vectors using the following primers to create 5' FLAG/HA epitope-tagged constructs (Forward: GAAGATCTAGATCTGCCATGGACTACAAGGACGACGATGACAAATACCCATACGAC GTCCCAGACTACGCTGCCTCAGCTCCTTCTGTG, Reverse: CGGAATTCCAGCACTTCTGGATGGGT). The RING-dead Trim58 construct, containing Cys>Ala missense mutations at residues 55 and 58 (within the RING domain), was created from a full length Trim58 construct using a two-step PCR method using the above full length Trim58 Forward and Reverse primers and the following mutation-generating primers (Forward: GGACCCCTGGCCTGGGGTGCGGCGTAGAC, Reverse: GTCTACGCCGCACCCCAGGCCAGGGGTCC). The Trim58 PRY-SPRY domain, including residues 281-485, was subcloned from a full length Trim58 construct using the following primers (Forward: AGAAGATCTAGATCTGCCATGAGGGAGATG, Reverse: CGGAATTCCAGCACTTCTGGATGGGT). This construct begins 8 amino acids upstream and extends 25 amino acids downstream of the predicted PRY-SPRY domain. Live cell imaging plasmids were cloned into the BglII/EcoRI site of a pK1 vector

containing amino-terminal FLAG and carboxy-terminal mCherry tags (S. Kadauke & G. Blobel, Children's Hospital of Philadelphia) using the following primers (Forward: GAAGATCTAGATCTATGGCCACGGCACCCG, Reverse: CCGGAATTCGAATTCGTATTCCTCACTTCTGGCAG).

Trim58 constructs were cloned into the BamHI/EcoRI or BglII/EcoRI sites in several expression vectors for this study, including pCRII-Dual (Invitrogen), retroviral MIGR1 (Murine Stem Cell Virus (MSCV) promoter-driven construct with downstream IRES-GFP), retroviral pK1 (MSCV-driven construct with downstream IRES-puromycin), and pGEX6P1 (GE Healthcare) for GST-tagged constructs.

B. Radioactive in situ hybridization

Embryonic day 14.5 (E14.5) murine embryos were fixed, dehydrated, paraffin-embedded, sectioned, and stained with an antisense probe targeting Trim58 nucleotides 841-1455 per protocols from the University of Pennsylvania Molecular Cardiology Research Center Histology and Gene Expression Core Facility (http://www.med.upenn.edu/mcrc/histology_core/).

C. Flow cytometry

For fluorescence activated cell sorting of primary murine fetal liver erythroblasts, single cell suspensions from whole fetal livers were stained with Ter119-APC (BioLegend) and CD71-PE (BD Pharmingen) for 45 min at 4 °C in PBS and sorted on a

FACSAria instrument (BD Biosciences) per a previously described gating strategy (Pop et al., 2010).

For cultured murine fetal liver erythroblast analysis, $5x10^5$ cells were stained sequentially with 5 μM Hoescht33342 (Sigma) for 1 hr at 37 °C in fetal liver maturation medium, Live/Dead near-IR fixable dead cell stain (Invitrogen) for 30 min at 4 °C in PBS, and Ter119-PerCP-Cy5.5 and CD44-AF647 (BioLegend) for 45 min at 4 °C in PBS with 2% fetal bovine serum (FBS). Cells were analyzed on an LSR Fortessa instrument (BD Biosciences) maintained by the Flow Cytometry Core Laboratory of The Children's Hospital of Philadelphia Research Institute. Data were analyzed using FlowJo software (TreeStar).

D. Semiquantitative real time PCR

RNA was extracted using the RNeasy kit (Qiagen) with on-column DNAse treatment. cDNA was prepared using the iScript cDNA kit (BioRad). Semiquantitative real-time PCR was done using the standard curve method and SYBR green dye on a ViiA 7 real-time PCR system (Life Technologies). Real time primers used in this study probed for murine Trim58 (*Trim58*; Forward: GAGCGTCTTTGGAACTTGTG, Reverse: ACCCTCTGTGTTTCTCAAACTC), dynein heavy chain (*Dync1h1*; Forward: TTGTACCGCATCCAAGAGAAG, Reverse: GTTGTAGTCATTCACCGTTTCC), dynein intermediate chain (*Dync1i2*, Forward: ACAGTCAAAGGCAGTAGCTG, Reverse: CTGGTGTCCCTCAAACATCTC), actin (*Actb*; Forward: CCTTCCTTCTTGGGTATGGAATC, Reverse: AGCACTGTGTTGGCATAGAGGT), hypoxanthine guanine phosphoribosyl transferase (*Hprt*; Forward:

TCAGTCAACGGGGGACATAAA, Reverse: GGGGCTGTACTGCTTAACCAG), and glyceraldehyde-3-phosphate dehydrogenase (*Gapdh*, Forward: AGGTTGTCTCCTGCGACTTCA, Reverse: CCAGGAAATGAGCTTGACAAA). Target gene expression was normalized to the average of *Actb, Gapdh,* and *Hprt* values.

E. *In silico* analyses of Trim58 gene regulation and expression

ChIP-Seq data at the murine *Trim58* locus were obtained from the Penn State University Bioinformatics Genome Browser (https://mery.genome-browser.bx.psu.edu/). The data presented in Figures 3.2C and 3.23 were generated from primary fetal liver erythroblasts by ChIP-Sequencing and RNA-Sequencing, respectively (Pimkin *et al,* in revision). Human *TRIM58* mRNA tissue expression patterns were obtained from publicly available microarray data (Figures 3.1A (Wu et al., 2009) and 3.1B (Novershtern et al., 2011)). Erythroid *TRIM58* expression data were obtained from microarray analysis of FACS-purified human erythroblasts cultured from peripheral blood buffy coat mononucleocytes (Figure 3.1C (Merryweather-Clarke et al., 2011)).

F. Murine fetal liver erythroblast isolation

E14.5 murine fetal livers were harvested from pregnant CD1 mice (Charles River Laboratories), triturated, and passed through a cell strainer (BD Biosciences) to yield stroma-free single cell suspensions. Erythroid progenitors were purified by negative selection on magnetic beads using the EasySep Mouse Hematopoietic Progenitor Cell

Enrichment Kit (STEMCELL Technologies) according to the manufacturer's instructions, with the addition of biotin-conjugated anti-mCD71 (eBioscience).

G. Short hairpin RNA cloning

Short hairpin RNAs from pGIPZ vectors (Open Biosystems) were subcloned into the "PIG" (MSCV-Puromycin-IRES-GFP) retroviral vector (Hemann et al., 2003). These shRNA constructs are within a miR30 stem-loop structure to aid processing. Primers (Forward: AGATCTAGATCTTGCTGTTGACAGTGAGCG, Reverse: CTCGAGCTCGAGTCCGAGGCAGTAGGC) were used to clone the following shRNAs into the MSCV-PIG vector BglII and XhoI sites. The sense strand is indicated in red, antisense in blue, loop in green, and the common miR-30 context in black.

shLuciferase (RHS1705)

TGCTGTTGACAGTGAGCGCCCGCCTGAAGTCTCTGATTAATAGTGAAGCCACAGAT
GTATTAATCAGAGACTTCAGGCGGTTGCCTACTGCCTCGGA

shScrambled (RHS4346)

TGCTGTTGACAGTGAGCGATCTCGCTTGGGCGAGAGTAAGTAGTGAAGCCACAGA
TGTACTTACTCTCGCCCAAGCGAGAGTGCCTACTGCCTCGGA

shTrim58 #3 (V3LMM_487333)

TGCTGTTGACAGTGAGCGACCGAGACTCAGTGCTGAGAAATAGTGAAGCCACAGAT

GTATTTCTCAGCACTGAGTCTCGGCTGCCTACTGCCTCGGA

shTrim58 #4 (V3LMM_487334)

TGCTGTTGACAGTGAGCGCCTCCTTCTACAATGTCACAAATAGTGAAGCCACAGAT

GTATTTGTGACATTGTAGAAGGAGATGCCTACTGCCTCGGA

shTrim58 #5 (V3LMM_487335)

TGCTGTTGACAGTGAGCGCTTGGACTACGAAGCTGGTGAATAGTGAAGCCACAGAT

GTATTCACCAGCTTCGTAGTCCAAATGCCTACTGCCTCGGA

shTrim58 #7 (V3LMM_487337)

TGCTGTTGACAGTGAGCGCCGGGATCTTTTTGGACTACGATAGTGAAGCCACAGAT

GTATCGTAGTCCAAAAAGATCCCGATGCCTACTGCCTCGGA

H. Retroviral infection

Retroviral PIG constructs were packaged by co-transfection of pCL-Eco into 293T

cells via calcium phosphate transfection. To create retrovirus for human (HeLa) cell infection, constructs were packaged by co-transfection of pVSVG and pCPG into 293T cells. Retroviral supernatants were collected 24 and 48 hr post-transfection and kept at -80 ^{o}C until use. Cells were infected with retroviral supernatant containing 8 μg/mL polybrene (Sigma) and 10 mM Hepes (Gibco) by centrifugation at 2800 rpm for 90 min at 30 °C.

I. Erythroblast culture conditions

Our methods were based on those initially devised by Zhang *et al* (Zhang et al., 2003) with some modifications. Erythroid progenitors were "expanded" for 24-72 hrs in StemPro-34 serum free media (Gibco) containing 10% SP34 supplement, 2 mM L-glutamine (Gibco), 1% Penicillin/Streptomycin (Gibco), 0.1 mM 1-thioglycerol (Sigma), 1 μM dexamethasone (Sigma), 0.5 Units/mL Erythropoietin (Amgen), and 1% mSCF-conditioned medium. At 18-24 hrs post-infection, puromycin (1 μg/mL) was added to select for infected cells. Following expansion, cells were pelleted at 800 rpm for 3 min, washed thrice in PBS, and cultured in fetal liver maturation medium (IMDM (Mediatech/Cellgro), 10% BenchMark fetal bovine serum (Gemini Bioproducts), 10% plasma derived serum (Animal Technologies), 5% Protein Free Hybridoma Media II (Gibco), 2 mM L-glutamine (Gibco), 1% Pen/Strep (Gibco), 0.1 mM 1-thioglycerol (Sigma), and 2 Units/mL Erythropoietin (Amgen)) for up to 48 hrs. After 48 hrs, maturation was complete, cultures began to die, and analyses became unreliable. Expansion and maturation cultures were kept below 1 million cells per mL at all times.

J. Erythroblast morphology analysis

Cells were centrifuged onto a glass slide and stained with May Grünwald-Giemsa (Sigma). Light microscopy images were obtained with a Zeiss Axioskope 2 microscope, Zeiss Axiocam camera, and Zeiss AxioVision 3.1 software (Carl Zeiss Microimaging) at room temperature. Multinuclearity was assessed by visual inspection of May Grünwald-Giemsa-stained slides. The “Analyze Particles” feature within FIJI (Schindelin et al., 2012) was used to quantify nuclear sizes from slide images.

K. Western blot analysis

Sample loading was normalized to protein content. Proteins were resolved on Tris-Glycine gels (BioRad), transferred to 0.45 μm PVDF (Whatman) or Nitrocellulose membrane (BioRad), and blocked in 5% milk. Primary antibodies included Dynein Heavy Chain (R-325, Santa Cruz), Dynein Intermediate Chain (MAB #1618, Millipore), Nup153 (QE5, Abcam), Gapdh (FL-335, Santa Cruz), α globin (custom rabbit polyclonal, Covance), Hemagglutinin (Y-11, Santa Cruz), FLAG (M2, Sigma), Codanin1 (G-1, Santa Cruz), and β actin-HRP (Sigma). Anti-Trim58 antibodies were raised against a peptide from the N-terminus (ERLQEEARCSVCLDFLQEPISVD) of murine Trim58 (Thermo Scientific). HRP-conjugated anti-mouse and anti-rabbit secondary antibodies, protein size markers, and other reagents were from Thermo Scientific.

L. Cell counting

Cultured erythroblasts were analyzed on a C6 Accuri Flow Cytometer (BD Biosciences) at medium flow rate to quantify the number of GFP+ cells.

M. Hemoglobin content quantification

Hemoglobin content in mature erythroblast cultures was quantified by Drabkin's assay as described (Campbell et al., 2013). Culture pellets were imaged in 1.1 mL FACS tubes (VWR) with an iPhone 4.

N. Immunoprecipitation assays

For all immunoprecipitation (IP) experiments, cells were lysed in buffer containing 10 mM Tris (pH 7.4), 150 mM sodium chloride, 0.5% NP-40 (Sigma), 1 mM EDTA (pH 8.0), 10 μM proteasome inhibitor (MG132, Enzo), and 1:500 protease inhibitor cocktail (Sigma). For FLAG- PS immunoprecipitation, 400 million FACS-purified GFP+ G1E cells, cultured as described (Weiss et al., 1997), were lysed, precleared with a 1:1 mix of Protein A and rProtein G agarose (Invitrogen), and incubated overnight with EZView Red Anti-Flag M2 Affinity Gel (Sigma) at 4 ^{o}C. After washing thrice with IP buffer, immunoprecipitated material was eluted off of beads with 100 μg/mL 3X FLAG peptide (Sigma) at 4 °C for 1 hr with intermittent agitation and used for further analyses.

For DIC immunoprecipitation, precleared lysate from 15 freshly isolated whole E14.5 murine fetal livers (~300 million cells) were incubated with anti-DIC antibody (Millipore MAB #1618) overnight. rProtein G agarose beads (Invitrogen) were then added for 4 hrs

at 4 °C. Beads containing immunoprecipitated material were washed thrice in IP buffer, boiled in 2X Laemmli Sample Buffer (Sigma), and analyzed immediately.

O. Mass spectrometry

Immunoprecipitates were size-fractionated by SDS-PAGE (4-15% gradient gel, BioRad) and stained with Coomassie Blue Silver overnight. Following washing in deionized water, the indicated bands were manually extracted, digested with trypsin, and subjected to liquid chromatography and nanospray/linear trap quadrupole mass spectrometry using a ThermoFinnigan LTQ linear ion trap mass spectrometer at the University of Pennsylvania Proteomics Core Facility. Data were analyzed via Sequest and Scaffold3 software packages. Presented data represent unweighted spectral counts, unique peptide counts, and percent protein coverage for proteins identified by ≥2 peptides with >99% protein/>95% peptide confidence.

P. *In vitro* GST pull down assays

For the *in vitro* binding experiments shown in Figures 3.10A and 3.10B, GST and GST-PS proteins were prepared in previously described conditions (Kihm et al., 2002). *E. coli* BL21 cells were grown at 37 °C for 3 hrs and induced to express protein by addition of 0.1 mM isopropyl-β-D-1-thiogalactopyranoside (IPTG) for 3 hrs at 30 °C. Cell pellets were resuspended in BC500 buffer (10 mM Tris-HCl (pH 8.0), 500 mM KCl, 20% glycerol, 1% NP-40, 0.5 mM EDTA, 1 mM DTT, 0.5 mg/mL lysozyme, 0.05 mg/mL DNAse I, and protease inhibitor cocktail (Sigma)) and sonicated. Lysates were clarified

by centrifugation at 10,000 rpm for 10 min at 4 °C. Cleared lysates were incubated with washed glutathione-Sepharose beads (GE Health Sciences) overnight at 4 °C, washed thrice in BC500, and eluted off of beads with 20 mM reduced glutathione solution containing 50 mM Tris-HCl (pH 8.8), 100 mM NaCl, 1 mM DTT, and protease inhibitor cocktail (Sigma).

Bovine brain holodynein was purified as described (Bingham et al., 1998). pCMV-based HA-tagged portions of rat dynein intermediate chain were introduced into 293T cells by calcium phosphate transfection. Transfected 293T cells expressing HA-tagged DIC constructs were lysed in pull down (PD) Buffer (20 mM Tris pH 7.4, 150 mM potassium chloride, 1 mg/mL BSA, 1:500 protease inhibitor cocktail (Sigma)) 24 hrs after transfection.

For pull down assays, recombinant GST or GST-PS (1 μmol at 4 mM final concentration) was incubated with substrate (5 μg holodynein (~4 fmol at 16 nM final concentration) or 400 μg 293T lysate containing DIC truncation) and 20 μL glutathione-Sepharose beads (GE Healthcare) in PD Buffer for 2 hrs at 4 °C with rotation. All pipette tips and Eppendorf tubes were passivized with 1 mg/mL bovine serum albumin (Sigma) prior to use. Beads were subsequently pelleted, washed thrice with PD Buffer, boiled in 2X Laemmli Sample Buffer (Sigma), and analyzed.

Q. SEC-MALLS experiments

Our collaborators, Drs. Joel Mackay and Ana Silva, of the School of Molecular Bioscience at the University of Sydney, Australia, conducted these experiments. Trim58

PS (residues 281-485) and dynein intermediate chain (residues 1-120) were expressed separately in *E. coli* Rosetta 2 (DE3) cells at 25 °C for 16 hrs. Cell pellets were resuspended in 50 mM sodium phosphate (pH 7.5) and 0.5 M sodium chloride for GST-PS, or 50 mM CHES pH 10 and 1 M sodium chloride for GST-DIC(1-120). Cells were lysed by sonication following the addition of 1 mg/mL lysozyme, 1 mM DTT, 1 mM PMSF, 0.05 mg/mL DNAse I, 0.05 mg/mL RNAse A and Complete EDTA-free protease inhibitors (Roche). Cell lysates were incubated with glutathione-Sepharose resin (Novagen) for 1 hr at 4 °C and washed. GST-DIC(1-120) was eluted using 30 mM glutathione, whereas PS was cleaved from the GST tag with HRV-3C protease overnight at 4 °C. Both proteins were then purified by size exclusion chromatography, using a Superdex 75 HiLoad 16/600 column. PS was eluted in 20 mM sodium phosphate (pH 7.5) and 50 mM sodium chloride, and GST-DIC(1-120) in 20 mM CHES pH 10 and 100 mM sodium chloride.

Purified PS (200 μL at 3.3 μM) and GST-DIC(1-120) (200 μL at 16.4 μM) were run separately on a Superdex 200 10/300 GL column connected to a MiniDawn Treos (Wyatt Technology). A mixture of PS and GST-DIC (200 μL of a mixture of PS at 13.2 μM and GST-DIC at 16.4 μM) was incubated for 1 hr at room temperature and then eluted on the same SEC-MALLS setup. All samples were eluted in 20 mM Tris pH 8 and 100 mM sodium chloride at 0.5 mL/min. Molecular masses were calculated using a dn/dc value of 0.185 mL/g.

R. Immunofluorescence assay sample preparation

HeLa cells were transiently transfected on 12 mm coverslips (VWR) with pK1-based Trim58 constructs or pEGFP-based mCherry-CC1 (human), using Lipofectamine 2000 reagent (Invitrogen) per the manufacturer's instructions. After 36 hrs, cells were fixed in 4% paraformaldehyde for 5 min, permeabilized in 0.1% Triton-X 100 for 5 min, and blocked in PBS containing 3% FBS for 1 hr at room temperature. Transfected HeLa cells were stained with GM130 (BD Biosciences) overnight at 4 °C, and then with goat anti-mouse Alexa Fluor 488 (Invitrogen) for 1 hr at room temperature. Cells were mounted on glass slides with Prolong Gold Antifade Reagent with DAPI (Invitrogen).

For erythroblast immunofluorescence assays, cells were layered onto glass slides previously treated with Vectabond reagent (Vector Laboratories) and incubated for 10 min at 37 °C. Erythroblasts were fixed and permeabilized as described above, stained with Alexa Fluor 488-conjugated anti-αTubulin (Millipore) overnight at 4 °C, and mounted.

S. Time lapse imaging set up

HeLa cell lines were plated on a FluoroDish (World Precision Instruments, 0.17 mm-thick glass bottom) in DMEM (Gibco) containing 10% FBS and 1% sodium pyruvate at a concentration of 250,000-500,000 cells per mL. Beginning 24-36 hrs later, cells were imaged at 5 min intervals for 12 hrs in an environmental chamber at 37 °C and 5% carbon dioxide.

T. Microscopy and image analysis

Time lapse and static erythroblast imaging were performed on an Olympus IX70 inverted microscope with a Photometrics CoolSnap HQ high-resolution CCD camera. Images were acquired and processed using Deltavision Softworx software. Static HeLa cell imaging was performed on a Zeiss LSM 710 Confocal microscope with ZEN 2011 acquisition software. The University of Pennsylvania Perelman School of Medicine Cell and Developmental Biology Microscopy Core maintained these microscopes. Images were analyzed using FIJI (Schindelin et al., 2012) and Volocity Software (PerkinElmer).

U. Imaging flow cytometry

For ImageStream analysis, erythroid cultures were fixed in 4% paraformaldehyde for 15 min at room temperature, washed in PBS, stained with Draq5 (Abcam), and analyzed on an Amnis ImageStream Mark II instrument at 40x magnification. GFP+ cells were gated using IDEAS software (Amnis) and comprised the base population for morphologic analysis based on aspect ratio and Δ centroid values. “Spherical” and “Oblong” cell gates were set by manual inspection of fluorescent cell images. A MATLAB program was used to identify nucleated cells within the spherical cell population by excluding anucleate reticulocytes (Draq5-negative) and multinucleated cells (detected by multiple Draq5-positive regions). The efficacy of this program was validated by manual inspection. Nuclear diameter, measured by Draq5 diameter, was quantified in MATLAB. IDEAS software was used to calculate Δ centroid values within the Draq5-positive, spherical cell population for nuclear polarization assessment. For some experiments, 16

μM nocodazole (Sigma) was added directly to culture media for the indicated amount of time.

V. Mouse work

Animal protocols were approved by the Institutional Animal Care and Use Committee of The Children's Hospital of Philadelphia (Philadelphia, PA).

W. Statistics

Statistical analysis was performed using GraphPad Prism 6.0 software (GraphPad Software). All multigroup comparisons were done using one-way ANOVA analysis. Comparisons between two groups were done using Student's t-test. Significance was set at $p<0.05$.

CHAPTER 3:

THE ROLE OF TRIM58 IN ERYTHROPOIESIS

Additional co-authors who contributed to this work:

From the Division of Hematology at the Children's Hospital of Philadelphia:

Elizabeth A Traxler, Eugene Khandros, Jenna M Nickas, Olivia Y Zhou, Dolly Prabhu, Yu Yao and Mitchell J Weiss

From the Department of Physiology and the Pennsylvania Muscle Institute at the University of Pennsylvania Perelman School of Medicine:

Jacob E Lazarus and Erika L Holzbaur

From the School of Molecular Bioscience at the University of Sydney:

Ana PG Silva and Joel P Mackay

Chapter Summary

TRIM58 is an E3 ubiquitin ligase superfamily member implicated by genome wide association studies (GWAS) to regulate human erythrocyte traits. Here we show

that Trim58 expression is induced during late erythropoiesis. Trim58 depletion in primary murine erythroid precursors inhibits their maturation from late stage nucleated erythroblasts to anucleate reticulocytes. Specifically, imaging flow cytometry studies demonstrate that Trim58 regulates polarization and/or extrusion of erythroblast nuclei. Protein interaction studies demonstrate that Trim58 binds directly to the intermediate chain of the microtubule motor dynein and induces degradation of the dynein complex. During erythropoiesis, Trim58 expression, dynein loss and enucleation occur concomitantly and all are inhibited by Trim58 shRNAs. Dynein regulates nuclear positioning and microtubule organization, both of which undergo changes during erythroblast enucleation. Thus, we propose that Trim58 regulates this process by eliminating dynein. Our findings identify the first erythroid-specific regulator of enucleation and elucidate a previously unrecognized mechanism for controlling dynein activity.

Figures and Tables can be found at the end of the text.

Introduction

Humans produce about 2 million red blood cells each second to replace those lost by senescence (McGrath and Palis, 2008) in a process termed erythropoiesis. Mature red blood cells (erythrocytes) contain high levels of the O_2 carrier hemoglobin and are distensible enough to withstand repeated passages through narrow capillary beds. These properties are acquired during precursor maturation through specialized cell divisions associated with activation of erythroid specific genes (Cheng et al., 2009; Welch et al., 2004), repression of alternate lineage genes (Cheng et al., 2009; Kingsley

et al., 2013; Welch et al., 2004), global DNA demethylation (Shearstone et al., 2011), reduced cell volume (Dolznig et al., 1995) and ejection of the nucleus to yield a reticulocyte, which develops further into a mature red blood cell (Liu et al., 2010). The mechanisms that govern these changes in cell structure and morphology are incompletely understood.

The process of nuclear expulsion from erythroblasts (Keerthivasan et al., 2011; Konstantinidis et al., 2012b) occurs exclusively in mammals and may represent an evolutionary adaptation to optimize erythrocyte rheology for transport through small capillary beds (Gaehtgens et al., 1981a; Mueller et al., 2008). Erythroblast enucleation is preceded by nuclear condensation and requires histone deacetylation (Ji et al., 2010; Popova et al., 2009) and suppression of the *Myc* proto-oncogene (Jayapal et al., 2010). The condensed nucleus polarizes to one side of the cell via transport mechanisms that require microtubules and phosphoinositide 3-kinase (Wang et al., 2012), followed by Rac GTPase-mediated formation of a contractile actomyosin ring between the incipient reticulocyte and nucleus (Ji et al., 2008; Konstantinidis et al., 2012b). Forces generated by the contractile ring promote further nuclear extrusion (Ji et al., 2008; Wang et al., 2012). Final separation between the reticulocyte and nucleus is facilitated by transport of lipid vesicles to the interface, which facilitates remodeling and resolution of the plasma membrane surrounding both structures (Keerthivasan et al., 2010; Keerthivasan et al., 2011). The ejected nucleus with surrounding plasma membrane is termed a pyrenocyte (McGrath et al., 2008). *In vivo*, free pyrenocytes are scavenged by macrophages (Soni et al., 2006), while reticulocytes are released into the circulation and undergo further maturation (Gifford et al., 2006). This process shares several features with cytokinesis (Keerthivasan et al., 2010; Konstantinidis et al., 2012b). Moreover, all of the proteins

currently known to participate in erythroblast enucleation are ubiquitously expressed and most function in mitosis. How erythroblasts co-opt generalized mitotic machinery for the lineage specific process of enucleation is unknown. Presumably, this is mediated in part by the expression of one or more erythroid restricted proteins.

Here, we identify a role for the erythroid protein Trim58 in erythroblast enucleation. Trim58 is a member of the tripartite motif-containing family of proteins, whose members function as E3 ubiquitin ligases broadly in physiology and disease (Napolitano and Meroni, 2012). Genome-wide association studies (GWAS) show that single nucleotide polymorphisms (SNPs) linked to the human *TRIM58* gene associate with variations in the size and/or number of circulating erythrocytes (Kamatani et al., 2010; van der Harst et al., 2012). Here we identify Trim58 as an erythroid restricted protein that facilitates erythroblast enucleation. Mechanistic studies suggest that Trim58 exerts this function by inducing degradation of the microtubule motor dynein. These findings are the first to identify an erythroid specific protein that participates in erythroblast enucleation, likely by targeting a ubiquitous protein complex that is essential for normal function in virtually all other eukaryotic cells.

Results

Trim58 is induced during late stage erythropoiesis

High-level human *TRIM58* expression is specific to the erythroid lineage (Figures 3.1A and 3.1B) and is strongly induced during the late stages of maturation (Figure

3.1C). *In situ* hybridization analysis of embryonic day 14.5 (E14.5) mouse embryos showed predominant *Trim58* mRNA expression in the fetal liver, an erythropoietic tissue (Figure 3.2A). Semiquantitative real-time PCR showed that Trim58 mRNA is upregulated >100-fold in late stage murine fetal liver erythroid precursors (Figure 3.2B). Chromatin immunoprecipitation-sequencing (ChIP-Seq) of primary erythroblasts demonstrated that the essential erythroid transcription factors Gata1 and SCL/Tal1 bind the *Trim58* locus within the first intron, a common location for erythroid specific enhancers (Figure 3.2C) ((Cheng et al., 2009) and Pimkin *et al*, in revision). Thus, the *Trim58* gene is strongly and specifically induced during terminal erythroid maturation, in part via direct activation by key hematopoietic transcription factors.

Trim58 regulates erythroblast enucleation

We used shRNAs to suppress *Trim58* expression during the *in vitro* maturation of primary fetal liver erythroblasts (Zhang et al., 2003). We infected purified E14.5 murine fetal liver erythroid precursors with retroviruses encoding *Trim58*-directed or control shRNAs along with a puromycin resistance cassette and green fluorescent protein (GFP) (Figure 3.3A) (Hemann et al., 2003). Infected cells were cultured for 1-3 days with dexamethasone, stem cell factor (SCF), erythropoietin (Epo) and puromycin to promote immature erythroblast expansion and select for infected cells. The erythroblasts were then switched to medium containing Epo only, which induced maturation to the reticulocyte stage. Four different shRNAs reduced *Trim58* mRNA and protein by 60-90% (Figures 3.3B and 3.3C). During late erythroid maturation, erythroblasts expel their nuclei to become anucleate reticulocytes that are Hoechst-negative by flow cytometry

(Figure 3.4A). The kinetics of enucleation were delayed in Trim58-deficient cultures (Figure 3.4B), and enucleation was consistently inhibited at 48 hrs maturation by all four Trim58-directed shRNAs analyzed compared to controls (Figures 3.4C). Histological staining confirmed these findings, showing reduced proportions of reticulocytes in *Trim58*-deficient cultures (Figures 3.4D and 3.4E). *Trim58* suppression also increased the proportions of mature erythroblasts containing two or more nuclei (Figure 3.5).

Several parameters of erythroid maturation were not altered by *Trim58* knockdown, including downregulation of the cell surface marker CD44 (Figure 3.6) (Chen et al., 2009). *Trim58* knockdown produced only small and inconsistent effects on erythroblast proliferation (Figure 3.7A) and viability (Figure 3.7B). Hemoglobin accumulation (Figure 3.8A) and nuclear condensation (Figure 3.8B) occurred normally after Trim58 knockdown. Overall, these findings demonstrate that Trim58 depletion caused selective defects during late stage erythropoiesis, including reduced enucleation and also increased formation of multinucleated cells.

Trim58 binds the molecular motor dynein

Trim58 is predicted to be an E3 ubiquitin ligase with characteristic functional modules, including a PRY-SPRY (PS) domain that mediates substrate interactions (Figure 3.9A) (James et al., 2007; Woo et al., 2006b). We performed pull down studies to identify Trim58 protein-binding partners, including potential degradation substrates. We used the isolated PS domain for these studies because ectopic expression of full-length wild type (WT) Trim58 was toxic to erythroblasts (data not shown). We expressed FLAG epitope-tagged PS domain in the erythroblast cell line G1E (Weiss et al., 1997),

which contains no endogenous Trim58 protein, immunoprecipitated (IP) with FLAG antibody and analyzed the recovered proteins by SDS-polyacrylamide gel electrophoresis. This analysis identified five discrete protein bands (Figure 3.9B). Mass spectrometry of these bands identified multiple subunits of the cytoplasmic microtubule motor protein complex dynein (Table 3.1), as well as nuclear pore complex proteins, a Golgi component, and several other proteins (Table 3.2). Dynein regulates nuclear positioning and microtubule structure within cells (McKenney et al., 2010; Splinter et al., 2010) and it was already known that erythroblast enucleation is microtubule-dependent (Konstantinidis et al., 2012b; Wang et al., 2012). Therefore, to investigate further a potential role for Trim58 in erythroblast enucleation, we focused on its interactions with dynein.

We confirmed the Trim58-dynein interaction in G1E cells by FLAG-IP followed by Western blotting for dynein intermediate chain (DIC) and dynein heavy chain (DHC) (Figure 3.9C). Immunoprecipitation of DIC from mouse fetal liver recovered Trim58, demonstrating an interaction between the endogenous proteins (Figure 3.9D). *In vitro* pull down assays showed that recombinant GST-tagged PS interacted with purified holodynein, indicating a direct and specific interaction (Figure 3.10A). Dynein is a multi-subunit complex that includes DHC, DIC, light intermediate chains, and light chains. The DIC mediates dynein interactions with several accessory proteins, mainly via the amino terminus (McKenney et al., 2011; Vallee et al., 2012). To test whether Trim58 interacted with DIC, we expressed hemagglutinin (HA)-tagged segments of the DIC amino terminus in 293T cells, incubated lysates with GST proteins and glutathione-Sepharose beads, and analyzed interacting polypeptides (Figure 3.10B). Western blotting for HA showed that PS interacted with DIC through an interface within the first 73 amino acids. We then

used size-exclusion chromatography coupled to multiangle laser light scattering (SEC-MALLS) to confirm this interaction *in vitro* using purified PS and DIC (residues 1-120). Bacterially expressed PS and GST-DIC(1-120) each eluted in gel filtration as a single peak when run individually (Figure 3.10C). MALLS data, which provide a reference-free estimate of solution molecular weight, showed that PS eluted as a monomer (observed MW = 25.6 kD; expected mass = 23.3 kD), whereas GST-DIC(1-120) ran as a dimer (observed MW = 91.2 kD; expected mass of dimer = 79.6 kD), as a result of the known dimerization of GST (Fabrini et al., 2009). A ~1:1 mixture of the two proteins also eluted predominantly as a single peak with a lower retention time, as expected for the formation of a complex. The molecular weight of this signal calculated from MALLS data (126.2 kD) is consistent with a 2:2 complex (expected mass = 114.4 kD) that represented a 1:1 Trim58-DIC complex that additionally dimerized through the GST moiety. Together, these data show that Trim58 binds dynein directly through physical interactions between its PS domain and the DIC amino-terminus (Figure 3.10D). This region of DIC contains a coiled coil domain that interacts with other dynein regulatory proteins, including the dynactin subunit $p150^{Glued}$ and NudE (Ma et al., 1999; McKenney et al., 2011).

Trim58 promotes dynein degradation

Next, we expressed FLAG/mCherry-tagged full length WT Trim58 in HeLa cells, which do not express endogenous Trim58, and assessed the effects on dynein protein levels. As controls, we expressed vector alone (V) or a “RING-dead” (RΔ) Trim58 containing two missense mutations predicted to abrogate E3 ligase activity (Figure 3.11A) (Zhang et al., 2012a). The cultures were treated with puromycin for 3 days to

enrich for infected cells and analyzed by Western blotting (Figure 3.11B). Although WT Trim58 slowed cell proliferation, we were able to create viable, stably expressing lines. Compared to the RΔ mutant, WT Trim58 was poorly expressed, likely due its autoubiquitylation and subsequent proteasomal degradation, which occur with other Trim proteins (Versteeg et al., 2013). Dynein subunits DHC and DIC were nearly absent from cells expressing WT Trim58, but not from cells expressing the RΔ version or the vector alone (Figure 3.11B and data not shown). In order to assess the mechanism through which Trim58 expression causes dynein loss, Trim58-expressing HeLa cells were treated with the proteasome inhibitor MG132. As shown in the right-hand panel of Figure 3.11B, MG132 increased the expression of dynein and WT Trim58. Thus, Trim58 promotes the degradation of itself and of dynein via mechanisms that require E3 ubiquitin ligase activity and proteasomes.

We then investigated whether Trim58 expression elicited cellular phenotypes characteristic of dynein loss. Dynein transports Golgi bodies along microtubules into perinuclear stacks at the microtubule organizing center (MTOC) (Quintyne et al., 1999). Inhibition of dynein by overexpression of CC1, a portion of $p150^{Glued}$ that interferes with the DIC-dynactin interaction, causes Golgi fragmentation and dispersal throughout the cytoplasm (Quintyne et al., 1999). We verified this result in HeLa cells and showed that WT Trim58, but not the RΔ mutant, produced a similar effect (Figure 3.12). Dynein also functions in mitotic spindle checkpoint inactivation to facilitate anaphase onset (Howell et al., 2001). Ectopic expression of WT Trim58 in HeLa cells caused mitotic defects characteristic of dynein inhibition, including prolonged interval between cell rounding and anaphase (Figures 3.13A and 3.13B) and cell death after rounding (Figure 3.13B right

panel) that were significantly worse than cells expressing vector or RΔ Trim58. Thus, ectopic expression of Trim58 in heterologous cells induces phenotypes that are consistent with dynein deficiency.

Trim58 expression in erythroblasts coincides with loss of dynein and enucleation

We investigated whether endogenous Trim58 expression promotes dynein loss during erythropoiesis. In murine erythroblast cultures undergoing semi-synchronous maturation, the induction of Trim58 protein at 24 hours correlated with loss of dynein subunits (DIC and DHC, Figure 3.14A) and the onset of enucleation (Figure 3.14C, black bars). The absence of dynein in late stages of erythroid maturation is consistent with proteomic studies of murine (Pasini et al., 2008) and human (Goodman et al., 2007) erythrocytes. In contrast, Trim58-deficient cells retained dynein protein aberrantly (Figures 3.14B and 3.15) and enucleation was delayed (Figures 3.14C gray bars). Dynein expression still declined in Trim58 knockdown erythroblasts, but with a ~12 hr delay. The eventual degradation of most dynein by 44 hours may be due to incomplete suppression of Trim58 and/or alternate protein degradation mechanisms. Overall, our findings demonstrate that expression of Trim58 destabilizes dynein and promotes enucleation. These findings are consistent with a model in which Trim58-mediated degradation of dynein and erythroblast enucleation are mechanistically linked.

Trim58 regulates nuclear polarization

We used the Amnis ImageStream, which combines flow cytometry with fluorescent microscopy, to compare specific steps of enucleation in Trim58-depleted and control erythroid cultures undergoing semi-synchronous maturation (see Figures 3.3, 3.4, and 3.14) (Konstantinidis et al., 2012b). Erythroblasts infected with shRNA retroviruses were identified by GFP expression, and nuclei were stained with the cell permeable DNA dye Draq5. We first measured changes in nuclear diameter as a function of time to assess nuclear condensation during maturation (Figures 3.16A-C and 3.17A). Overall, no significant differences in condensation were observed between control and Trim58-depleted cells (Figure 3.17A), in agreement with findings obtained by microscopic analysis of cytocentrifuged cells (Figure 3.8B). We next measured the aspect ratio (minor/major axis) and Δ centroid (distance between centers of the nucleus and cytoplasm) to distinguish spherical nucleated cells from oblong ones that were extruding their nuclei (Figures 3.16A-C). Spherical cells accumulated in Trim58-depleted cultures (Figure 3.17B), while the production of oblong cells undergoing nuclear extrusion was delayed (Figure 3.17C). Thus, Trim58 facilitates enucleation after the step of nuclear condensation.

We next assessed whether Trim58 regulated nuclear positioning specifically within the population of spherical cells depicted in Figure 3.17B, by measuring their Δ centroid distribution (Figures 3.18A and 3.18B). At 32 and 36 hours maturation, the mean Δ centroid was significantly reduced in Trim58 depleted spherical cells, indicating impaired nuclear polarization. Treatment of control erythroblasts with nocodazole produced similar, albeit stronger effects (Figure 3.19), consistent with previous studies

(Konstantinidis et al., 2012b; Wang et al., 2012). Thus, erythroblast nuclear polarization is Trim58- and microtubule-dependent.

We then used immunofluorescence to examine relationships between microtubule structure and nuclear positioning during enucleation. Erythroblast nuclei are surrounded by a network or “cage” of microtubules, similar to what occurs in most cells (Figure 3.20i) (Tsai et al., 2010; Wilson and Holzbaur, 2012). During enucleation, the nucleus moves away from the MTOC (Figure 3.20 and (Konstantinidis et al., 2012b; Wang et al., 2012)), opposite to what would occur with minus end-directed dynein transport. Later, the microtubule cage partially collapses, becoming detached from the cell cortex and nucleus as the latter is extruded (Figures 3.20ii-iv). Dynein stabilizes microtubules and tethers them to the cell cortex (Hendricks et al., 2012). Thus, events observed during enucleation, including directional nuclear movement and microtubule cage collapse (Figure 3.21), may be facilitated by dynein loss (see Figure 3.14).

Discussion

Genome wide association studies suggest that the E3 ubiquitin ligase superfamily member TRIM58 regulates human erythrocyte traits, including cell size and number (Kamatani et al., 2010; van der Harst et al., 2012). Here we support further a role for Trim58 in erythropoiesis and provide insight into the associated mechanisms. Trim58 binds dynein directly through its intermediate chain subunit and promotes proteasomal degradation of the holocomplex. During erythropoiesis, Trim58 expression correlates with dynein loss and enucleation. Both of these processes are inhibited by Trim58 depletion. Thus, we propose that Trim58 mediates erythroblast enucleation by

interfering with the established ability of dynein to regulate nuclear positioning and/or microtubule structure within cells (Figure 3.21) (McKenney et al., 2010; Splinter et al., 2010; Tanenbaum et al., 2011; Tsai et al., 2010; Wilson and Holzbaur, 2012). Our findings provide functional correlates for GWAS findings and identify a lineage-specific protein that alters the ubiquitous process of microtubule motor dynamics to regulate the highly specialized process of erythroblast enucleation.

According to our model (Figure 3.21), delayed enucleation caused by Trim58 deficiency should be alleviated by inhibiting dynein through alternate mechanisms. However, our attempts to inhibit dynein in wild type and Trim58-deficient erythroblasts using dynein intermediate chain-directed shRNAs, dynein heavy chain-directed shRNAs, overexpressed CC1 (Quintyne et al., 1999) or the chemical inhibitor ciliobrevin (Firestone et al., 2012) caused cell death in maturing erythroblasts prior to enucleation (data not shown), which undermined our ability to discern whether these treatments augmented enucleation. Similarly, retroviral expression of Trim58 in erythroblasts prior to their enucleation was toxic. These findings indicate that the physiological timing and magnitude of Trim58 expression and consequent dynein degradation must be exquisitely regulated to occur exclusively in post-mitotic erythroblasts during enucleation, in order to preserve dynein-dependent processes required for earlier stages of cellular maturation.

In most cells, networks or “cages” of microtubules surround the nucleus and regulate its spatial orientation through the actions of directionally opposed dynein and kinesin motors (Wilson and Holzbaur, 2012). During erythroblast enucleation, the nucleus moves away from the MTOC (Konstantinidis et al., 2012b; Wang et al., 2012) and is ultimately released from the encompassing microtubule cage (Figure 3.20). By

degrading dynein, Trim58 could facilitate these processes via two potential mechanisms (Figure 3.21). On one hand, movement of the nucleus during enucleation is directionally opposed to the minus end-directed motor actions of dynein. Thus, Trim58-mediated suppression of dynein may create a “microtubule motor imbalance”, allowing the plus end-directed actions of kinesins to polarize the nucleus away from the MTOC. Alternatively, dynein normally stabilizes microtubules and mediates their attachment to the cell cortex (see (Hendricks et al., 2012) and references therein). Thus, Trim58-mediated dynein degradation in late stage erythroblasts may destabilize microtubules, promoting their detachment from both the cell cortex and nuclear membrane (i.e., “microtubule cage collapse”) thereby facilitating nuclear movement and release. Of note, dynein loss and enucleation are significantly delayed, but not eliminated by Trim58 shRNAs (see Figure 3.14). This may be explained by incomplete suppression of Trim58. Alternatively, redundant systems, including other ubiquitin ligases, autophagy, and/or proteases, may cooperate with Trim58 to degrade dynein during late stage erythropoiesis. We favor the latter possibility, which is consistent with the extensive repertoire of proteolytic systems present in late stage erythroblasts (Khandros and Weiss, 2010).

Kinesin-1 regulates nuclear movement in numerous cell types (Tanenbaum et al., 2011) and its Kif5b isoform is abundant in murine (Kingsley et al., 2013) and human (Merryweather-Clarke et al., 2011) erythroblasts. However, shRNA-mediated knockdown of Kif5b did not antagonize the deleterious effects of Trim58 deficiency on enucleation’ as would be predicted by the “microtubule motor imbalance” model (Figure 3.22). This finding supports the alternative mechanism of “microtubule cage collapse”. However, at least 10 additional kinesin family members are expressed during erythropoiesis

((Kingsley et al., 2013; Merryweather-Clarke et al., 2011) and Figure 3.22), making it difficult to draw a definitive conclusion from the Kif5b knockdown data. Systematic inhibition of these kinesin genes, either separately or in combinations, may determine whether any participate in nuclear polarization during erythroblast enucleation.

Several lines of evidence suggest important roles for proteasome-mediated protein degradation during erythroblast maturation (Khandros and Weiss, 2010) and enucleation (Chen et al., 2002)., but only a few specific pathways are currently defined. For example, the ubiquitin ligases Mdm2 and Mdm4 foster erythropoiesis by inhibiting p53 (Maetens et al., 2007) and the ubiquitin ligase Cul4A regulates erythropoiesis by targeting the cell cycle inhibitor p27 (Li et al., 2006). To our knowledge, Trim58 represents the first lineage-specific ubiquitin ligase shown to be involved in erythroid maturation and in particular the enucleation step. There are two likely mechanisms by which Trim58 might mediate degradation of bound dynein. First, Trim58 might promote the transfer of K48-linked polyubiquitin onto DIC and/or other subunits, targeting dynein to the proteasome. Alternatively, Trim58 might autoubiquitylate, stimulating its own proteasomal targeting along with that of bound dynein, similar to the mechanism by which the related protein Trim21 mediates degradation of IgG-bound intracellular virions (Mallery et al., 2010).

It is also possible that Trim58 promotes erythroid maturation via dynein-independent mechanisms through interactions with other binding partners, including those identified by our IP studies (Table 3.2). For example, Trim58 binds several nuclear pore complex proteins, including Nup153 and Nup50. These proteins function in mitosis (Chatel and Fahrenkrog, 2011; Mackay et al., 2009), a process that shares some

features with enucleation (Keerthivasan et al., 2011). Like dynein, Nup153 is downregulated during erythropoiesis, but the latter process does not appear to be dependent on Trim58 (Figures 3.14A and 3.14B). However, some Trim family members function through proteasome-independent mechanisms, for example by catalyzing SUMOylation of substrates (Chu and Yang, 2011; Napolitano and Meroni, 2012); this may also be the case for Trim58 interactions with Nup153/50 and/or other proteins.

Genome wide association studies offer a population-based approach to identify genes that regulate health-related traits. However, GWAS typically identify single nucleotide polymorphisms within linkage disequilibrium blocks that contain multiple genes, and it can be challenging to identify the specific gene(s) that influence the trait of interest (Hindorff et al., 2009; Peters and Musunuru, 2012). Moreover, alleles discovered by GWAS usually cause subtle alterations in gene expression or function, providing a minimal estimate of the role of a particular gene in the biological process of interest (Sankaran and Orkin, 2013). Our gain- and loss-of-function studies address these general issues by demonstrating a specific role for Trim58 in erythroid cells and by identifying a relevant molecular pathway. Of note, GWAS also identify *TRIM58* as a candidate gene for regulating human platelet numbers (Gieger et al., 2011). Consistent with this observation, Trim58 expression is induced in megakaryocytes, likely via Gata1 and SCL/Tal1 (Figure 3.23), similar to what we observed in erythroid cells. These observations are interesting in light of findings that dynein promotes platelet production by regulating microtubule dynamics in megakaryocytes (Patel et al., 2005). Thus, Trim58 might regulate platelet formation through its interactions with dynein. Overall, our findings illustrate how mechanism-based investigations can synergize with GWAS to elucidate new biological pathways.

Dynein is expressed ubiquitously in eukaryotes and performs a wide array of functions. Consequently, considerable efforts have been directed toward understanding how dynein activities are regulated during cellular development, cell cycle progression, and in different lineages. Dynein cargo preference and motor activity are modulated largely by protein interactions and perhaps by post-translational modifications (Vallee et al., 2012). Our findings demonstrate that dynein is also regulated by precisely timed, lineage-specific degradation. It will be interesting to explore the generality of this finding by investigating whether dynein stability is regulated in non-erythroid tissues through interactions with Trim58 or other ubiquitin ligases.

Tables

Table 3.1. Dynein subunits identified by mass spectrometric analysis of proteins that coimmunoprecipitated with the Trim58 PRY-SPRY domain in erythroid cells. The bands in Figure 3.9B that contained each protein are noted. MW, molecular weight.

Protein Name	Accession	MW	Band	Unweighted Spectra	Unique Peptides	Percent Coverage
Cytoplasmic dynein 1						
Heavy chain 1	IPI00119876	532 kD	1	189	95	19
Intermediate chain 2	IPI00131086	68 kD	3	16	7	14
Light intermediate chain 1	IPI00153421	57 kD	3,4	38	12	27
Light intermediate chain 2	IPI00420806	54 kD	4	12	7	16
Trim58 PRY-SPRY (Bait)						
Trim58	IPI00353647	55 kD	4,5	91	14	26

Table 3.2. Proteins other than dynein subunits that were identified by mass spectrometry in FLAG-PS or Vector control IP samples. The bands in Figure 3.9B that contained each protein are noted. MW, molecular weight; % Cvg, % coverage. Spc, Spectra. Unq Pep, Unique Peptides.

				FLAG-PS			Vector		
Protein Name	**Accession**	**MW**	**Band**	**Spectra**	**Unique Peptides**	**% Cvg**	**Spc**	**Unq Pep**	**% Cvg**
Golgin α3	IPI00336281	163 kD	2	67	28	20			
Nucleoporin 153	IPI00330624	152 kD	2	48	25	18			
Importin α2	IPI00124973	58 kD	3,4	38	9	21			
Nucleoporin 50	IPI00120572	49 kD	4,5	34	13	32			
Ig kappa chain V-II region 26-10	IPI00464378	12 kD	5	20	5	26	10	3	22
dehydrogenase/reductase SDR family member 4 isoform 1	IPI00318750	30 kD	5	17	7	22	10	5	18

Ig gamma-1 chain C region, membrane-bound form	IPI00308213	43 kD	4,5	16	5	14	4	2	6
Importin β1	IPI00323881	97 kD	3	12	5	6			
Similar to Chain L, Structural Basis Of Antigen Mimicry In A Clinically Relevant Melanoma Antigen System isoform 1	IPI00406213	26 kD	5	10	5	22	7	4	18
Isoform 3 of A-kinase anchor protein 9	IPI00623749	434 kD	1	9	7	2			
Tubulin beta-2B chain	IPI00109061	50 kD	4	9	5	12			
Isoform 1 of 6-phosphofructokinase type C	IPI00124444	85 kD	2	6	4	4			
Tubulin alpha-1A chain	IPI00110753	50 kD	4	6	4	11			

DNA replication licensing factor MCM5	IPI00309398	82 kD	3	5	3	4
Elongation factor 1-alpha 2	IPI00119667	50 kD	4	5	2	5
Splicing factor 4	IPI00454015	73 kD	3	5	3	5
6-phosphofructokinase, muscle type	IPI00331541	85 kD	3	4	3	3
ATP synthase subunit alpha, mitochondrial	IPI00130280	60 kD	4	4	2	4
Phosphate carrier protein, mitochondrial	IPI00124771	40 kD	5	4	2	6
Serine/threonine-protein kinase 38	IPI00126943	54 kD	4	4	3	7
ADP/ATP translocase 2	IPI00127841	33 kD	5	3	2	6
cAMP-dependent protein kinase type II-beta	IPI00224570	46 kD	4	3	2	5

regulatory subunit						
Putative uncharacterized protein	IPI00396787	67 kD	4	3	2	3
Heat shock cognate 71 kD protein	IPI00323357	71 kD	3	2	2	4
Isoform 2 of DNA-directed RNA polymerase I subunit RPA49	IPI00120981	49 kD	4	2	2	4
Protein LSM14 homolog A	IPI00172202	51 kD	4	2	2	4
RuvB-like 1	IPI00133985	50 kD	4	2	2	6

Figures

Figure 3.1. Human Trim58 expression is restricted to late stage erythroblasts. Human *TRIM58* mRNA expression levels were measured by microarray analysis in (A) a panel of human tissue types (Wu et al., 2009), (B) a panel of human hematopoietic tissues (Novershtern et al., 2011), and (C) cultured primary human erythroblasts from peripheral blood buffy coat mononucleocytes (Merryweather-Clarke et al., 2011). The results in panel C represent mean ± SD for 3 biological replicates normalized to the average expression level in CFU-E cells, which were assigned a value of 1. **p<0.01. CFU-E, erythroid colony-forming units; Pro-E, proerythroblasts; Int-E, intermediate (basophilic) erythroblasts; Late-E, late (orthochromatic) erythroblasts.

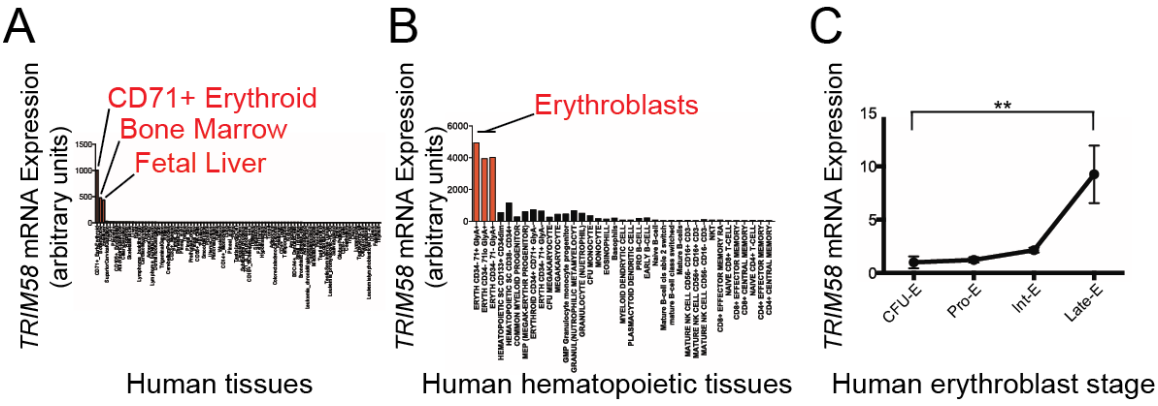

Figure 3.2. Murine Trim58 is expressed during late stage erythropoiesis. (A) RNA *in situ* hybridization for *Trim58* mRNA in a day 14.5 mouse embryo showing strong expression (red) in fetal liver, the site of definitive erythropoiesis. (B) Primary murine fetal liver erythroblasts were FACS-purified using a previously described gating strategy (Pop et al., 2010) and *Trim58* mRNA was analyzed by semiquantitative real-time PCR. The y-axis shows relative mRNA expression, normalized to S0 cells, which were assigned a value of 1. The results represent mean ± SEM for 3 biological replicates. *p<0.05. (C) Chromatin immunoprecipitation-sequencing (ChIP-Seq) analysis of transcription factor binding to the *Trim58* locus in primary murine erythroblasts (data from Pimkin *et al*, in revision). The blue line depicts the *Trim58* gene, with exons shown as rectangles. Transcription factor binding sites are indicated in red.

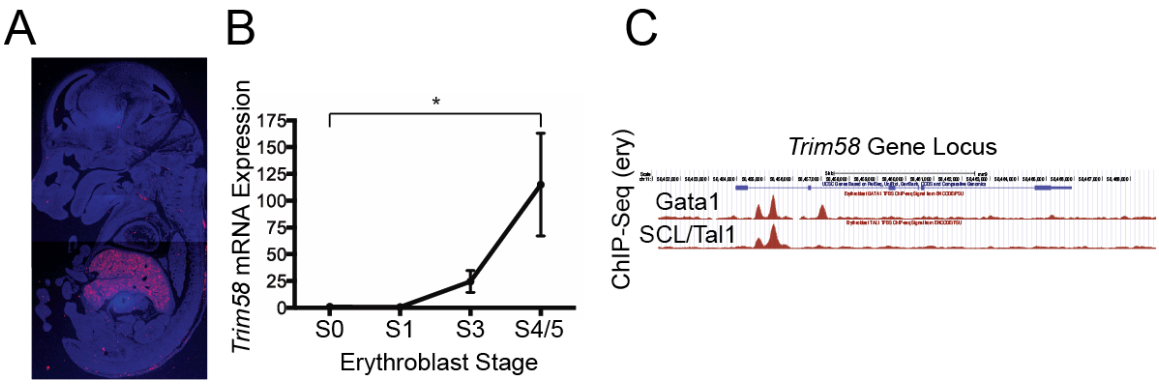

Figure 3.3. Trim58-directed shRNAs reduce expression in murine erythroblast cultures. (A) Embryonic day 14.5 murine fetal liver erythroid precursors were purified, infected with retroviruses encoding *Trim58* or control shRNAs, and cultured for 24-72 hrs in expansion medium with puromycin (Puro) to select for infected cells. The cells were then switched to maturation medium, which facilitates development to the reticulocyte stage over ~48 hrs. Epo, erythropoietin; SCF, stem cell factor; Dex, dexamethasone. Scale bar, 10μm. (B) Western blot for Trim58 in erythroblasts expressing Trim58-directed or control shRNAs at 48 hrs maturation. Luc, luciferase; Scr, scrambled. The asterisk (*) represents a nonspecific band. “Long” and “short” exposures are from the same blot. (C) Suppression of *Trim58* mRNA expression by four shRNAs. *Trim58* mRNA levels were measured at 48 hrs maturation by semiquantitative real time PCR and normalized to the average expression value for *Gapdh*, *Actin*, and *Hprt* mRNA levels. The y-axis represents mRNA expression level compared to the average value for control-treated samples (Vector, shLuc, shScr), which was set at 1. Results represent mean ± SD for 4 biological replicates.

Figure 3.3

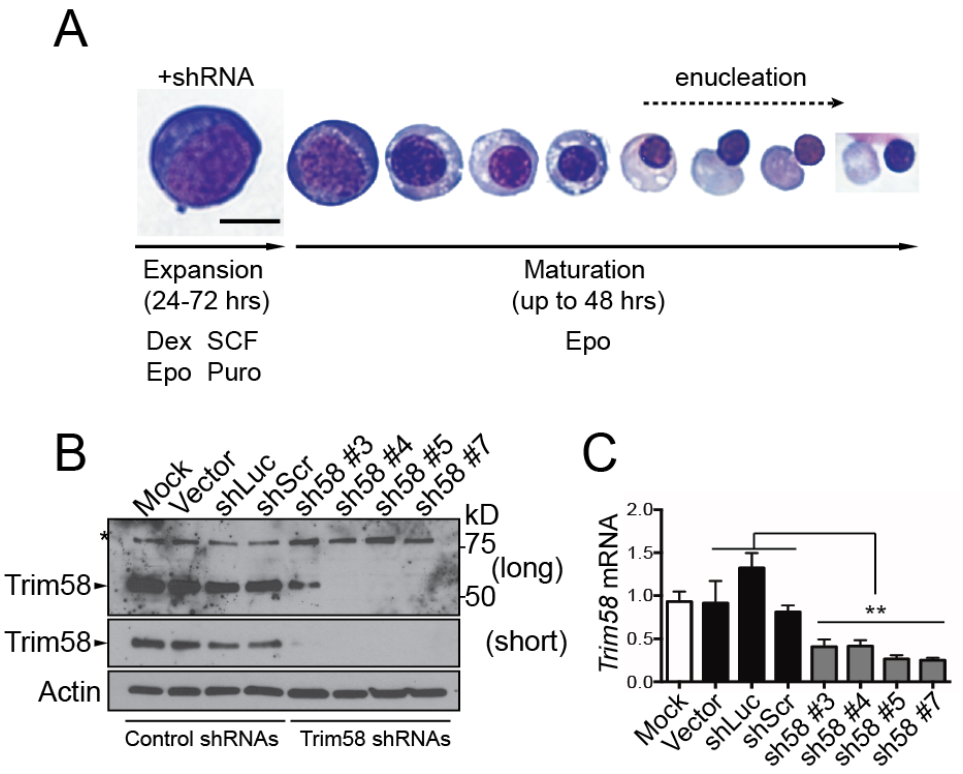
A
+shRNA
enucleation
Expansion
(24-72 hrs)
Dex SCF
Epo Puro
Maturation
(up to 48 hrs)
Epo
B
Mock
Vector
shLuc
shScr
sh58 #3
sh58 #4
sh58 #5
sh58 #7
kD
75
50
(long)
(short)
Trim58
Trim58
Actin
Control shRNAs
Trim58 shRNAs
C
Trim58 mRNA
2.0
1.5
1.0
0.5
0.0
**
Mock
Vector
shLuc
shScr
sh58 #3
sh58 #4
sh58 #5
sh58 #7

Figure 3.4. Trim58 knockdown inhibits murine erythroblast enucleation. (A) FACS analysis for enucleation of control (shLuc) and Trim58-deficient (shTrim58 #4) erythroid cultures at the indicated time points. During maturation, erythroblasts become smaller, indicated by decreased forward scatter, and ultimately enucleate to become Hoechst-negative reticulocytes (boxed regions). (B) Summary of percent (%) enucleation at the indicated time points in cultures treated with control (shLuc) or Trim58-directed (#4) shRNAs. Results represent mean ± SD for 3 biological replicates. (C) Four Trim58-directed shRNAs inhibit enucleation. Following 48 hrs maturation, erythroblasts treated with the indicated shRNAs were analyzed by FACS for enucleation. (D) Representative histologies of control (shLuc) and Trim58-deficient (shTrim58 #4) erythroid cultures after 36 hrs maturation. Red arrows denote anucleate reticulocytes. Scale bar, 20 μm. R, reticulocyte; E, erythroblast; N, extruded nucleus. (E) Summary of cell counts from panel D showing percent (%) reticulocytes. Six hundred cells were counted on each slide.

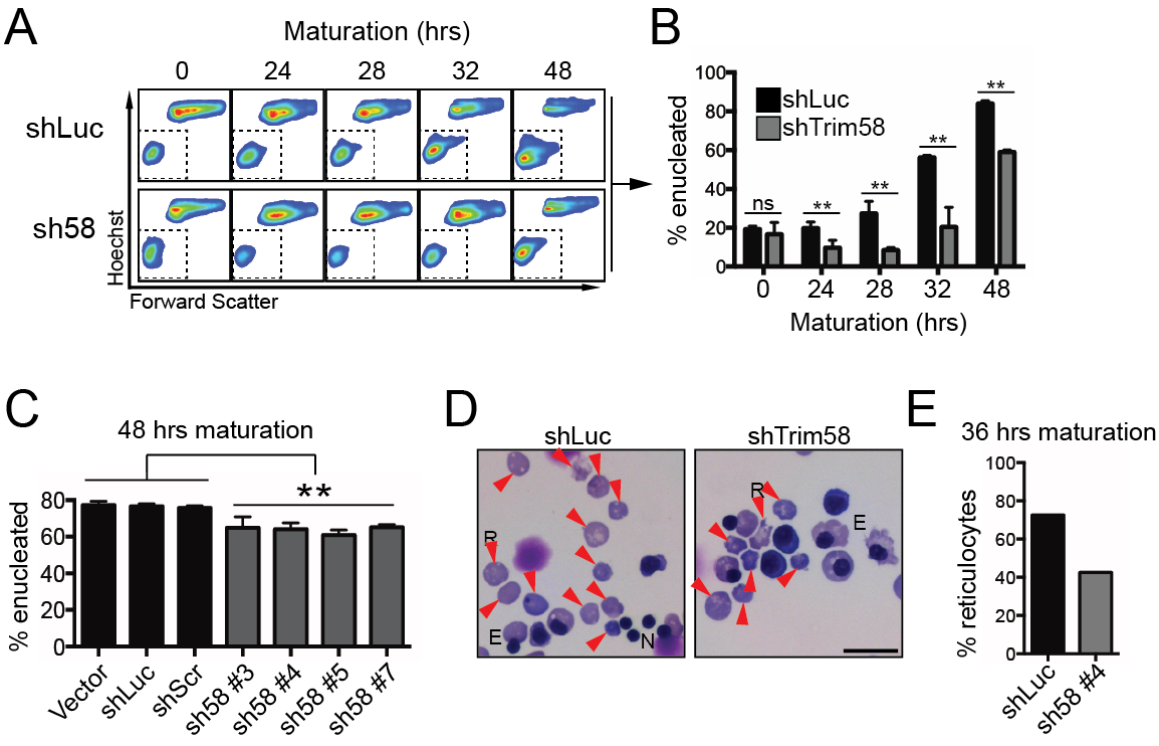

Figure 3.5. Trim58 knockdown results in multinucleated erythroblasts. Murine fetal liver erythroblasts were infected with control retrovirus(es) (empty Vector; shLuc, Luciferase; and/or shScr, Scrambled), *Trim58*-directed shRNA(s) (sh58 #3, #4, #5, and/or #7) and/or mock-treated. Infected cells were expanded with puromycin for 72 hrs and then induced to mature at time 0. (A) At 48 hrs maturation, erythroblasts treated with shTrim58 #4 were cytocentrifuged onto a glass slide, stained with May Grünwald and Giemsa reagents, and visualized by light microscopy. Arrows denote binucleate erythroblasts (BE). Scale bar, 10 μm. (B) The percentage of cells containing 2 or more nuclei was quantified by visual inspection. Results represent mean ± SD for 3 independent experiments with >200 cells counted per treatment group per experiment.

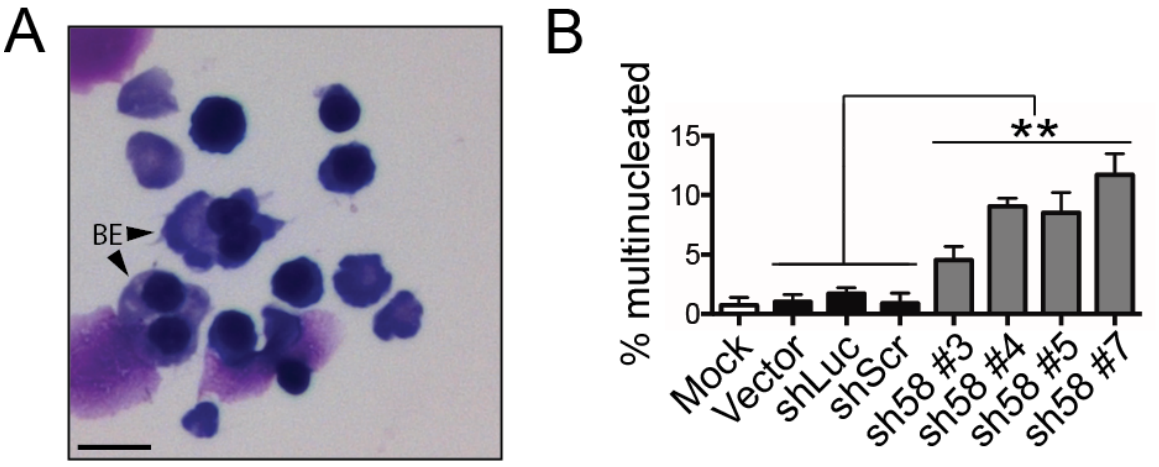

Figure 3.6. Trim58 knockdown does not affect CD44 downregulation kinetics during erythroid maturation. Erythroblasts expressing control (shLuc, black) or Trim58 (sh58 #4, gray) shRNAs were analyzed serially by flow cytometry for CD44, a cell surface marker that progressively decreases during erythroid maturation (Chen et al., 2009). Representative histogram plots of FACS data are shown. Below the histograms are line graphs depicting CD44 mean fluorescence intensity (mfi) over time (mean ± SD for 4 biological replicates). % max, percent (%) of maximum cell count.

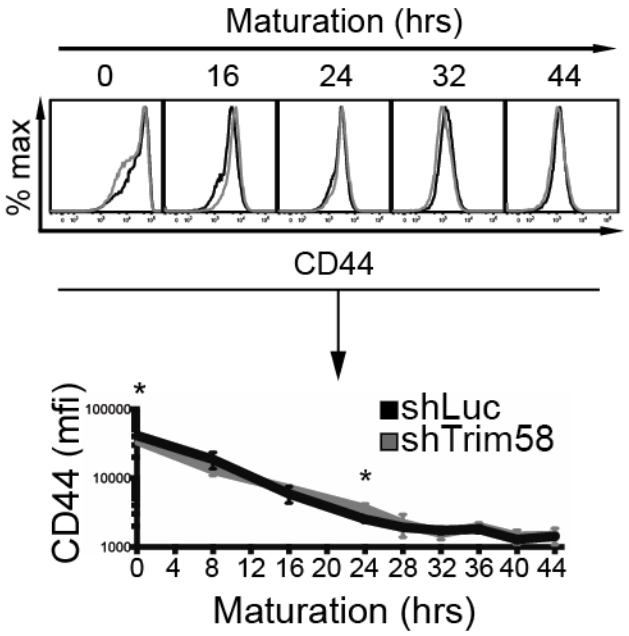

Figure 3.7. Trim58 knockdown does not affect cell proliferation or viability. Murine fetal liver erythroblasts were infected with control retrovirus(es) (empty Vector; shLuc, Luciferase; and/or shScr, Scrambled), *Trim58*-directed shRNA(s) (sh58 #3, #4, #5, and/or #7) and/or mock-treated. Infected cells were expanded with puromycin for 72 hrs and then induced to mature at time 0. (A) Infected erythroblast proliferation was quantified at 0, 24, and 48 hrs maturation. Cell numbers were normalized to the cell count at 0 hrs. Results represent mean ± SD for 4 biological replicates. (B) Cell viability was measured by fluorescent amino-reactive (LiveDead) staining at 0, 24, and 48 hrs maturation. Results represent mean ± SD for 4 biological replicates. A key depicting the color of each treatment group is shown to the right.

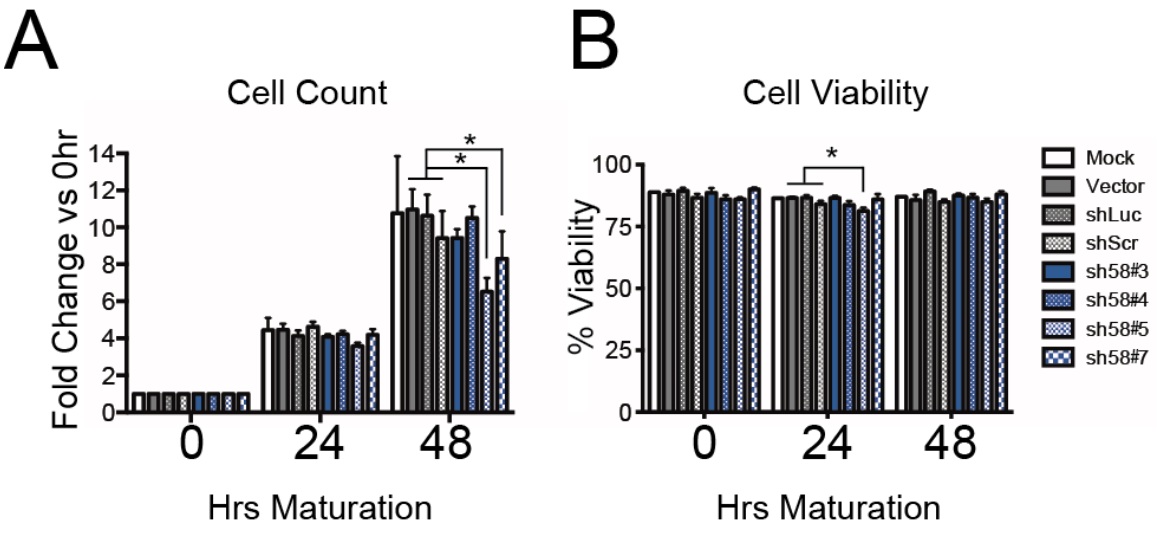

Figure 3.8. Trim58 knockdown does not affect Hb content or nuclear condensation. Murine fetal liver erythroblasts were infected with control retrovirus(es) (empty Vector; shLuc, Luciferase; and/or shScr, Scrambled), *Trim58*-directed shRNA(s) (sh58 #3, #4, #5, and/or #7) and/or mock-treated. Infected cells were expanded with puromycin for 72 hrs and matured for 48 hours. (A) Hemoglobin content measured at 48 hrs maturation, normalized to total cellular protein. Results represent mean ± SD for 3 independent experiments. The top panel shows the red color of cell pellets. (B) Nuclear size quantification at 48 hrs maturation. Erythroblasts treated with the indicated shRNAs were centrifuged onto a slide and stained with May Grünwald and Giemsa reagents. The area encompassed by each nucleus was quantified by microscopy using the Analyze Particles feature in FIJI (Schindelin et al., 2012). Results represent mean ± SD for 3 independent experiments with >50 cells counted per treatment group per experiment. *p<0.05, **p<0.01.

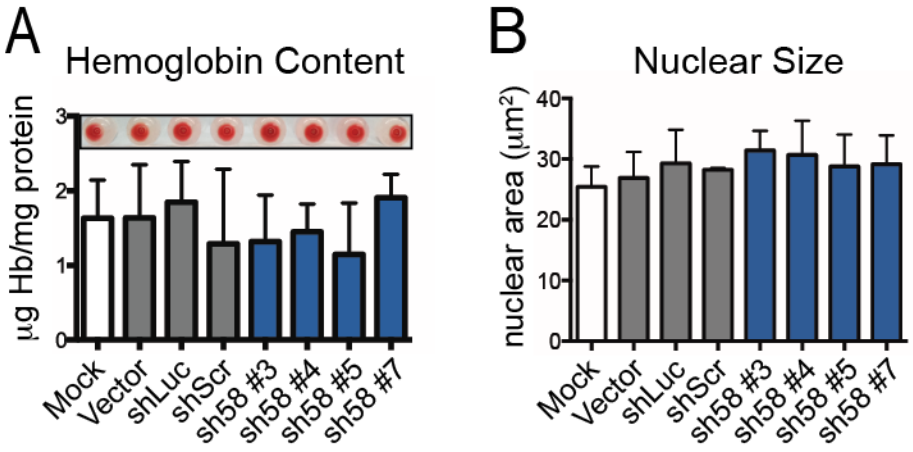

Figure 3.9. The Trim58 PRY-SPRY domain binds the molecular motor dynein. (A) Domain structures of Trim58 showing the “tripartite” RING-BBox-Coiled Coil (CC) motif and the immunoglobulin-like PRY-SPRY domain. Amino acid numbers are indicated. In some TRIM proteins, the RING domain recruits E2 conjugases carrying activated ubiquitin and the PRY-SPRY domain binds substrates. (B) FLAG-tagged Trim58 PRY-SPRY domain (PS), or vector (V), were stably expressed in G1E proerythroblast cells. Lysates were immunoprecipitated (IP) with FLAG antibody, fractionated by SDS-polyacrylamide gel electrophoresis, and stained with Coomassie Blue Silver. Numbered arrows denote the regions of the gel from which bands were excised for mass spectrometric (MS) analysis. Bands from both V and PS IPs were analyzed. MS identified peptides from dynein heavy chain (DHC), dynein intermediate chain (DIC), dynein light intermediate chains 1/2 (DLIC), and Trim58 PRY-SPRY (PS) predominantly in Bands 1, 3, 4, and 5, respectively. These proteins were only identified in bands from the PS IP lane. See Tables 3.1 and 3.2 for a full listing of identified proteins. Inp, input (1%). (C) Lysates of G1E cells expressing FLAG-PS or vector (V) were immunoprecipitated with FLAG antibody and analyzed by Western blotting (immunoblotting, IB) for DHC, DIC, FLAG and Codanin1 (Cdan1, negative control). Inp, input (5%). (D) Embryonic day 14.5 murine fetal liver erythroblasts were lysed, immunoprecipitated with anti-DIC antibody or IgG control and analyzed by Western blotting for the indicated proteins. α globin was included as a negative control. Inp, input (0.5%).

Figure 3.9

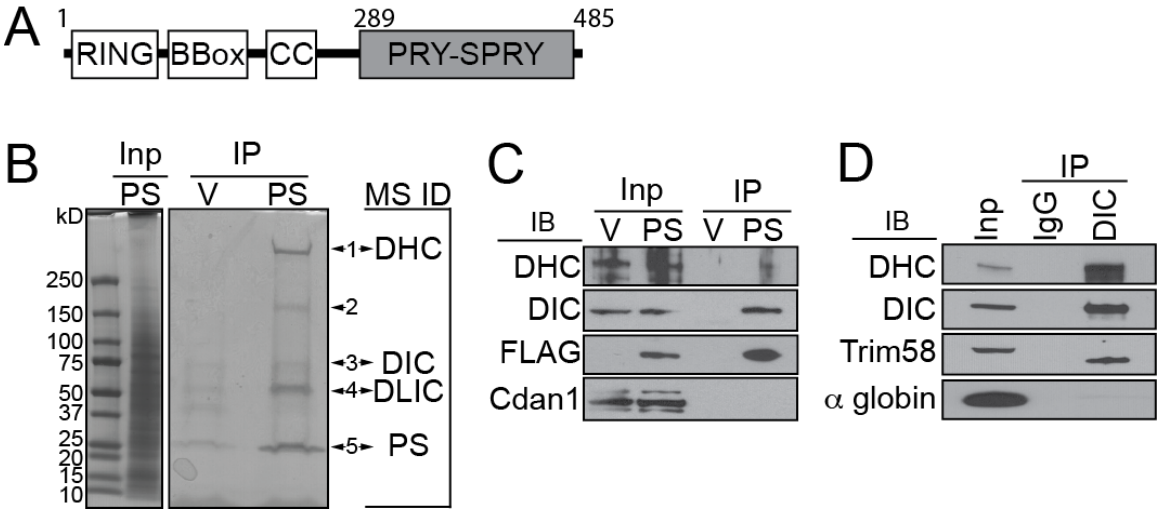
A
1
289
485
RING
BBox
CC
PRY-SPRY
B
Inp
IP
PS
V
PS
MS ID
kD
250
150
100
75
50
37
25
20
15
10
1 DHC
2
3 DIC
4 DLIC
5 PS
C
Inp
IP
IB
V PS V PS
DHC
DIC
FLAG
Cdan1
D
IP
IB
Inp
IgG
DIC
DHC
DIC
Trim58
α globin

Figure 3.10. Trim58 binds directly to the DIC amino terminus. (A) Recombinant purified GST-Trim58 PS domain (GST-PS) or GST alone were incubated with purified bovine holodynein complex and glutathione-Sepharose beads. Bound proteins were analyzed by Western blotting. Equal percentages of total input (Inp), pull down (PD) and supernatant (SN) samples were loaded. (B) 293T cells were transfected with expression plasmids encoding hemagglutinin (HA) fused to the indicated DIC amino acids. After 24 hrs, cells were lysed and incubated with GST-PS or GST and glutathione-Sepharose beads. Bound proteins were analyzed by anti-HA Western blotting. PD, pull down. SN, supernatant (1%). (C) SEC-MALLS data for PS, GST-DIC(1-120) and a 1:1 mixture. Protein concentration was measured on an inline refractive index detector. Light scattering data converted to molecular weight are shown above each chromatography trace and relate to the right-hand y-axis. The observed molecular weights are consistent with a 1:1 interaction between the two proteins augmented by the dimerization of the GST tag appended to DIC(1-120). (D) DIC domain structure showing the amino-terminal coiled coil (CC) motif, which binds Trim58. This region of DIC also binds dynactin/p150^{Glued} and NudE, which are previously characterized regulators of dynein function (McKenney et al., 2011). The DIC carboxy-terminal domain contains WD repeats that interact with DHC. Amino acid numbers are indicated (aa#).

Figure 3.10

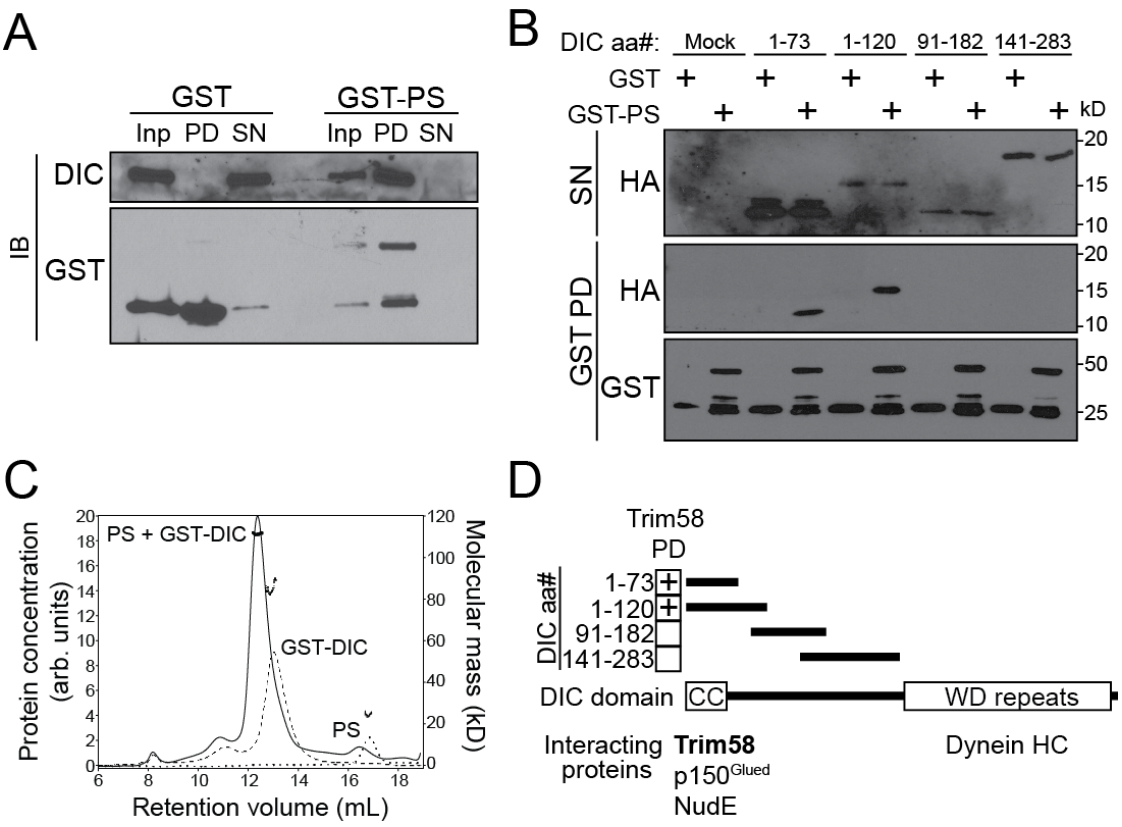
A
GST
GST-PS
Inp PD SN
Inp PD SN
IB
DIC
GST
B
DIC aa#: Mock 1-73 1-120 91-182 141-283
GST + + + + +
GST-PS + + + + +
kD
SN
HA
20
15
10
GST PD
HA
20
15
10
GST
50
25
C
PS + GST-DIC
GST-DIC
PS
Protein concentration (arb. units)
Molecular mass (kD)
Retention volume (mL)
D
Trim58
PD
DIC aa#
1-73 +
1-120 +
91-182
141-283
DIC domain
CC
WD repeats
Interacting proteins
Trim58
p150Glued
NudE
Dynein HC

Figure 3.11. Trim58 facilitates dynein degradation. (A) Schematic diagram showing full length Trim58 constructs with amino-FLAG and carboxyl-mCherry tags. The RΔ mutant contains two missense mutations in the RING domain that abrogate ubiquitin ligase activity. (B) Western blot analysis of Trim58-expressing HeLa cells. Cells were infected with retrovirus encoding FLAG-Trim58 (WT or RΔ) or vector (V), selected in puromycin for 3 days, then analyzed by Western blotting before or after treatment with the proteasome inhibitor MG132 (10 μM) for 4 hrs at 37 ºC.

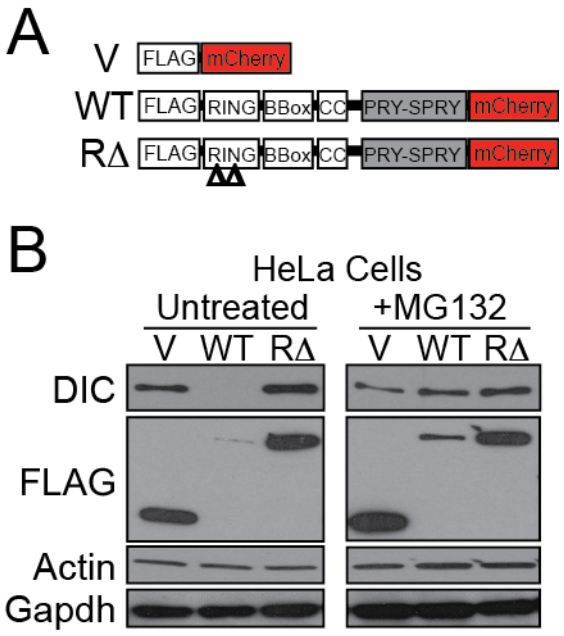

Figure 3.12. Trim58 expression causes Golgi spreading, a marker of dynein dysfunction. Assessment of Golgi structure in HeLa cells expressing Trim58. HeLa cells were transfected with expression plasmids encoding Trim58-mCherry or CC1-mCherry, a dynein inhibitor (Quintyne et al., 1999). After 36 hrs, the cells were fixed, stained for the Golgi matrix protein GM130 and DNA (DAPI), and visualized by confocal microscopy. The percentage (%) of mCherry (mCh) positive cells that displayed normal punctate perinuclear Golgi body distribution is shown at right. The results represent mean ± SD for 3 independent experiments, with >100 cells counted per experiment. **p<0.01 vs. Vector control.

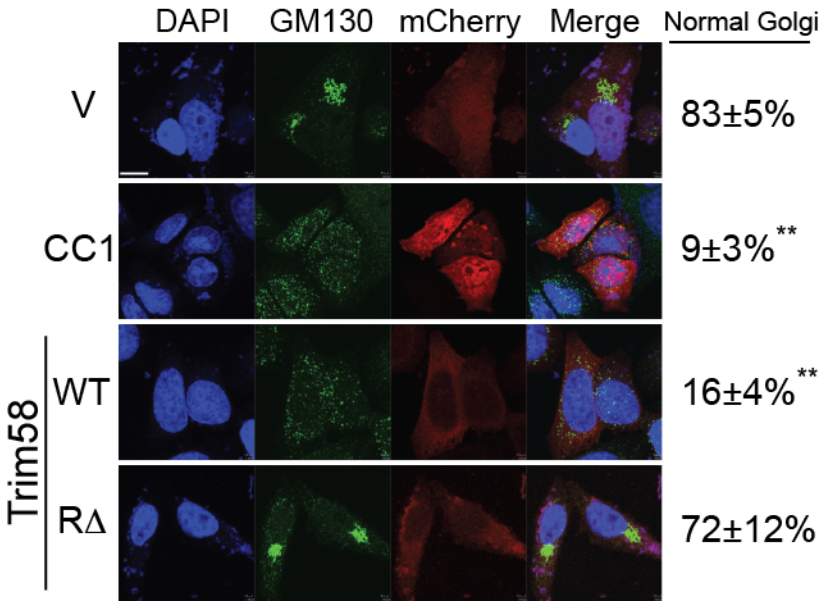

Figure 3.13. Trim58 expression perturbs mitotic progression. (A) Mitotic progression in HeLa cells expressing Trim58-mCherry constructs was analyzed by time-lapse microscopy. Representative images show mitotic progression in outlined cells. Cells expressing WT Trim58 exhibit delayed progression from cell rounding (~metaphase) to anaphase, compared to cells expressing vector or RΔ Trim58. BF, Brightfield; mCh, mCherry. Scale bar, 16μm. (B) Quantitative analysis of mitosis in Trim58-expressing HeLa cells. The graph on the left shows time elapsed between cell rounding and anaphase. The results represent mean ± SD for all observed mitotic cells. **p<0.01. The graph on the right shows the percentages of cells with delayed (>200 min) or failed mitosis manifested as cell death between rounding and anaphase. (V, n=134 normal mitoses; WT, n=50 normal, 13 delayed, 11 failed mitoses; RΔ, n=100 normal, 7 delayed mitoses).

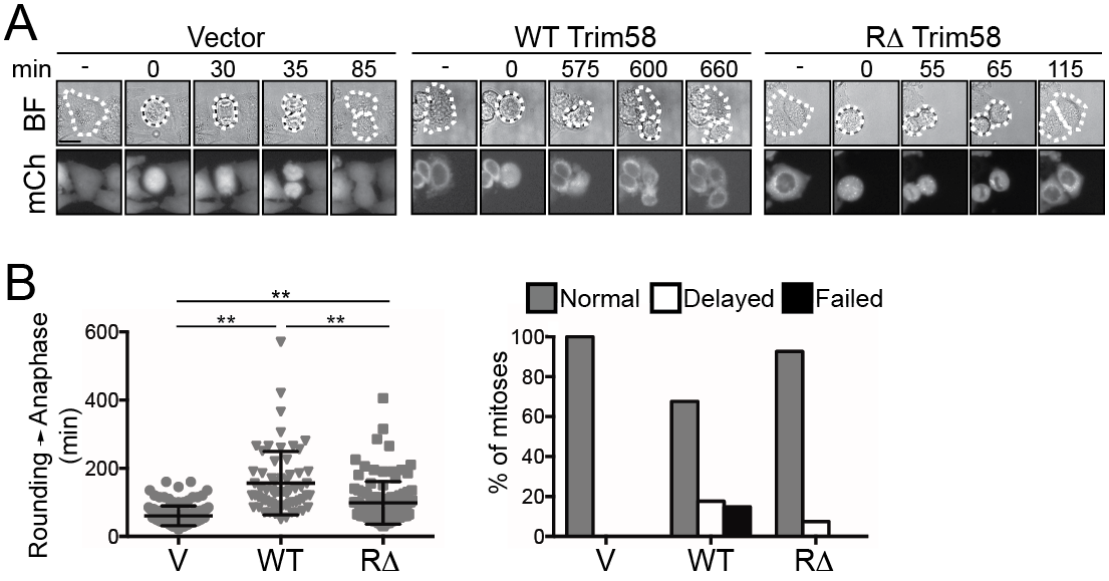

Figure 3.14. Trim58 expression correlates with loss of dynein and enucleation during erythroid maturation. Fetal liver erythroblasts were infected with retrovirus encoding shRNA against (A) luciferase (shLuc) or (B) Trim58 (shRNA #4), cultured in expansion medium for 72 hrs, and shifted to maturation medium at time 0. Whole cell lysates were prepared at the indicated time points and analyzed by Western blotting. A control sample from 44 hrs maturation was run in the lane marked "+" as a positive control for Trim58. (C) Rate of enucleation in cells from panels A and B, determined as shown in Figure 3.4A. The results represent mean ± SD for 4 biological replicates. *$p<0.05$; **$p<0.01$; ns, not significant.

Figure 3.14.

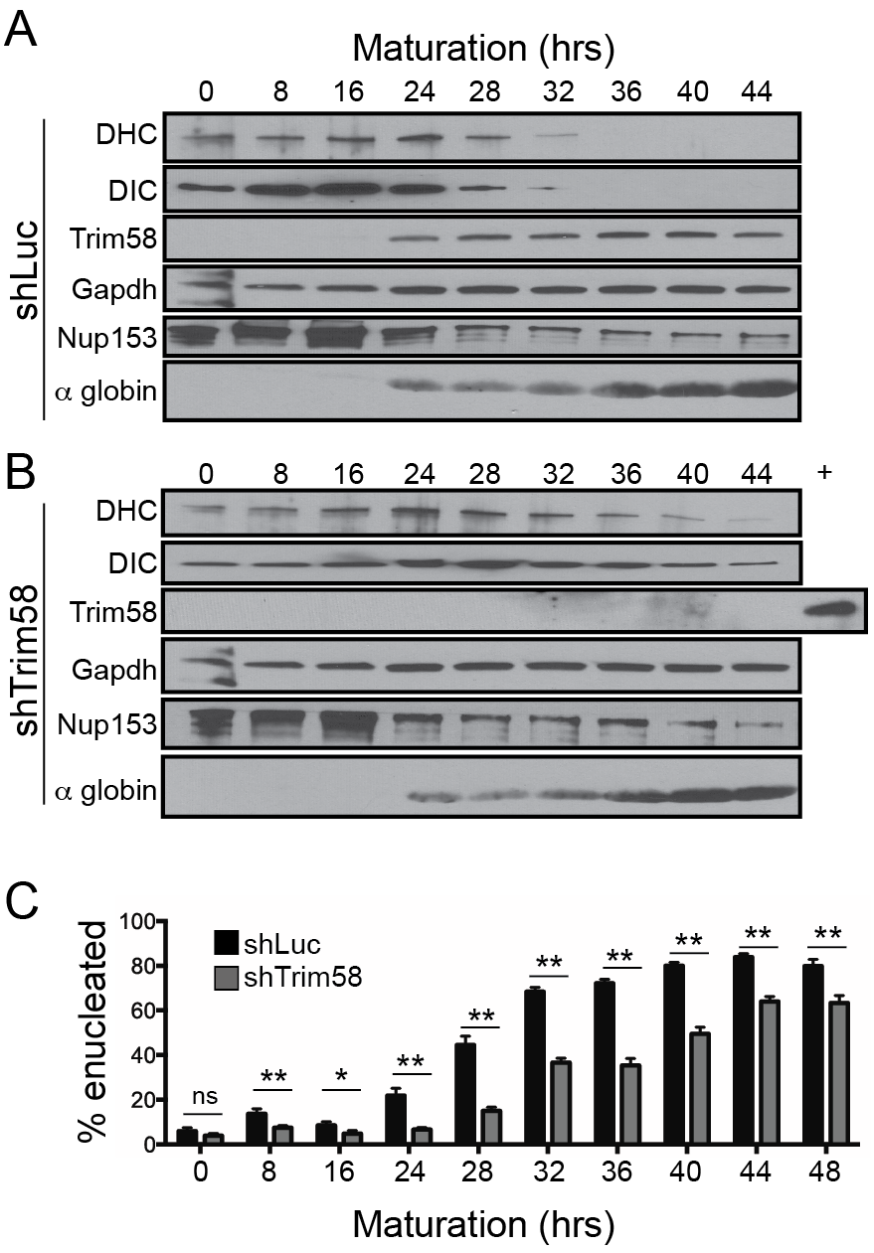
A
Maturation (hrs)
0 8 16 24 28 32 36 40 44
shLuc
DHC
DIC
Trim58
Gapdh
Nup153
α globin
B
0 8 16 24 28 32 36 40 44 +
shTrim58
DHC
DIC
Trim58
Gapdh
Nup153
α globin
C
% enucleated
shLuc
shTrim58
ns
**
*
**
**
**
**
**
**
0 8 16 24 28 32 36 40 44 48
Maturation (hrs)

Figure 3.15. Trim58 deficiency causes aberrant dynein protein retention in late stage erythroblasts. Erythroblast cultures expressing control constructs (Vector, shLuc) or Trim58-directed shRNAs (sh58 #4, sh58 #7) were expanded in puromycin for 72 hrs, then induced to mature for 48 hrs and collected for analysis. (A) Whole cell lysates were analyzed by Western blotting for the indicated proteins. DHC, dynein heavy chain; DIC, dynein intermediate chain. (B) Whole cell lysate cDNA was analyzed by semiquantatitive real time PCR for dynein intermediate chain (*Dync1i2*), dynein heavy chain (*Dync1h1*) and *Trim58*. The y-axis represents mRNA expression level compared to the average value for control-treated samples (Vector, shLuc), which was set at 1. Results represent mean ± SD for 4 biological replicates. **p<0.01; ns, not significant.

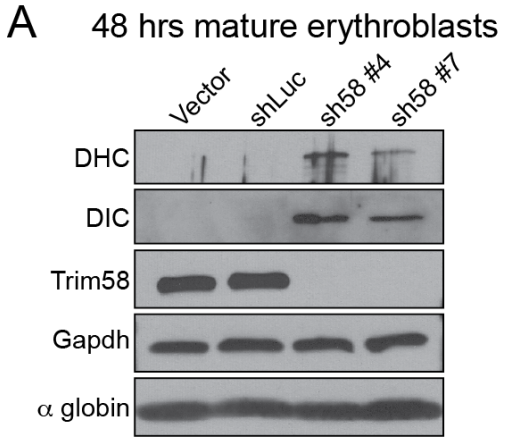

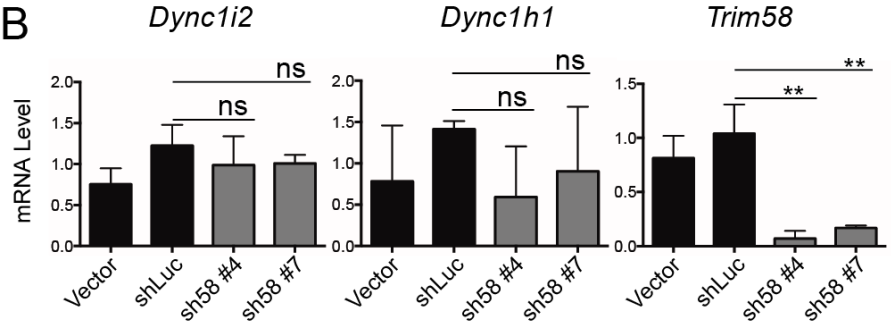

Figure 3.16. Overview of the parameters used to analyze erythroblasts by imaging flow cytometry. (A) Morphology parameters used to assess the steps of erythroblast enucleation during imaging flow cytometry. Nuclear condensation is reflected by reduced nuclear diameter (broken line). The aspect ratio (minor axis (blue line) divided by major axis (red line)) decreases as cells become oblong during nuclear extrusion. The Δ centroid (distance between centers of the nucleus (red) and cytoplasm (green)) increases during nuclear polarization and extrusion. (B) Representative analysis of fetal liver erythroblasts at 36 hrs maturation. Spherical nucleated erythroblasts are pink. Oblong cells extruding their nuclei (decreased aspect ratio and increased Δ centroid) are orange. Cells in late mitosis, visualized to the left of the orange gate, exhibit low aspect ratio and low Δ centroid. (C) Representative images of cells from panel B that are, 1) Spherical with a non-condensed centralized nucleus; 2) spherical with a condensed centralized nucleus; 3) spherical with a condensed polarized nucleus; and 4) oblong with a condensed extruding nucleus.

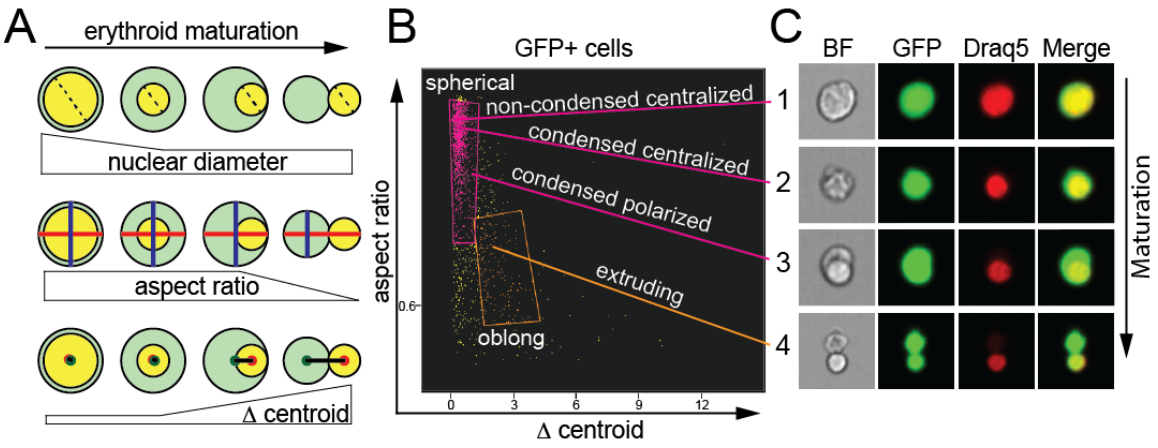

Figure 3.17. Trim58 functions between nuclear condensation and nuclear extrusion during erythroblast enucleation. Erythroblasts expressing GFP and control (shLuc) or Trim58 shRNA #4 were analyzed by imaging flow cytometry at the indicated times during maturation. The results represent mean ± SD for 4 biological replicates, ~3000 cells analyzed per replicate. (A) Plot of the average nuclear diameter, demonstrating condensation over time. (B) Plot of the percent (%) spherical cells, including those that were centralized or polarized. (C) Plot of percent (%) oblong cells with extruding nuclei.

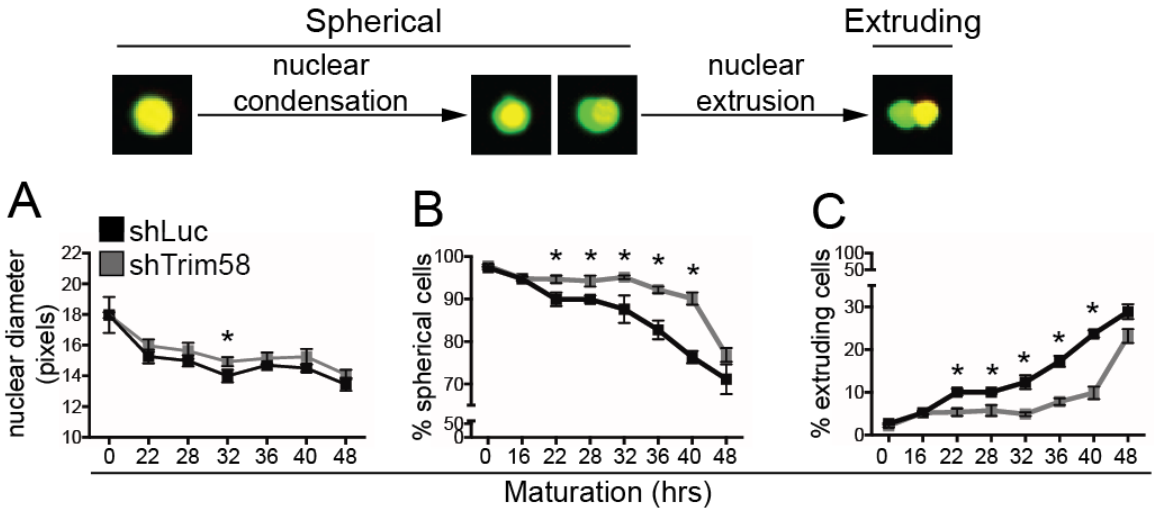

Figure 3.18. Trim58 regulates nuclear polarization during erythroblast enucleation. (A) Δ centroid distribution within spherical erythroblasts depicted in Figure 3.17B. Higher Δ centroid values indicate more polarized nuclei. Representative histograms are shown for three time points. Dashed white bars indicate the mean Δ centroid value for each plot. (B) Quantification of mean Δ centroid values in control (shLuc) or Trim58-deficient (shTrim58 #4) erythroblast maturation cultures. The results represent mean ± SD for 3 biological replicates, ~3000 cells analyzed per replicate. *p<0.05, **p<0.01.

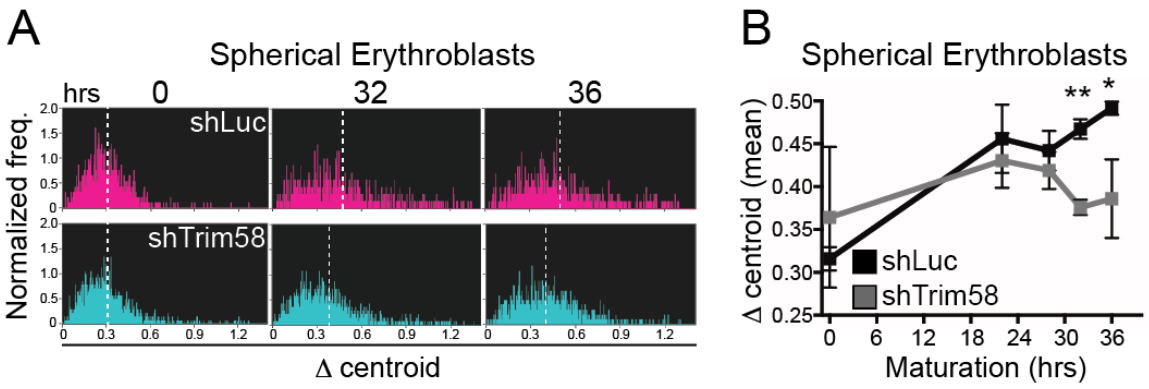

Figure 3.19. Trim58 and an intact microtubule network regulate nuclear polarization. (A) Erythroblast cultures were infected with retrovirus encoding Luciferase- (shLuc) or Trim58-directed shRNA (shTrim58 #4), expanded for 72 hrs in puromycin, then induced to mature for 26 hrs, fixed in paraformaldehyde and analyzed by imaging flow cytometry. In the bottom panel, shLuc-expressing cells were treated with 16 μM nocodazole at 37 °C from 22-26 hrs of maturation. Histograms show Δ centroid distribution within spherical erythroblasts from each treatment condition (see Figure 3.16A). Higher Δ centroid values indicate more polarized nuclei. (B) Mean Δ centroid values for each treatment condition were calculated using the IDEAS software (Amnis) from the histograms in panel A.

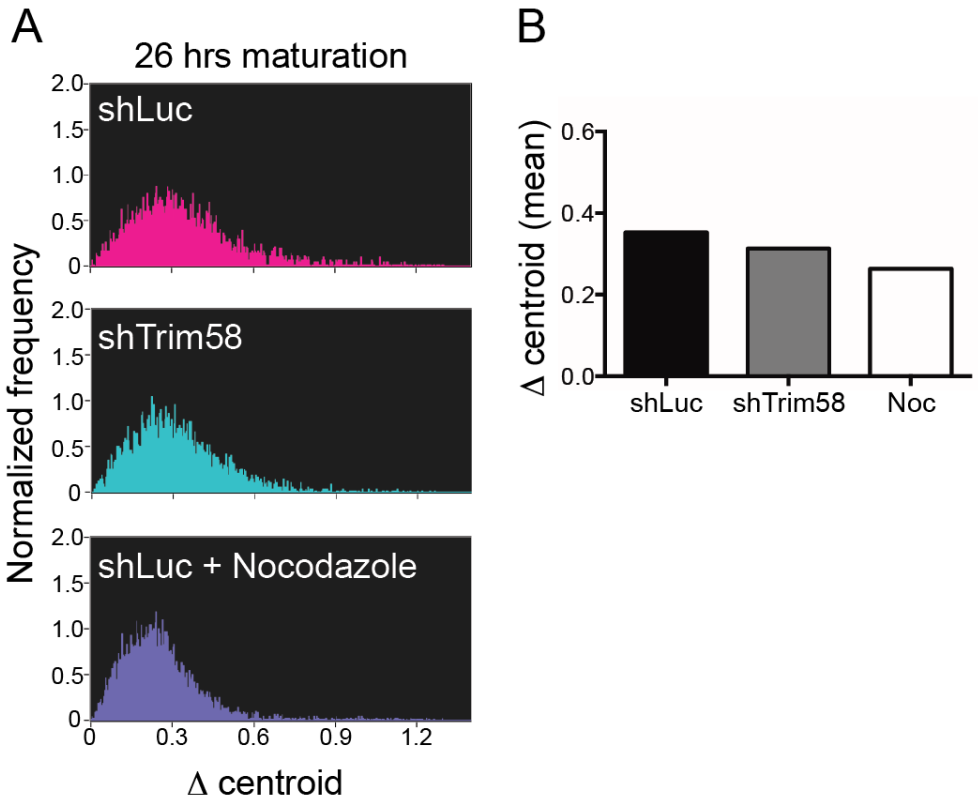

Figure 3.20. Directional nuclear movement during erythroblast enucleation. Primary murine fetal liver erythroblasts were fixed, stained for microtubules (α tubulin, green) and DNA (DAPI, blue), and imaged by deconvolution fluorescent microscopy. Arrow indicates the microtubule organizing center (MTOC). Scale bar, 2 μm.

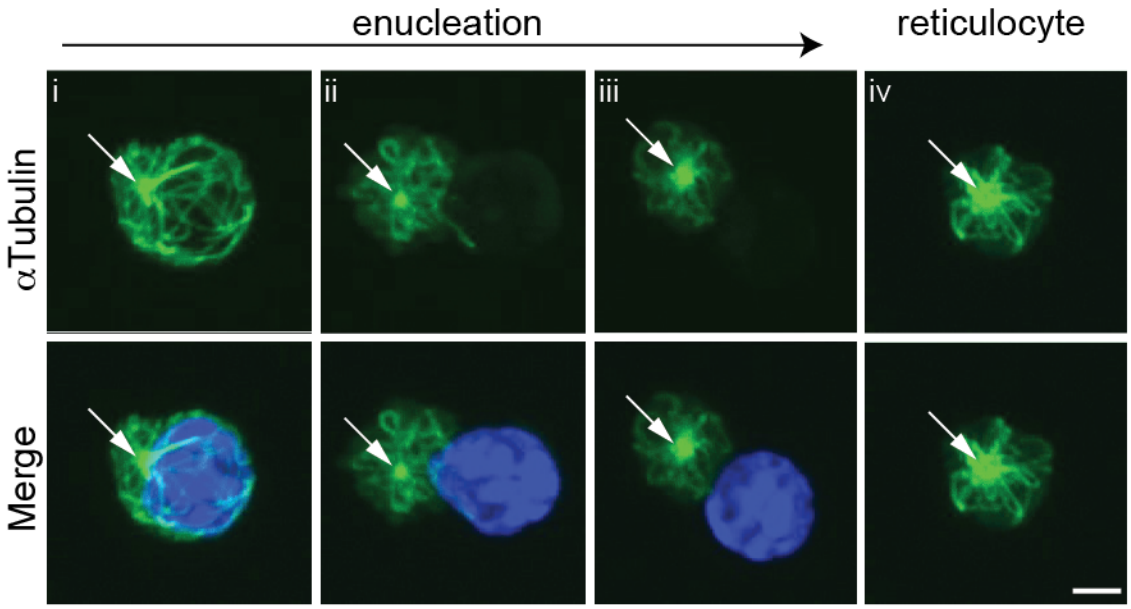

Figure 3.21. Model for the actions of Trim58 during erythroblast enucleation. In early maturation, the nucleus resides within a cage of microtubules (green) and dynein (blue) keeps the nucleus in close proximity to the MTOC (yellow). Induction of Trim58 causes dynein degradation, which may promote nuclear polarization through multiple mechanisms. A microtubule motor imbalance may allow unopposed kinesin molecular motors to polarize the nucleus within a microtubule cage (top) and/or microtubule cage collapse could free the nucleus to polarize. Following polarization and microtubule disassembly, nuclear extrusion occurs.

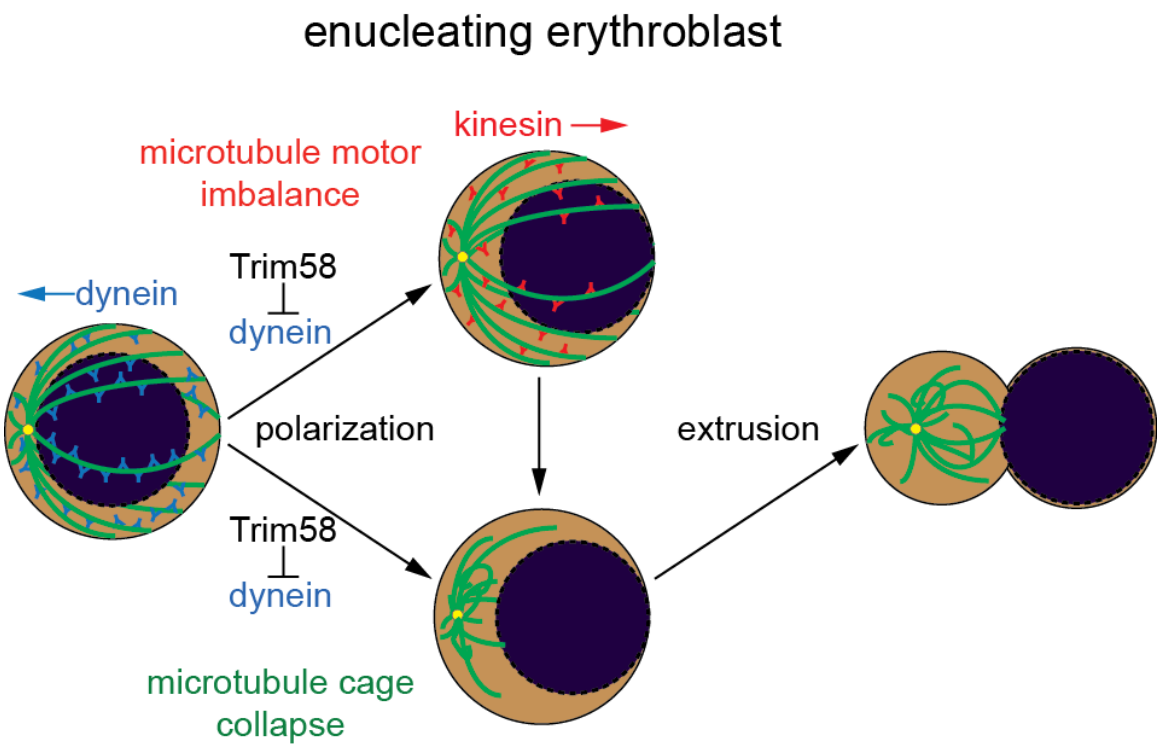

Figure 3.22. Several kinesin family genes are expressed in late erythroblasts. Definitive murine orthochromatic erythroblasts were collected from (A) E14.5 fetal liver or (B) adult bone marrow and FACS-purified. Gene expression in these samples was analyzed by microarray (Kingsley et al., 2013). (C) Gene expression in primary human late (orthochromatic) erythroblasts, cultured from peripheral blood buffy coat mononucleocytes, was analyzed by microarray (Merryweather-Clarke et al., 2011).

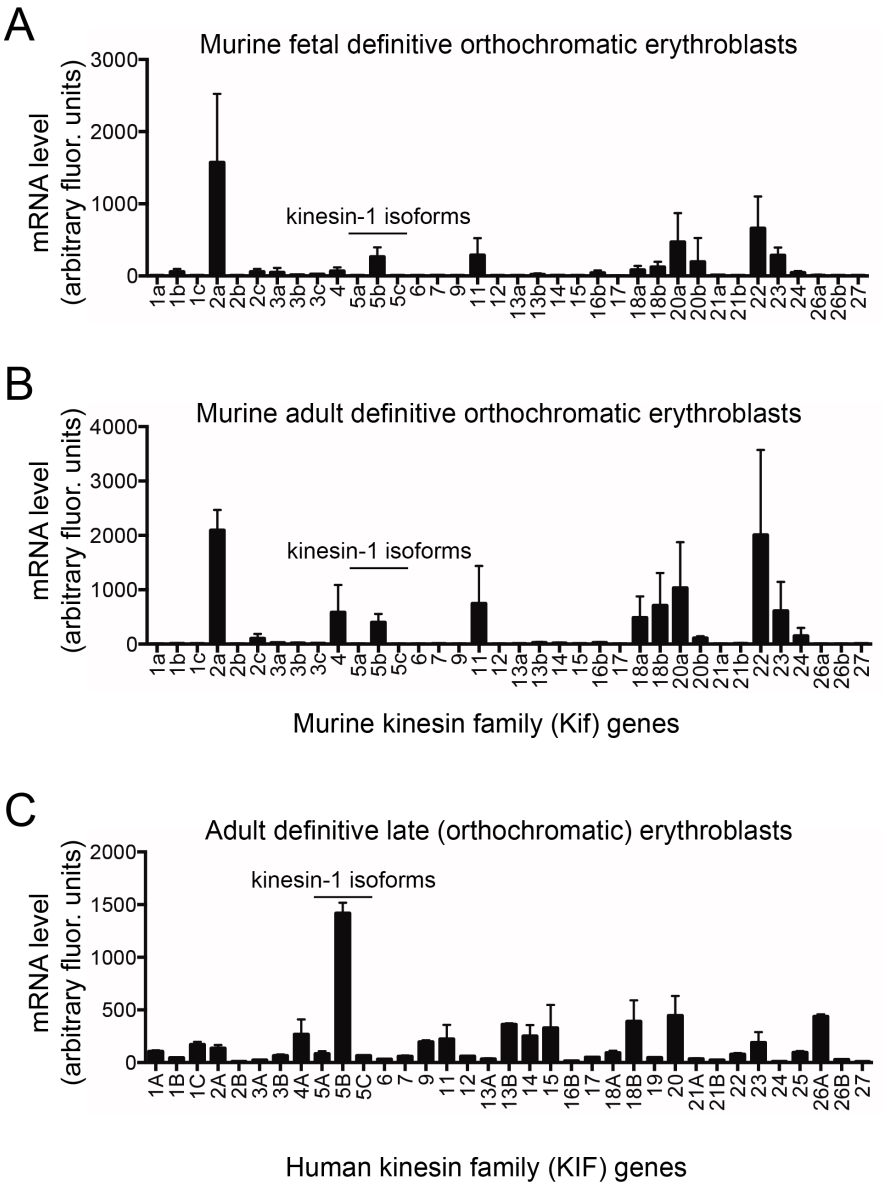

Figure 3.23. Trim58 is expressed in megakaryocytes. (A) Trim58 mRNA levels were analyzed by RNA-Sequencing (RNA-Seq) in megakaryocyte-erythroid progenitor (MEP) cells, erythroblasts (Ery), and megakaryocytes (Mk) (data from Pimkin *et al*, in revision). The mRNA expression is quantitated as FPKM (fragments per kilobase of transcript per million reads). (B) Chromatin immunoprecipitation-sequencing (ChIP-Seq) analysis of transcription factor binding to the *Trim58* locus in primary murine megakaryocytes (data from Pimkin *et al*, in revision). The blue line depicts the *Trim58* gene, with exons shown as rectangles. Transcription factor binding sites are indicated in cyan.

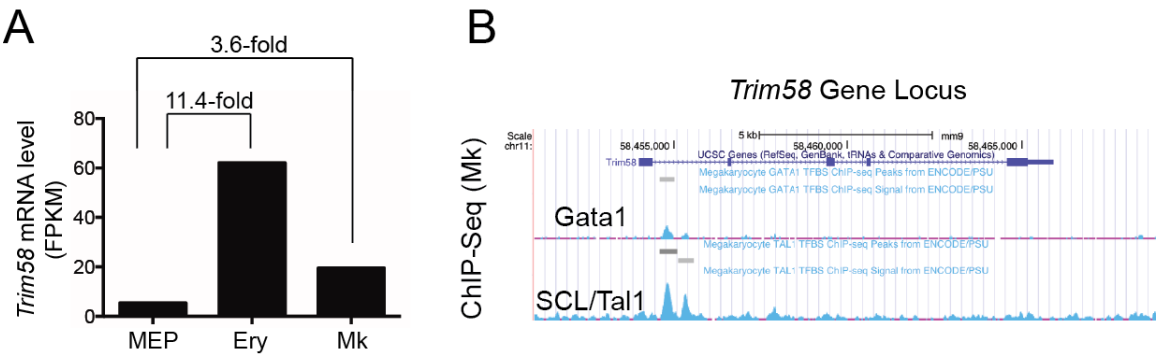

CHAPTER 4:

CONCLUSIONS AND FUTURE DIRECTIONS

Summary statement

Consistent with GWAS that linked *TRIM58* SNPs with altered erythrocyte parameters (Kamatani et al., 2010; van der Harst et al., 2012) and gene expression studies that suggested Trim58 might be active during late erythroid maturation (Figures 3.1 and 3.2), our investigation identified a role for this putative E3 ubiquitin ligase in erythroblast enucleation. Trim58 degrades dynein in temporal correlation with enucleation, whereas Trim58-deficient erythroblasts aberrantly retain dynein and fail to polarize, extrude, or expel their nuclei efficiently. Given the established role for dynein in regulating nuclear positioning (Fridolfsson and Starr, 2010; Splinter et al., 2010; Tanenbaum et al., 2011; Wilson and Holzbaur, 2012) and in preventing microtubule catastrophe at the cell periphery (Hendricks et al., 2012; Moore and Cooper, 2010), as well as studies implicating microtubule-based activities in nuclear polarization and extrusion during erythroblast enucleation (Figures 3.16-3.18 and (Konstantinidis et al., 2012b; Wang et al., 2012)), we propose that Trim58-mediated dynein degradation is responsible for some aspects of nuclear movement during enucleation.

Many questions are raised by our initial characterization of Trim58 biology, including: By what mechanism(s) does Trim58 promote enucleation? What is the role of Trim58 *in vivo*? How does Trim58 deficiency lead to multinuclearity? Does Trim58

function biochemically as an E3 ubiquitin ligase? How do *TRIM58* SNP(s) alter its function? How do other GWAS-identified putative E3 ligases regulate erythropoiesis*?*

Our findings identify a previously unappreciated role for regulated proteolysis in dynein regulation. It is possible that proteasomal degradation regulates dynein activity outside of the erythroid compartment, potentially making our findings broadly applicable for studies of dynein biology. Future studies will address the following questions: Does Trim58 regulate non-erythroid biology? Does regulated proteolysis influence dynein activities in non-erythroid cells?

Ongoing and future studies

By what mechanism(s) does Trim58 promote enucleation?

Our model proposes that Trim58-mediated dynein degradation promotes enucleation by allowing unopposed kinesin(s) to polarize the nucleus and/or by depolymerizing microtubules to free the nucleus for extrusion (Figure 3.21). During erythroid maturation, dynein degradation must be exquisitely timed to promote enucleation without compromising dynein-dependent processes in earlier erythroblasts (Figure 3.14). This complicated our efforts to delineate the mechanism by which dynein promotes enucleation and also prevented us from analyzing whether dynein manipulations rescued enucleation in Trim58-deficient cells. Retroviral introduction of dynein-directed shRNAs or ectopic CC1 expression in cultured erythroblasts caused toxicity in early erythroblasts that precluded reliable analysis.

Rescue of Trim58-deficiency phenotypes will therefore likely require temporal treatment with a small molecule. Treatment with the cell permeable dynein motility inhibitor Ciliobrevin (Firestone et al., 2012) did not rescue enucleation in Trim58-deficient cultures (data not shown), suggesting that tonic motility-independent dynein forces may retain a condensed nucleus in the center of the cell. This is consistent with models in which dynein exerts tonic force on neuronal nuclei through a microtubule cage-like structure (Shu et al., 2004; Tsai et al., 2007; Xie et al., 2003). A similar microtubule structure exists in early erythroblasts (Figure 3.20).

However, temporal dynein inhibition in late stage erythroblasts with CC1 protein should theoretically disengage aberrantly retained dynein from the nucleus in Trim58-deficient cells. This may promote enucleation. We are therefore working to purify recombinant CC1 protein that contains a cell-permeable TAT tag (Wadia and Dowdy, 2002, 2005). This TAT tag allows proteins to enter cells, including erythroblasts (Keerthivasan et al., 2012), via an endocytic process called macropinocytosis (Wadia and Dowdy, 2002, 2005). If successful, the addition of cell permeable CC1 to erythroid cultures could boost enucleation in our studies of Trim58-deficient erythroblasts. It also might augment enucleation in untreated murine erythroblasts. Furthermore, this reagent might promote enucleation in cultured human erythroblasts, which would aid investigations aimed to generate human erythrocytes for transfusion medicine (Migliaccio et al., 2012). Recombinant cell-permeable CC1 protein might also provide an easier alternative to microinjecting CC1 protein, which is a commonly used technique to temporally inhibit dynein activity in large adherent cells (i.e., U2OS or HeLa cells).

To discern whether nuclear polarization and enucleation depend on motor-based nuclear transport and/or microtubule cage collapse (Figure 3.21), we have investigated the effects of kinesin knockdown on enucleation. We hypothesized that Trim58-mediated dynein degradation would allow unopposed kinesin(s) to facilitate nuclear polarization. Although kinesin-1 regulates nuclear movement in multiple organisms and cell types (Fridolfsson and Starr, 2010; Splinter et al., 2010; Wilson and Holzbaur, 2012), our studies did not reveal a role for Kif5b in murine erythroid enucleation. This supports our microtubule cage collapse mechanism for enucleation (Figure 3.21). Alternatively, this could be due to compensation from other kinesin-1 isoforms, or other kinesins that are expressed in late erythroblasts might directly promote nuclear migration (Figures 3.22A and 3.22B).

Other kinesins that are expressed in late erythroblasts might regulate enucleation in different ways (Figures 3.22A and 3.22B). *Kif2a* mRNA is abundant in murine orthochromatic erythroblasts, suggesting that this gene might regulate murine enucleation. Kif2a depolymerizes microtubules (Uehara et al., 2013), and microtubule depolymerization seems to be necessary for nuclear polarization and/or expulsion (Figures 3.20 and 3.21). Kif2a might therefore contribute to the microtubule cage collapse mechanism (Figure 3.21), which is otherwise difficult to investigate experimentally due to its highly temporal nature and the fragility of late erythroblasts in suspension culture. *Kif20a* and *Kif23* are highly expressed in late stage murine erythroblasts (Figures 3.22A and 3.22B). These proteins localize to the central spindle during mitosis and regulate cell division (Hummer and Mayer, 2009; Uehara et al., 2013). Targeted knockdown of *Kif2a*, *Kif20a*, or *Kif23* in erythroblast cultures will determine whether these genes regulate enucleation and/or other aspects of late

erythroblast development. Protein interaction studies will investigate whether these kinesins have erythroid-specific isoforms or binding partners.

Interestingly, the kinesins expressed in mouse and human orthochromatic erythroblasts differ (Figure 3.22). This is consistent with previous observations that many erythroid-specific RNAs are expressed differently in these two species (Paralkar et al., 2014). Whereas *Kif5b* does not stand out as being highly expressed in murine orthochromatic erythroblasts (Figures 3.22A and 3.22B), *KIF5B* is clearly enriched among kinesin genes in late stage human erythroblasts (Figure 3.22C). Thus, *KIF5B* knockdown might inhibit nuclear polarization during enucleation of cultured human CD34+ cells, despite our negative results in murine erythroblast cultures.

In addition to our proposed mechanisms (Figure 3.21), Trim58-mediated dynein proteolysis could promote enucleation via alternative, less well-characterized mechanisms. For example, Trim58-mediated dynein degradation may promote enucleation by inhibiting the dynein light chain Tctex-1, which binds and inactivates the RhoA guanine exchange factor GEF-H1 through holodynein-dependent microtubule recruitment (Meiri et al., 2012). Upon microtubule disassembly, Tctex-1 releases GEF-H1, which in turn promotes GTPase-mediated actin stress fiber formation and actomyosin contractility. Work presented in abstract form suggests that RhoA promotes erythroblast enucleation by stimulating contraction of the actomyosin ring (Konstantinidis et al., 2012a). Thus, Trim58-mediated dynein elimination may facilitate nuclear extrusion by de-repressing GEF-H1, which in turn activates RhoA, a positive regulator of the contractile ring. Pull down assays will examine whether activation of RhoA or its downstream effectors temporally correlates with enucleation and/or Trim58 activity.

Trim58-mediated dynein degradation might also regulate enucleation independent of nuclear movement. For example, lipid raft-containing vesicles are transported in a polarized fashion to the nucleus-reticulocyte boundary to facilitate enucleation (Keerthivasan et al., 2010). Mitochondria are also transported to the nucleus-reticulocyte boundary, although the reason for this is unclear (Simpson and Kling, 1967). The directional movement of these cargoes away from the MTOC is consistent with kinesin-mediated transport. Hence, dynein degradation might facilitate transport by allowing unopposed kinesins to perform this function. Morphologic and immunofluorescence assays will assess whether these cargoes are properly localized in control and late stage Trim58-deficient erythroblasts during enucleation.

Trim58 could also facilitate erythroblast enucleation through interactions with other proteins that we identified in our screen, such as Nup153, Nup50, importin α, and importin β (Table 3.2). Nup153 provides a scaffold that recruits Nup50, importin α, and other factors to the nuclear pore (Makise et al., 2012). Nup153 also regulates mitotic progression (Mackay et al., 2009), which is particularly interesting in light of the fact that enucleation shares many processes with cell division (Keerthivasan et al., 2011; Konstantinidis et al., 2012b). Several studies have shown that dynein is localized to nuclear pores under certain conditions (Bolhy et al., 2011; Hu et al., 2013; Splinter et al., 2010). Nuclear pore complex proteins may recruit Trim58 to the nuclear envelope in order to enhance dynein degradation at this location, which would be particularly important for release of the nucleus during enucleation. Immunofluorescence studies will investigate whether Trim58, NPC proteins, and dynein colocalize at the nuclear envelope during enucleation. However, these studies will first require the generation of a reliable antibody to detect endogenous Trim58 by immunofluorescence assay.

Furthermore, it is possible that Trim58 promotes enucleation through interactions with as-yet-unidentified proteins. RING (Brzovic et al., 2001), BBox (Schweiger and Schneider, 2003; Trockenbacher et al., 2001), and Coiled Coil (CC) (Endo et al., 2012) domains from Trim proteins and other E3 ligases (i.e., BRCA1 and BARD1 (Brzovic et al., 2001)) mediate protein interactions. Proteins that interact with the BBox or CC domains of some Trim proteins are degradation substrates (Endo et al., 2012; Trockenbacher et al., 2001). Immunoprecipitation-mass spectrometry studies utilizing full length Trim58 may identify novel protein interactors. Quantitative approaches (for example, stable isotope labeling by amino acids in cell culture (SILAC) (Geiger et al., 2011)) could also be used to identify Trim58 degradation substrates in HeLa cells ectopically expressing Trim58, or in Trim58-deficient late erythroblasts, compared to controls.

What is the role of Trim58 *in vivo*?

We have recently generated a mouse lacking Trim58 exon 3, which contains the coiled coil region of the Trim58 protein ($Trim58^{CC-/CC-}$). The coiled coil domain is critical for the functions of other Trim proteins (Javanbakht et al., 2006; Reymond, 2001; Streich et al., 2013). Initial erythroid phenotypic analyses in mixed-background knockouts were conducted with Elizabeth Traxler (U. Pennsylvania Perelman School of Medicine Medical Scientist Training Program and Children's Hospital of Philadelphia). These revealed a mild reduction in reticulocyte counts in juvenile mice (~5 weeks old) that resolved by ~16 weeks of age. Recovery from phenylhydrazine-induced hemolytic stress was normal in 12-16 week-old mice. We have not observed defective enucleation in

cultured Trim58$^{CC-/CC-}$ murine erythroblasts, and are currently investigating whether dynein degradation is delayed during maturation of Trim58$^{CC-/CC-}$ erythroblasts.

There are two potential reasons for our negative findings in adult mice. First, it is possible that hypomorphic Trim58$^{CC-/CC-}$ protein is expressed, and that this protein retains some ability to interact and degrade dynein. Indeed, messenger RNA encoding Trim58$^{CC-/CC-}$ is expressed in late erythroblasts, although protein levels were reduced by western blot analysis (data not shown). We will assess whether Trim58$^{CC-/CC-}$ protein binds recombinant purified GST-DIC(1-120) through *in vitro* pull down assays. Ectopic expression of Trim58$^{CC-/CC-}$ in HeLa cells will examine whether the truncated protein can promote dynein degradation. If this protein retains activity, this would be important knowledge for the field as it would go against the prevailing dogma for how Trim proteins function. In this case, we will also consider new strategies to generate true Trim58 knockout mice.

Alternatively, Trim58$^{CC-/CC-}$ mice may indeed be “true knockouts” if this protein is unstable and/or dysfunctional. Compensatory processes in Trim58$^{CC-/CC-}$ cells might therefore be expected to facilitate efficient enucleation of knockout fetal liver erythroblasts. Microarray analysis of late stage murine fetal liver erythroblasts from WT and Trim58$^{CC-/CC-}$ mice might reveal the identities of compensatory genes. Protein interaction and/or proteomic studies in control and Trim58$^{CC-/CC-}$ erythroblasts might also reveal whether other E3 ubiquitin ligases can target dynein for degradation in the absence of Trim58.

Trim58$^{CC-/CC-}$ or other Trim58-knockout mice will help us investigate whether Trim58 influences erythropoiesis outside of its role in enucleation. Most Trim proteins are

thought to regulate innate immunity (Napolitano and Meroni, 2012; Versteeg et al., 2013), commonly by suppressing immune response pathways (see for example (Booth et al., 1998)). Trim58 expression in late erythroblasts may negatively modulate immune signaling. Indeed, nucleated avian and fish erythrocytes play incompletely understood roles in immune response regulation (Morera et al., 2011; Passantino et al., 2007), and late stage nucleated murine erythroblasts were recently shown to have immune-regulatory functions in neonatal mice (Elahi et al., 2013). Given these findings, enucleation could be viewed as a Trim58-mediated immunosuppressive event, since anucleate erythrocytes cannot respond transcriptionally to cytokine signals. Alternatively, Trim58 might regulate immune functions in late stage nucleated erythroblasts. Co-culture of neonatal control or Trim58-deficient late stage erythroblasts with adult immune cells (Elahi et al., 2013) will test whether Trim58 is important for erythroblast-mediated cytokine production and other immune cell responses to bacterial infection.

How does Trim58 deficiency lead to multinuclearity?

Several diseases that affect erythroid development yield multinucleated erythroblasts in the bone marrow, including CDA (Renella and Wood, 2009) and myelodysplastic syndrome (Yoshida, 1996). KIF23, which regulates mitotic progression in many cell types, is the causative gene for CDA type III (Liljeholm et al., 2013b). This finding suggests that defective cell division during terminal erythropoiesis yields multinucleated erythroblasts and underlies at least some aspects of disease pathology (Traxler and Weiss, 2013).

We noted increased multinuclearity in mature Trim58-knockdown erythroblasts (Figure 3.5). Thus, in addition to its role in enucleation, Trim58 might regulate the "normal" cell division(s) during terminal erythropoiesis. Many proteins regulate cytokinesis (Eggert et al., 2006), including Trim58-interactors dynein (Moore and Cooper, 2010) and Nup153 (Mackay et al., 2009). Histologic analysis of bone marrow from $Trim58^{CC-/CC-}$ mice did not demonstrate multinucleate erythroblasts, but as discussed previously this could be the result of retained $Trim58^{CC-/CC-}$ protein activity. Future studies will be aimed at identifying what steps of mitosis, if any, are deregulated in the absence of Trim58 through immunofluorescence and/or time lapse microscopy of developing Trim58-knockdown or Trim58-knockout erythroblasts.

Does Trim58 function biochemically as an E3 ubiquitin ligase?

Ectopic Trim58 expression in HeLa cells causes proteasome-mediated dynein degradation (Figure 3.11). There are multiple mechanisms by which this could occur. Trim58 could facilitate transfer of ubiquitin directly onto bound DIC and/or other dynein subunits. This is the canonical mechanism of action for E3 ubiquitin ligases (Komander, 2009). Alternatively, the interaction between Trim58 and DIC could stimulate Trim58 autoubiquitylation and subsequent translocation of Trim58, DIC, and any other bound proteins to the proteasome for degradation. This is the mechanism by which Trim21 degrades IgG-bound viral particles (Mallery et al., 2010). Denaturing immunoprecipitation experiments using HeLa cells ectopically expressing WT or RING-dead Trim58 protein are currently in progress to answer this question.

The nature of the polyubiquitin chains catalyzed by Trim58 activity will also be interesting to investigate. Polyubiquitin chains formed through linkage at lysine 48 (K48) are typically thought to target substrates for degradation by the 26S proteasome (Komander, 2009). However, several other lysine linkage options exist. These possibilities will be addressed through *in vitro* ubiquitylation experiments utilizing recombinant WT or RING-dead Trim58, purified holodynein and/or DIC truncations as substrates, and commercially available UPS reagents including E1 and E2 enzymes, and ubiquitin variants that contain single lysine mutations (i.e., K48A or K63A). Moreover, some Trim proteins promote transfer of ubiquitin-like moieties, such as SUMO (Chu and Yang, 2011) or ISG15 (Napolitano and Meroni, 2012), onto substrates. We will assess whether Trim58 mediates such activity through *in vitro* and cell-based assays and, if so, to determine the identities of its targets.

How do *TRIM58* SNP(s) alter its function?

TRIM58 single nucleotide polymorphisms (SNPs) have been linked with microcytosis (small erythrocytes) and higher erythrocyte count (van der Harst et al., 2012). It will be interesting and important to identify the causative polymorphism(s). There are no common polymorphisms in gene regulatory regions within linkage disequilibrium of the identified *TRIM58* SNPs (analyzed with the help of Dr. Daniel Bauer, Children's Hospital Boston). However, SNPs within *TRIM58* exons are predicted to cause missense mutations in the resulting protein. For example, the polymorphism rs3811444, which occurs in 20-25% of all chromosomes, causes a T394M mutation in a variable loop within the TRIM58 PRY-SPRY domain. A potentially disruptive missense

mutation at the analogous position in a TRIM20/Pyrin PRY-SPRY loop causes Familial Mediterranean Fever (Booth et al., 1998), although the functions of this mutant protein have not been specifically investigated. Protein interaction studies using a TRIM58 PRY-SPRY domain that contains this missense mutation may reveal defects in its association with DIC or other known interactors (see Tables 3.1 and 3.2).

How do other GWAS-identified E3 ligases regulate erythropoiesis?

GWAS have also linked SNPs associated with several other putative and validated E3 ligases with altered erythrocyte parameters (Kamatani et al., 2010; Nuinoon et al., 2009; Soranzo et al., 2009; van der Harst et al., 2012). The work in this thesis demonstrates that functional follow-up studies on GWAS hits can elucidate novel and interesting biology (see for example (Sankaran et al., 2012)). Studies of other E3 ligases implicated in regulating erythrocyte parameters might elucidate new and exciting aspects of erythroid biology.

Does Trim58 regulate non-erythroid biology?

A *TRIM58* SNP has been associated with altered platelet count (Gieger et al., 2011), implicating TRIM58 in megakaryocyte development and/or platelet formation. Megakaryocyte development involves endomitosis, which entails DNA replication without cell division, and later the elaboration of long tubular cytoplasmic protrusions called proplatelets (Italiano et al., 2007). Proplatelets ultimately separate from the megakaryocyte and undergo further maturation into platelets. The cellular and molecular basis for proplatelet formation is not well understood (Italiano et al., 2007).

Proplatelets use bipolar microtubule arrays to elongate from differentiated megakaryocytes (Patel et al., 2005). Rather than strict addition of tubulin subunits to growing microtubules, this occurs in part via dynein-dependent sliding of antiparallel microtubules (Patel et al., 2005). Trim58-mediated effects on dynein might regulate this process. Given that dynein has been implicated in microtubule sliding dynamics during proplatelet production, Trim58-mediated dynein degradation might inhibit sliding to signal completion of proplatelet elongation and/or instigate proplatelet separation from megakaryocyte.

Trim58 could also influence platelet maturation from proplatelets. While proteomic studies indicate that both dynein and TRIM58 protein are retained in mature platelets (Burkhart et al., 2012), immunofluorescence images demonstrate that the levels of dynein are substantially lower in platelets versus proplatelets (Patel et al., 2005). Platelets contain 0.8 μg dynein per gram of tissue (Rothwell and Calvert, 1997). This is ~30% of the dynein levels found in neurons (Paschal and Vallee, 1987; Schnapp and Reese, 1989). This could indicate that TRIM58 degrades some, but not all dynein in proplatelets. Consistent with this hypothesis, *Trim58* mRNA is induced ~3.6-fold versus megakaryocyte-erythroid precursors during megakaryopoiesis (Figure 3.23). This is decreased compared with the 11.4-fold induction seen during erythropoiesis, which is associated with complete dynein loss.

TRIM58 might also regulate aspects of platelet function. Platelet activation causes dynein redistribution from soluble cytoplasmic granules to an insoluble, perhaps microtubule-associated fraction by immunofluorescence and sedimentation assays (Rothwell and Calvert, 1997). Murine fetal liver megakaryocyte cultures treated with

control or Trim58-directed shRNAs will be used to assess proplatelet elongation, platelet formation, and/or platelet function by time-lapse microscopy, immunofluorescence, and Immunoprecipitation assays.

It is also possible that transient or low-level Trim58 expression regulates biological processes outside of hematopoiesis. For example, in keeping with an immunomodulatory role for Trim proteins (Napolitano and Meroni, 2012; Versteeg et al., 2013), it is possible that Trim58 is upregulated in response to viral infection and/or interferon signaling. In fact, ectopically expressed Trim58 enhanced nuclear factor kappa-light-chain-enhancer of activated B cells (NF-κB) and interferon β (IFNβ) signaling in HEK293T cells, and Trim58 knockdown interfered with the latter upon viral infection (Versteeg et al., 2013). Interestingly, dynein mediates retroviral integration (Bremner et al., 2009), and microtubule depolymerization, dynein, and dynactin can regulate NF-κB signaling (Rosette and Karin, 1995; Shrum et al., 2009). It is possible that acute Trim58 induction may transiently degrade dynein to prevent retroviral integration without adversely affecting cell viability. Furthermore, Trim58 might competitively inhibit viral association with dynein, since Trim58 and adenoviral hexon both interact with a similar region on DIC (Bremner et al., 2009). HeLa cells infected with virus and/or treated with interferon will be used to assess endogenous Trim58 induction under these conditions. If this proves true, it would provide a more rapid and facile system in which to study endogenous Trim58 functions compared to our current fetal liver erythroblast culture model. Further studies would examine Trim58-mediated dynein ubiquitylation and/or proteolysis in response to viral infection, and also biochemically investigate whether Trim58 competitively inhibits viral binding to DIC using purified proteins.

Does regulated proteolysis influence dynein activities in non-erythroid cells?

Although this thesis has focused primarily on the role of Trim58, our studies have uncovered new and interesting aspects of dynein biology. With the exception of late stage erythroid cells, dynein is expressed in all mammalian cell types. This makes our findings potentially relevant for many aspects of cell biology, since dynein proteolysis would be expected to potently regulate cell division, intracellular transport, and cell migration. Notably, Trim58 need not be expressed in these cells, as alternative dynein-specific E3 ligases might exist. In fact, other Trim proteins might function in this way. Trim5α colocalizes with dynein by immunofluorescence (Diaz-Griffero et al., 2006) and Trim50 promotes PI3K-dependent gastric vesicle secretion (a plus end-directed process, directionally consistent with nuclear movement during erythroid enucleation) (Nishi et al., 2012). An initial screen for dynein ubiquitylation in several different tissue types may reveal the generality of this mechanism, and protein interaction studies may reveal other E3 ligases that facilitate dynein ubiquitylation. The results could impact our understanding of tissue development, neurodegenerative diseases, oncogenesis and metastasis.

BIBLIOGRAPHY

Alkuraya, F.S., Cai, X., Emery, C., Mochida, G.H., Al-Dosari, M.S., Felie, J.M., Hill, R.S., Barry, B.J., Partlow, J.N., Gascon, G.G.*, et al.* (2011). Human mutations in NDE1 cause extreme microcephaly with lissencephaly. Am J Hum Genet *88*, 536-547.

Allan, V.J. (2011). Cytoplasmic dynein. Biochem Soc Trans *39*, 1169-1178.

Anstee, D.J., Gampel, A., and Toye, A.M. (2012). Ex-vivo generation of human red cells for transfusion. Curr Opin Hematol *19*, 163-169.

Arnaud, L., Saison, C., Helias, V., Lucien, N., Steschenko, D., Giarratana, M.C., Prehu, C., Foliguet, B., Montout, L., de Brevern, A.G.*, et al.* (2010). A dominant mutation in the gene encoding the erythroid transcription factor KLF1 causes a congenital dyserythropoietic anemia. Am J Hum Genet *87*, 721-727.

Asthana, J., Kuchibhatla, A., Jana, S.C., Ray, K., and Panda, D. (2012). Dynein light chain 1 (LC8) association enhances microtubule stability and promotes microtubule bundling. J Biol Chem *287*, 40793-40805.

Bakkaloglu, A. (2003). Familial Mediterranean fever. Pediatr Nephrol *18*, 853-859.

Balarajan, Y., Ramakrishnan, U., Ozaltin, E., Shankar, A.H., and Subramanian, S.V. (2011). Anaemia in low-income and middle-income countries. Lancet *378*, 2123-2135.

Bard, H., Rosenberg, A., and Huisman, T.H. (1998). Hemoglobinopathies affecting maternal-fetal oxygen gradient during pregnancy: molecular, biochemical and clinical studies. Am J Perinatol *15*, 389-393.

Barr, F.A., and Gruneberg, U. (2007). Cytokinesis: placing and making the final cut. Cell *131*, 847-860.

Bement, W.M., Benink, H.A., and von Dassow, G. (2005). A microtubule-dependent zone of active RhoA during cleavage plane specification. J Cell Biol *170*, 91-101.

Billat, J.N. (1974). [The erythroblast island, an anatomic unit of the hematopoietic tissue of fetal rat liver]. Archives d'anatomie microscopique et de morphologie experimentale *63*, 147-161.

Bingham, J.B., King, S.J., and Schroer, T.A. (1998). Purification of dynactin and dynein from brain tissue. Methods Enzymol *298*, 171-184.

Boehm, D., Mazurier, C., Giarratana, M.C., Darghouth, D., Faussat, A.M., Harmand, L., and Douay, L. (2013). Caspase-3 is involved in the signalling in erythroid differentiation by targeting late progenitors. PLoS ONE *8*, e62303.

Bolhy, S., Bouhlel, I., Dultz, E., Nayak, T., Zuccolo, M., Gatti, X., Vallee, R., Ellenberg, J., and Doye, V. (2011). A Nup133-dependent NPC-anchored network tethers centrosomes to the nuclear envelope in prophase. J Cell Biol *192*, 855-871.

Booth, D.R., Gillmore, J.D., Booth, S.E., Pepys, M.B., and Hawkins, P.N. (1998). Pyrin/marenostrin mutations in familial Mediterranean fever. QJM *91*, 603-606.

Boylan, J.W., Van Liew, J.B., and Feig, P.U. (1991). Inverse changes in erythroid cell volume and number regulate the hematocrit in newborn genetically hypertensive rats. Proc Natl Acad Sci U.S.A. *88*, 9848-9852.

Bremner, K.H., Scherer, J., Yi, J., Vershinin, M., Gross, S.P., and Vallee, R.B. (2009). Adenovirus transport via direct interaction of cytoplasmic dynein with the viral capsid hexon subunit. Cell Host Microbe *6*, 523-535.

Brzovic, P.S., Rajagopal, P., Hoyt, D.W., King, M.C., and Klevit, R.E. (2001). Structure of a BRCA1-BARD1 heterodimeric RING-RING complex. Nat Struct Biol *8*, 833-837.

Burgess, S.A., Walker, M.L., Sakakibara, H., Knight, P.J., and Oiwa, K. (2003). Dynein structure and power stroke. Nature *421*, 715-718.

Burgess, S.A., Walker, M.L., Sakakibara, H., Oiwa, K., and Knight, P.J. (2004). The structure of dynein-c by negative stain electron microscopy. J Struct Biol *146*, 205-216.

Burkhart, J.M., Vaudel, M., Gambaryan, S., Radau, S., Walter, U., Martens, L., Geiger, J., Sickmann, A., and Zahedi, R.P. (2012). The first comprehensive and quantitative analysis of human platelet protein composition allows the comparative analysis of structural and functional pathways. Blood *120*, e73-82.

Cammas, F., Khetchoumian, K., Chambon, P., and Losson, R. (2012). TRIM involvement in transcriptional regulation. Adv Expt Med Biol *770*, 59-76.

Campbell, A.E., Wilkinson-White, L., Mackay, J.P., Matthews, J.M., and Blobel, G.A. (2013). Analysis of disease-causing GATA1 mutations in murine gene complementation systems. Blood *121*, 5218-5227.

Carlile, G.W., Smith, D.H., and Wiedmann, M. (2004). Caspase-3 has a nonapoptotic function in erythroid maturation. Blood *103*, 4310-4316.

Carter, A.P. (2013). Crystal clear insights into how the dynein motor moves. J Cell Sci *126*, 705-713.
Carter, A.P., Cho, C., Jin, L., and Vale, R.D. (2011). Crystal structure of the dynein motor domain. Science *331*, 1159-1165.
Chatel, G., and Fahrenkrog, B. (2011). Nucleoporins: leaving the nuclear pore complex for a successful mitosis. Cell Signal *23*, 1555-1562.
Chen, C.Y., Pajak, L., Tamburlin, J., Bofinger, D., and Koury, S.T. (2002). The effect of proteasome inhibitors on mammalian erythroid terminal differentiation. Exp Hematol *30*, 634-639.
Chen, K., Liu, J., Heck, S., Chasis, J.A., An, X., and Mohandas, N. (2009). Resolving the distinct stages in erythroid differentiation based on dynamic changes in membrane protein expression during erythropoiesis. Proc Natl Acad Sci U S A *106*, 17413-17418.
Cheng, Y., Wu, W., Kumar, S.A., Yu, D., Deng, W., Tripic, T., King, D.C., Chen, K.B., Zhang, Y., Drautz, D.*, et al.* (2009). Erythroid GATA1 function revealed by genome-wide analysis of transcription factor occupancy, histone modifications, and mRNA expression. Genome Res *19*, 2172-2184.
Cho, C., and Vale, R.D. (2012). The mechanism of dynein motility: insight from crystal structures of the motor domain. Biochim Biophys Acta *1823*, 182-191.
Chu, Y., and Yang, X. (2011). SUMO E3 ligase activity of TRIM proteins. Oncogene *30*, 1108-1116.
Chuang, J.Z., Yeh, T.Y., Bollati, F., Conde, C., Canavosio, F., Caceres, A., and Sung, C.H. (2005). The dynein light chain Tctex-1 has a dynein-independent role in actin remodeling during neurite outgrowth. Dev Cell *9*, 75-86.
Ciechanover, A., Hod, Y., and Hershko, A. (1978). A heat-stable polypeptide component of an ATP-dependent proteolytic system from reticulocytes. Biochem Biophys Res Commun *81*, 1100-1105.
Cohen, W.D., and Terwilliger, N.B. (1979). Marginal bands in camel erythrocytes. J Cell Sci *36*, 97-107.
Collins, E.S., Balchand, S.K., Faraci, J.L., Wadsworth, P., and Lee, W.-L. (2012). Cell cycle-regulated cortical dynein/dynactin promotes symmetric cell division by differential pole motion in anaphase. Mol Biol Cell *23*, 3380-3390.

Coulombel, L., Tchernia, G., and Mohandas, N. (1979). Human reticulocyte maturation and its relevance to erythropoietic stress. J Lab Clin Med *94*, 467-474.
D'Avino, P.P., Savoian, M.S., and Glover, D.M. (2005). Cleavage furrow formation and ingression during animal cytokinesis: a microtubule legacy. J Cell Sci *118*, 1549-1558.
D'Cruz, A.A., Kershaw, N.J., Chiang, J.J., Wang, M.K., Nicola, N.A., Babon, J.J., Gack, M.U., and Nicholson, S.E. (2013). Crystal Structure of the TRIM25 B30.2 (PRYSPRY) domain: A Key Component of Antiviral Signaling. Biochem J *456,* 231-240.
Da Costa, L., Galimand, J., Fenneteau, O., and Mohandas, N. (2013). Hereditary spherocytosis, elliptocytosis, and other red cell membrane disorders. Blood Rev *27*, 167-178.
De Maria, R., Zeuner, A., Eramo, A., Domenichelli, C., Bonci, D., Grignani, F., Srinivasula, S.M., Alnemri, E.S., Testa, U., and Peschle, C. (1999). Negative regulation of erythropoiesis by caspase-mediated cleavage of GATA-1. Nature *401*, 489-493.
Deng, W., Lee, J., Wang, H., Miller, J., Reik, A., Gregory, P.D., Dean, A., and Blobel, G.A. (2012). Controlling long-range genomic interactions at a native locus by targeted tethering of a looping factor. Cell *149*, 1233-1244.
Deshaies, R.J., and Joazeiro, C.A.P. (2009). RING domain E3 ubiquitin ligases. Annu Rev Biochem *78*, 399-434.
Dgany, O., Avidan, N., Delaunay, J., Krasnov, T., Shalmon, L., Shalev, H., Eidelitz-Markus, T., Kapelushnik, J., Cattan, D., Pariente, A.*, et al.* (2002). Congenital dyserythropoietic anemia type I is caused by mutations in codanin-1. Am J Hum Genet *71*, 1467-1474.
Diaz-Griffero, F., Li, X., Javanbakht, H., Song, B., Welikala, S., Stremlau, M., and Sodroski, J. (2006). Rapid turnover and polyubiquitylation of the retroviral restriction factor TRIM5. Virology *349*, 300-315.
Dikic, I., and Robertson, M. (2012). Ubiquitin ligases and beyond. BMC Biol *10*, 22.
Dirlam, A., Spike, B.T., and Macleod, K.F. (2007). Deregulated E2f-2 underlies cell cycle and maturation defects in retinoblastoma null erythroblasts. Mol Cell Biol *27*, 8713-8728.
Dolznig, H., Bartunek, P., Nasmyth, K., Mullner, E.W., and Beug, H. (1995). Terminal differentiation of normal chicken erythroid progenitors: shortening of G1 correlates with loss of D-cyclin/cdk4 expression and altered cell size control. Cell Growth Differ *6*, 1341-1352.

Duden, R. (2001). A motor goes mitotic and divorces the Golgi complex. Trends Cell Biol *11*, 13.

Dujardin, D.L., Barnhart, L.E., Stehman, S.A., Gomes, E.R., Gundersen, G.G., and Vallee, R.B. (2003). A role for cytoplasmic dynein and LIS1 in directed cell movement. J Cell Biol *163*, 1205-1211.

Dzierzak, E., and Philipsen, S. (2013). Erythropoiesis: development and differentiation. Cold Spring Harb Perspect Med *3*, a011601.

Echard, A., Jollivet, F., Martinez, O., Lacapere, J.J., Rousselet, A., Janoueix-Lerosey, I., and Goud, B. (1998). Interaction of a Golgi-associated kinesin-like protein with Rab6. Science *279*, 580-585.

Eggert, U.S., Mitchison, T.J., and Field, C.M. (2006). Animal cytokinesis: from parts list to mechanisms. Annu Rev Biochem *75*, 543-566.

Eitan, A., Aloni, B., and Livne, A. (1976). Unique properties of the camel erythrocyte membrane, II. Organization of membrane proteins. Biochim Biophys Acta *426*, 647-658.

Elahi, S., Ertelt, J.M., Kinder, J.M., Jiang, T.T., Zhang, X., Xin, L., Chaturvedi, V., Strong, B.S., Qualls, J.E., Steinbrecher, K.A*., et al.* (2013). Immunosuppressive CD71 erythroid cells compromise neonatal host defence against infection. Nature (in press)

Endo, H., Ikeda, K., Urano, T., Horie-Inoue, K., and Inoue, S. (2012). Terf/TRIM17 stimulates degradation of kinetochore protein ZWINT and regulates cell proliferation. J Biochem *151*, 139-144.

Eshel, D., Urrestarazu, L.A., Vissers, S., Jauniaux, J.C., van Vliet-Reedijk, J.C., Planta, R.J., and Gibbons, I.R. (1993). Cytoplasmic dynein is required for normal nuclear segregation in yeast. Proc Natl Acad Sci U S A *90*, 11172-11176.

Etlinger, J.D., and Goldberg, A.L. (1977). A soluble ATP-dependent proteolytic system responsible for the degradation of abnormal proteins in reticulocytes. Proc Natl Acad Sci. U S A *74*, 54-58.

Fabrini, R., De Luca, A., Stella, L., Mei, G., Orioni, B., Ciccone, S., Federici, G., Lo Bello, M., and Ricci, G. (2009). Monomer-dimer equilibrium in glutathione transferases: a critical re-examination. Biochemistry *48*, 10473-10482.

Faulkner, N.E., Dujardin, D.L., Tai, C.Y., Vaughan, K.T., O'Connell, C.B., Wang, Y., and Vallee, R.B. (2000). A role for the lissencephaly gene LIS1 in mitosis and cytoplasmic dynein function. Nat Cell Biol *2*, 784-791.

Fededa, J.P., and Gerlich, D.W. (2012). Molecular control of animal cell cytokinesis. Nat Cell Biol *14*, 440-447.
Firestone, A.J., Weinger, J.S., Maldonado, M., Barlan, K., Langston, L.D., O'Donnell, M., Gelfand, V.I., Kapoor, T.M., and Chen, J.K. (2012). Small-molecule inhibitors of the AAA+ ATPase motor cytoplasmic dynein. Nature *484*, 125-129.
Fraser, S.T., Isern, J., and Baron, M.H. (2007). Maturation and enucleation of primitive erythroblasts during mouse embryogenesis is accompanied by changes in cell-surface antigen expression. Blood *109*, 343-352.
Fridolfsson, H.N., and Starr, D.A. (2010). Kinesin-1 and dynein at the nuclear envelope mediate the bidirectional migrations of nuclei. J Cell Biol *191*, 115-128.
Gaehtgens, P., Schmidt, F., and Will, G. (1981a). Comparative rheology of nucleated and non-nucleated red blood cells. I. Microrheology of avian erythrocytes during capillary flow. Pflugers Arch *390*, 278-282.
Gaehtgens, P., Will, G., and Schmidt, F. (1981b). Comparative rheology of nucleated and non-nucleated red blood cells. II. Rheological properties of avian red cells suspensions in narrow capillaries. Pflugers Arch *390*, 283-287.
Ganesh, S.K., Zakai, N.A., van Rooij, F.J.A., Soranzo, N., Smith, A.V., Nalls, M.A., Chen, M.-H., Kottgen, A., Glazer, N.L., Dehghan, A*., et al.* (2009). Multiple loci influence erythrocyte phenotypes in the CHARGE Consortium. Nat Genet *41*, 1191-1198.
Gee, M.A., Heuser, J.E., and Vallee, R.B. (1997). An extended microtubule-binding structure within the dynein motor domain. Nature *390*, 636-639.
Geiger, T., Wisniewski, J.R., Cox, J., Zanivan, S., Kruger, M., Ishihama, Y., and Mann, M. (2011). Use of stable isotope labeling by amino acids in cell culture as a spike-in standard in quantitative proteomics. Nat Protoc *6*, 147-157.
Gerdes, J.M., Davis, E.E., and Katsanis, N. (2009). The vertebrate primary cilium in development, homeostasis, and disease. Cell *137*, 32-45.
Gibbons, I.R., and Rowe, A.J. (1965). Dynein: A Protein with Adenosine Triphosphatase Activity from Cilia. Science *149*, 424-426.
Gieger, C., Radhakrishnan, A., Cvejic, A., Tang, W., Porcu, E., Pistis, G., Serbanovic-Canic, J., Elling, U., Goodall, A.H., Labrune, Y*., et al.* (2011). New gene functions in megakaryopoiesis and platelet formation. Nature *480*, 201-208.

Gifford, S.C., Derganc, J., Shevkoplyas, S.S., Yoshida, T., and Bitensky, M.W. (2006). A detailed study of time-dependent changes in human red blood cells: from reticulocyte maturation to erythrocyte senescence. Br J Haematol *135*, 395-404.
Glotzer, M. (2005). The molecular requirements for cytokinesis. Science *307*, 1735-1739.
Goodman, S.R., Kurdia, A., Ammann, L., Kakhniashvili, D., and Daescu, O. (2007). The human red blood cell proteome and interactome. Exp Biol Med (Maywood) *232*, 1391-1408.
Grebien, F., Dolznig, H., Beug, H., and Mullner, E.W. (2005). Cell size control: new evidence for a general mechanism. Cell Cycle *4*, 418-421.
Grigoryev, S.A., Solovieva, V.O., Spirin, K.S., and Krasheninnikov, I.A. (1992). A novel nonhistone protein (MENT) promotes nuclear collapse at the terminal stage of avian erythropoiesis. Exp Cell Res *198*, 268-275.
Gundersen, G.G., and Worman, H.J. (2013). Nuclear positioning. Cell *152*, 1376-1389.
Hammesfahr, B., and Kollmar, M. (2012). Evolution of the eukaryotic dynactin complex, the activator of cytoplasmic dynein. BMC Evol Biol *12*, 95.
Hammond, J.W., Cai, D., Blasius, T.L., Li, Z., Jiang, Y., Jih, G.T., Meyhofer, E., and Verhey, K.J. (2009). Mammalian Kinesin-3 motors are dimeric in vivo and move by processive motility upon release of autoinhibition. PLoS Biol *7*, e72.
Hanspal, M., and Hanspal, J.S. (1994). The association of erythroblasts with macrophages promotes erythroid proliferation and maturation: a 30-kD heparin-binding protein is involved in this contact. Blood *84*, 3494-3504.
Hanspal, M., Smockova, Y., and Uong, Q. (1998). Molecular identification and functional characterization of a novel protein that mediates the attachment of erythroblasts to macrophages. Blood *92*, 2940-2950.
Harms, M.B., Ori-McKenney, K.M., Scoto, M., Tuck, E.P., Bell, S., Ma, D., Masi, S., Allred, P., Al-Lozi, M., Reilly, M.M.*, et al.* (2012). Mutations in the tail domain of DYNC1H1 cause dominant spinal muscular atrophy. Neurology *78*, 1714-1720.
Hatakeyama, S. (2011). TRIM proteins and cancer. Nat Rev Cancer *11*, 792-804.
Hawkey, C.M., Bennett, P.M., Gascoyne, S.C., Hart, M.G., and Kirkwood, J.K. (1991). Erythrocyte size, number and haemoglobin content in vertebrates. Br J Haematol *77*, 392-397.

Hebbar, S., Mesngon, M.T., Guillotte, A.M., Desai, B., Ayala, R., and Smith, D.S. (2008). Lis1 and Ndel1 influence the timing of nuclear envelope breakdown in neural stem cells. J Cell Biol *182*, 1063-1071.

Hemann, M.T., Fridman, J.S., Zilfou, J.T., Hernando, E., Paddison, P.J., Cordon-Cardo, C., Hannon, G.J., and Lowe, S.W. (2003). An epi-allelic series of p53 hypomorphs created by stable RNAi produces distinct tumor phenotypes in vivo. Nat Genet *33*, 396-400.

Hendricks, A.G., Lazarus, J.E., Perlson, E., Gardner, M.K., Odde, D.J., Goldman, Y.E., and Holzbaur, E.L. (2012). Dynein tethers and stabilizes dynamic microtubule plus ends. Curr Biol *22*, 632-637.

Hendricks, A.G., Perlson, E., Ross, J.L., Schroeder, H.W., 3rd, Tokito, M., and Holzbaur, E.L. (2010). Motor coordination via a tug-of-war mechanism drives bidirectional vesicle transport. Curr Biol *20*, 697-702.

Hershko, A., Heller, H., Elias, S., and Ciechanover, A. (1983). Components of ubiquitin-protein ligase system. Resolution, affinity purification, and role in protein breakdown. J Biol Chem *258*, 8206-8214.

Hindorff, L.A., Sethupathy, P., Junkins, H.A., Ramos, E.M., Mehta, J.P., Collins, F.S., and Manolio, T.A. (2009). Potential etiologic and functional implications of genome-wide association loci for human diseases and traits. Proc Natl Acad Sci U S A *106*, 9362-9367.

Hirokawa, N. (1998). Kinesin and dynein superfamily proteins and the mechanism of organelle transport. Science *279*, 519-526.

Hirokawa, N., Noda, Y., and Okada, Y. (1998). Kinesin and dynein superfamily proteins in organelle transport and cell division. Curr Opin Cell Biol *10*, 60-73.

Holzbaur, E.L., and Vallee, R.B. (1994). Dyneins: Molecular structure and cellular function. Annu Rev Cell Biol *10*, 339-372.

Homma, N., Takei, Y., Tanaka, Y., Nakata, T., Terada, S., Kikkawa, M., Noda, Y., and Hirokawa, N. (2003). Kinesin superfamily protein 2A (KIF2A) functions in suppression of collateral branch extension. Cell *114*, 229-239.

Horgan, C.P., Hanscom, S.R., and McCaffrey, M.W. (2011). Dynein LIC1 localizes to the mitotic spindle and midbody and LIC2 localizes to spindle poles during cell division. Cell Biol Int *35*, 171-178.

Howell, B.J., McEwen, B.F., Canman, J.C., Hoffman, D.B., Farrar, E.M., Rieder, C.L., and Salmon, E.D. (2001). Cytoplasmic dynein/dynactin drives kinetochore protein transport to the spindle poles and has a role in mitotic spindle checkpoint inactivation. J Cell Biol *155*, 1159-1172.

Hu, D.J., Baffet, A.D., Nayak, T., Akhmanova, A., Doye, V., and Vallee, R.B. (2013). Dynein recruitment to nuclear pores activates apical nuclear migration and mitotic entry in brain progenitor cells. Cell *154*, 1300-1313.

Hummer, S., and Mayer, T.U. (2009). Cdk1 negatively regulates midzone localization of the mitotic kinesin Mklp2 and the chromosomal passenger complex. Curr Biol *19*, 607-612.

Iolascon, A., Esposito, M.R., and Russo, R. (2012). Clinical aspects and pathogenesis of congenital dyserythropoietic anemias: from morphology to molecular approach. Haematologica *97*, 1786-1794.

Iolascon, A., Russo, R., and Delaunay, J. (2011). Congenital dyserythropoietic anemias. Curr Opin Hematol *18*, 146-151.

Ishizaki, Y., Jacobson, M.D., and Raff, M.C. (1998). A role for caspases in lens fiber differentiation. J Cell Biol *140*, 153-158.

Italiano, J.E., Patel-Hett, S., and Hartwig, J.H. (2007). Mechanics of proplatelet elaboration. J Thromb Haemost *5 Suppl 1*, 18-23.

James, L.C., Keeble, A.H., Khan, Z., Rhodes, D.A., and Trowsdale, J. (2007). Structural basis for PRYSPRY-mediated tripartite motif (TRIM) protein function. Proc Natl Acad Sci U S A *104*, 6200-6205.

Javanbakht, H., Yuan, W., Yeung, D.F., Song, B., Diaz-Griffero, F., Li, Y., Li, X., Stremlau, M., and Sodroski, J. (2006). Characterization of TRIM5alpha trimerization and its contribution to human immunodeficiency virus capsid binding. Virology *353*, 234-246.

Jayapal, S.R., Lee, K.L., Ji, P., Kaldis, P., Lim, B., and Lodish, H.F. (2010). Down-regulation of Myc is essential for terminal erythroid maturation. J Biol Chem *285*, 40252-40265.

Ji, P., Jayapal, S.R., and Lodish, H.F. (2008). Enucleation of cultured mouse fetal erythroblasts requires Rac GTPases and mDia2. Nat Cell Biol *10*, 314-321.

Ji, P., Yeh, V., Ramirez, T., Murata-Hori, M., and Lodish, H.F. (2010). Histone deacetylase 2 is required for chromatin condensation and subsequent enucleation of cultured mouse fetal erythroblasts. Haematologica *95*, 2013-2021.

Joseph-Silverstein, J., and Cohen, W.D. (1984). The cytoskeletal system of nucleated erythrocytes. III. Marginal band function in mature cells. J Cell Biol *98*, 2118-2125.

Kadauke, S., Udugama, M.I., Pawlicki, J.M., Achtman, J.C., Jain, D.P., Cheng, Y., Hardison, R.C., and Blobel, G.A. (2012). Tissue-specific mitotic bookmarking by hematopoietic transcription factor GATA1. Cell *150*, 725-737.

Kamatani, Y., Matsuda, K., Okada, Y., Kubo, M., Hosono, N., Daigo, Y., Nakamura, Y., and Kamatani, N. (2010). Genome-wide association study of hematological and biochemical traits in a Japanese population. Nat Genet *42*, 210-215.

Kang, Y.-A., Sanalkumar, R., O'Geen, H., Linnemann, A.K., Chang, C.-J., Bouhassira, E.E., Farnham, P.J., Keles, S., and Bresnick, E.H. (2012). Autophagy driven by a master regulator of hematopoiesis. Mol Cell Biol *32*, 226-239.

Kawane, K. (2001). Requirement of DNase II for Definitive Erythropoiesis in the Mouse Fetal Liver. Blood *292*, 1546-1549.

Keerthivasan, G., Liu, H., Gump, J.M., Dowdy, S.F., Wickrema, A., and Crispino, J.D. (2012). A novel role for survivin in erythroblast enucleation. Haematologica *97*, 1471-1490.

Keerthivasan, G., Small, S., Liu, H., Wickrema, A., and Crispino, J.D. (2010). Vesicle trafficking plays a novel role in erythroblast enucleation. Blood *116*, 3331-3340.

Keerthivasan, G., Wickrema, A., and Crispino, J.D. (2011). Erythroblast enucleation. Stem Cells Int *2011*, 139851.

Khandros, E., Thom, C.S., D'Souza, J., and Weiss, M.J. (2012). Integrated protein quality-control pathways regulate free alpha-globin in murine beta-thalassemia. Blood *119*, 5265-5275.

Khandros, E., and Weiss, M.J. (2010). Protein quality control during erythropoiesis and hemoglobin synthesis. Hematol Oncol Clin North Am *24*, 1071-1088.

Kihm, A.J., Kong, Y., Hong, W., Russell, J.E., Rouda, S., Adachi, K., Simon, M.C., Blobel, G.A., and Weiss, M.J. (2002). An abundant erythroid protein that stabilizes free alpha-haemoglobin. Nature *417*, 758-763.

Kikkawa, M. (2013). Big steps toward understanding dynein. J Cell Biol *202*, 15-23.

Kingsley, P.D., Greenfest-Allen, E., Frame, J.M., Bushnell, T.P., Malik, J., McGrath, K.E., Stoeckert, C.J., and Palis, J. (2013). Ontogeny of erythroid gene expression. Blood *121*, e5-e13.

Kirschner, M., and Mitchison, T. (1986). Beyond self-assembly: from microtubules to morphogenesis. Cell *45*, 329-342.

Komander, D. (2009). The emerging complexity of protein ubiquitination. Biochem Soc Trans *37*, 937-953.

Kon, T., Mogami, T., Ohkura, R., Nishiura, M., and Sutoh, K. (2005). ATP hydrolysis cycle-dependent tail motions in cytoplasmic dynein. Nat Struct Mol Biol *12*, 513-519.

Kon, T., Oyama, T., Shimo-Kon, R., Imamula, K., Shima, T., Sutoh, K., and Kurisu, G. (2012). The 2.8 Å crystal structure of the dynein motor domain. Nature *484*, 345-350.

Kon, T., Sutoh, K., and Kurisu, G. (2011). X-ray structure of a functional full-length dynein motor domain. Nat Struct Mol Biol *18*, 638-642.

Konstantinidis, D., Pushkaran, S., Klingmuller, U., Palis, J., Zheng, Y., and Kalfa, T.A. (2012a). Erythroid Specific RhoA Deficiency Causes Dysplastic and Inefficient Fetal Erythropoiesis with Lethal Embryonic Anemia Due to Defects in Erythroblast Cytokinesis and Enucleation. Abstract presented at the 54th American Society of Hematology Annual Meeting and Exposition, Atlanta, GA.

Konstantinidis, D.G., George, A., and Kalfa, T.A. (2010). Rac GTPases in erythroid biology. Transfusion clinique et biologique *17*, 126-130.

Konstantinidis, D.G., Pushkaran, S., Johnson, J.F., Cancelas, J.A., Manganaris, S., Harris, C.E., Williams, D.A., Zheng, Y., and Kalfa, T.A. (2012b). Signaling and cytoskeletal requirements in erythroblast enucleation. Blood *119*, 6118-6127.

Kotak, S., Busso, C., and Gonczy, P. (2013). NuMA phosphorylation by CDK1 couples mitotic progression with cortical dynein function. EMBO J *32*, 2517-2529.

Koury, M.J., Sawyer, S.T., and Brandt, S.J. (2002). New insights into erythropoiesis. Curr Opin Hematol *9*, 93-100.

Koury, S.T., Koury, M.J., and Bondurant, M.C. (1988). Morphological changes in erythroblasts during erythropoietin-induced terminal differentiation in vitro. Exp Hematol *16*, 758-763.

Koury, S.T., Koury, M.J., and Bondurant, M.C. (1989). Cytoskeletal distribution and function during the maturation and enucleation of mammalian erythroblasts. J Cell Biol *109*, 3005-3013.

Krauss, S.W., Lo, A.J., Short, S.A., Koury, M.J., Mohandas, N., and Chasis, J.A. (2005). Nuclear substructure reorganization during late-stage erythropoiesis is selective and does not involve caspase cleavage of major nuclear substructural proteins. Blood *106*, 2200-2205.

Kuhlbrodt, K., Mouysset, J., and Hoppe, T. (2005). Orchestra for assembly and fate of polyubiquitin chains. Essays Biochem *41*, 1-14.

Lapillonne, H., Kobari, L., Mazurier, C., Tropel, P., Giarratana, M.-C., Zanella-Cleon, I., Kiger, L., Wattenhofer-Donzé, M., Puccio, H., Hebert, N.*, et al.* Red blood cell generation from human induced pluripotent stem cells: perspectives for transfusion medicine. Haematologica *95*, 1651-1659.

Lausen, J., Pless, O., Leonard, F., Kuvardina, O.N., Koch, B., and Leutz, A. (2010). Targets of the Tal1 transcription factor in erythrocytes: E2 ubiquitin conjugase regulation by Tal1. J Biol Chem *285*, 5338-5346.

Lawrence, C.J., Dawe, R.K., Christie, K.R., Cleveland, D.W., Dawson, S.C., Endow, S.A., Goldstein, L.S., Goodson, H.V., Hirokawa, N., Howard, J.*, et al.* (2004). A standardized kinesin nomenclature. J Cell Biol *167*, 19-22.

Lazarus, J.E., Moughamian, A.J., Tokito, M.K., and Holzbaur, E.L. (2013). Dynactin subunit p150(Glued) is a neuron-specific anti-catastrophe factor. PLoS Biol *11*, e1001611.

Lee, G., Spring, F.A., Parsons, S.F., Mankelow, T.J., Peters, L.L., Koury, M.J., Mohandas, N., Anstee, D.J., and Chasis, J.A. (2003). Novel secreted isoform of adhesion molecule ICAM-4: potential regulator of membrane-associated ICAM-4 interactions. Blood *101*, 1790-1797.

Li, B., Jia, N., Kapur, R., and Chun, K.T. (2006). Cul4A targets p27 for degradation and regulates proliferation, cell cycle exit, and differentiation during erythropoiesis. Blood *107*, 4291-4299.

Li, W., Bengtson, M.H., Ulbrich, A., Matsuda, A., Reddy, V.A., Orth, A., Chanda, S.K., Batalov, S., and Joazeiro, C.A. (2008). Genome-wide and functional annotation of

human E3 ubiquitin ligases identifies MULAN, a mitochondrial E3 that regulates the organelle's dynamics and signaling. PLoS ONE *3*, e1487.
Li, Y.Y., Yeh, E., Hays, T., and Bloom, K. (1993). Disruption of mitotic spindle orientation in a yeast dynein mutant. Proc Natl Acad Sci U S A *90*, 10096-10100.
Liang, Y., Yu, W., Li, Y., Yu, L., Zhang, Q., Wang, F., Yang, Z., Du, J., Huang, Q., Yao, X.*, et al.* (2007). Nudel modulates kinetochore association and function of cytoplasmic dynein in M phase. Mol Biol Cell *18*, 2656-2666.
Ligon, L.A., Tokito, M., Finklestein, J.M., Grossman, F.E., and Holzbaur, E.L. (2004). A direct interaction between cytoplasmic dynein and kinesin I may coordinate motor activity. J Biol Chem *279*, 19201-19208.
Liljeholm, M., Irvine, A.F., Vikberg, A.-L., Norberg, A., Month, S., Sandström, H., Wahlin, A., Mishima, M., and Golovleva, I. (2013a). Congenital dyserythropoietic anemia type III (CDA III) is caused by a mutation in kinesin family member, KIF23. Blood *121*, 4791-4799.
Liljeholm, M., Irvine, A.F., Vikberg, A.L., Norberg, A., Month, S., Sandstrom, H., Wahlin, A., Mishima, M., and Golovleva, I. (2013b). Congenital dyserythropoietic anemia type III (CDA III) is caused by a mutation in kinesin family member, KIF23. Blood *121*, 4791-4799.
Liu, J., Guo, X., Mohandas, N., Chasis, J.A., and An, X. (2010). Membrane remodeling during reticulocyte maturation. Blood *115*, 2021-2027.
Liu, J., Prickett, T.D., Elliott, E., Meroni, G., and Brautigan, D.L. (2001). Phosphorylation and microtubule association of the Opitz syndrome protein mid-1 is regulated by protein phosphatase 2A via binding to the regulatory subunit alpha 4. Proc Natl Acad Sci U S A *98*, 6650-6655.
Long, C.A. (2007). Evolution of function and form in camelid erythrocytes. BIO'07: Proceedings of the 3rd WSEAS International Conference on Cellular and Molecular Biology, 18-24.
Ma, S., Triviños-Lagos, L., Gräf, R., and Chisholm, R.L. (1999). Dynein Intermediate Chain Mediated Dynein–Dynactin Interaction Is Required for Interphase Microtubule Organization and Centrosome Replication and Separation in Dictyostelium. J Cell Biol *147*, 1261-1274.

Mackay, D.R., Elgort, S.W., and Ullman, K.S. (2009). The nucleoporin Nup153 has separable roles in both early mitotic progression and the resolution of mitosis. Mol Biol Cell *20*, 1652-1660.
Maday, S., Wallace, K.E., and Holzbaur, E.L. (2012). Autophagosomes initiate distally and mature during transport toward the cell soma in primary neurons. J Cell Biol *196*, 407-417.
Maetens, M., Doumont, G., Clercq, S.D., Francoz, S., Froment, P., Bellefroid, E., Klingmuller, U., Lozano, G., and Marine, J.C. (2007). Distinct roles of Mdm2 and Mdm4 in red cell production. Blood *109*, 2630-2633.
Makise, M., Mackay, D.R., Elgort, S., Shankaran, S.S., Adam, S.A., and Ullman, K.S. (2012). The Nup153-Nup50 protein interface and its role in nuclear import. J Biol Chem *287*, 38515-38522.
Makokha, M., Hare, M., Li, M., Hays, T., and Barbar, E. (2002). Interactions of cytoplasmic dynein light chains Tctex-1 and LC8 with the intermediate chain IC74. Biochemistry *41*, 4302-4311.
Mallery, D.L., McEwan, W.A., Bidgood, S.R., Towers, G.J., Johnson, C.M., and James, L.C. (2010). Antibodies mediate intracellular immunity through tripartite motif-containing 21 (TRIM21). Proc Natl Acad Sci U S A *107*, 19985-19990.
Malumbres, M., and Barbacid, M. (2009). Cell cycle, CDKs and cancer: a changing paradigm. Nat Rev Cancer *9*, 153-166.
Mandelkow, E., and Mandelkow, E.M. (1989). Microtubular structure and tubulin polymerization. Curr Opin Cell Biol *1*, 5-9.
Mankelow, T.J., Spring, F.A., Parsons, S.F., Brady, R.L., Mohandas, N., Chasis, J.A., and Anstee, D.J. (2004). Identification of critical amino-acid residues on the erythroid intercellular adhesion molecule-4 (ICAM-4) mediating adhesion to αV integrins. Blood *103*, 1503-1508.
Sardiello, M., Cairo, S., Fontanella, B., Ballabio, A., and Meroni, G. (2008). Genomic analysis of the TRIM family reveals two groups of genes with distinct evolutionary properties. BMC Evol Biol *8*, 225.
Massiah, M.A., Simmons, B.N., Short, K.M., and Cox, T.C. (2006). Solution structure of the RBCC/TRIM B-box1 domain of human MID1: B-box with a RING. J Mol Biol *358*, 532-545.

McGrail, M., Gepner, J., Silvanovich, A., Ludmann, S., Serr, M., and Hays, T.S. (1995). Regulation of cytoplasmic dynein function in vivo by the Drosophila Glued complex. J Cell Biol *131*, 411-425.

McGrath, K., and Palis, J. (2008). Ontogeny of erythropoiesis in the mammalian embryo. Curr Top Dev Biol *82*, 1-22.

McGrath, K.E., Kingsley, P.D., Koniski, A.D., Porter, R.L., Bushnell, T.P., and Palis, J. (2008). Enucleation of primitive erythroid cells generates a transient population of "pyrenocytes" in the mammalian fetus. Blood *111*, 2409-2417.

McKenney, R.J., Vershinin, M., Kunwar, A., Vallee, R.B., and Gross, S.P. (2010). LIS1 and NudE induce a persistent dynein force-producing state. Cell *141*, 304-314.

McKenney, R.J., Weil, S.J., Scherer, J., and Vallee, R.B. (2011). Mutually exclusive cytoplasmic dynein regulation by NudE-Lis1 and dynactin. J Biol Chem *286*, 39615-39622.

Meiri, D., Marshall, C.B., Greeve, M.A., Kim, B., Balan, M., Suarez, F., Bakal, C., Wu, C., LaRose, J., Fine, N.*, et al.* (2012). Mechanistic Insight into the Microtubule and Actin Cytoskeleton Coupling through Dynein-Dependent RhoGEF Inhibition. Mol Cell *45*, 642-655.

Mel, H.C., Prenant, M., and Mohandas, N. (1977). Reticulocyte motility and form: studies on maturation and classification. Blood *49*, 1001-1009.

Meroni, G., and Diez-Roux, G. (2005). TRIM/RBCC, a novel class of 'single protein RING finger' E3 ubiquitin ligases. BioEssays *27*, 1147-1157.

Merryweather-Clarke, A.T., Atzberger, A., Soneji, S., Gray, N., Clark, K., Waugh, C., McGowan, S.J., Taylor, S., Nandi, A.K., Wood, W.G.*, et al.* (2011). Global gene expression analysis of human erythroid progenitors. Blood *117*, e96-108.

Messick, T.E., and Greenberg, R.A. (2009). The ubiquitin landscape at DNA double-strand breaks. J Cell Biol *187*, 319-326.

Metzger, M.B., Hristova, V.A., and Weissman, A.M. (2012). HECT and RING finger families of E3 ubiquitin ligases at a glance. J Cell Sci *125*, 531-537.

Migliaccio, A.R., Masselli, E., Varricchio, L., and Whitsett, C. (2012). Ex-vivo expansion of red blood cells: How real for transfusion in humans? Blood Rev *26*, 81-95.

Mische, S., He, Y., Ma, L., Li, M., Serr, M., and Hays, T.S. (2008). Dynein light intermediate chain: an essential subunit that contributes to spindle checkpoint inactivation. Mol Biol Cell *19*, 4918-4929.
Mok, Y.K., Lo, K.W., and Zhang, M. (2001). Structure of Tctex-1 and its interaction with cytoplasmic dynein intermediate chain. J Biol Chem *276*, 14067-14074.
Monaco, G., Salustri, A., and Bertolini, B. (1982). Observations on the molecular components stabilizing the microtubular system of the marginal band in the newt erythrocyte. J Cell Sci *58*, 149-163.
Moore, J.K., and Cooper, J.A. (2010). Coordinating mitosis with cell polarity: Molecular motors at the cell cortex. Semin Cell Dev Biol *21*, 283-289.
Morera, D., Roher, N., Ribas, L., Balasch, J.C., Donate, C., Callol, A., Boltana, S., Roberts, S., Goetz, G., Goetz, F.W.*, et al.* (2011). RNA-Seq reveals an integrated immune response in nucleated erythrocytes. PLoS ONE *6*, e26998.
Moughamian, A.J., and Holzbaur, E.L. (2012). Dynactin is required for transport initiation from the distal axon. Neuron *74*, 331-343.
Moughamian, A.J., Osborn, G.E., Lazarus, J.E., Maday, S., and Holzbaur, E.L. (2013). Ordered recruitment of dynactin to the microtubule plus-end is required for efficient initiation of retrograde axonal transport. J Neurosci *33*, 13190-13203.
Mueller, R.L., Gregory, T.R., Gregory, S.M., Hsieh, A., and Boore, J.L. (2008). Genome size, cell size, and the evolution of enucleated erythrocytes in attenuate salamanders. Zoology *111*, 218-230.
Nagata, S. (2002). Breakdown of chromosomal DNA. Cornea *21*, S2-6.
Nans, A., Mohandas, N., and Stokes, D.L. (2011). Native ultrastructure of the red cell cytoskeleton by cryo-electron tomography. Biophys J *101*, 2341-2350.
Napolitano, L.M., Jaffray, E.G., Hay, R.T., and Meroni, G. (2011). Functional interactions between ubiquitin E2 enzymes and TRIM proteins. Biochem J *434*, 309-319.
Napolitano, L.M., and Meroni, G. (2012). TRIM family: Pleiotropy and diversification through homomultimer and heteromultimer formation. IUBMB Life *64*, 64-71.
Ney, P.A. (2011). Normal and disordered reticulocyte maturation. Curr Opin Hematol *18*, 152-157.

Nichols, K.E., Crispino, J.D., Poncz, M., White, J.G., Orkin, S.H., Maris, J.M., and Weiss, M.J. (2000). Familial dyserythropoietic anaemia and thrombocytopenia due to an inherited mutation in GATA1. Nat Genet *24*, 266-270.

Nishi, M., Aoyama, F., Kisa, F., Zhu, H., Sun, M., Lin, P., Ohta, H., Van, B., Yamamoto, S., Kakizawa, S.*, et al.* (2012). TRIM50 protein regulates vesicular trafficking for acid secretion in gastric parietal cells. J Biol Chem *287*, 33523-33532.

Nisole, S., Stoye, J.P., and Saib, A. (2005). TRIM family proteins: retroviral restriction and antiviral defence. Nat Rev Microbiol *3*, 799-808.

Novershtern, N., Subramanian, A., Lawton, L.N., Mak, R.H., Haining, W.N., McConkey, M.E., Habib, N., Yosef, N., Chang, C.Y., Shay, T.*, et al.* (2011). Densely interconnected transcriptional circuits control cell states in human hematopoiesis. Cell *144*, 296-309.

Nuinoon, M., Makarasara, W., Mushiroda, T., Setianingsih, I., Wahidiyat, P.A., Sripichai, O., Kumasaka, N., Takahashi, A., Svasti, S., Munkongdee, T.*, et al.* (2009). A genome-wide association identified the common genetic variants influence disease severity in β0-thalassemia/hemoglobin E. Hum Genet *127*, 303-314.

Nyarko, A., and Barbar, E. (2011). Light chain-dependent self-association of dynein intermediate chain. J Biol Chem *286*, 1556-1566.

Nyarko, A., Hare, M., Hays, T.S., and Barbar, E. (2004). The intermediate chain of cytoplasmic dynein is partially disordered and gains structure upon binding to light-chain LC8. Biochemistry *43*, 15595-15603.

Ori-McKenney, K.M., and Vallee, R.B. (2011). Neuronal migration defects in the Loa dynein mutant mouse. Neural Dev *6*, 26.

Orkin, S.H., and Zon, L.I. (2002). Hematopoiesis and stem cells: plasticity versus developmental heterogeneity. Nat Immunol *3*, 323-328.

Ozato, K., Shin, D.M., Chang, T.H., and Morse, H.C., 3rd (2008). TRIM family proteins and their emerging roles in innate immunity. Nature reviews. Immunology *8*, 849-860.

Paralkar, V.R., Mishra, T., Luan, J., Yao, Y., Kossenkov, A.V., Anderson, S.M., Dunagin, M., Pimkin, M., Gore, M., Sun, D., Konuthula, N., Raj, A., An, X., Mohandas, N., Bodine, D.M., Hardison, R.C., and Weiss, M.J. (2014). Lineage and species-specific long noncoding RNAs during erythro-megakaryocytic development. Blood [Epub ahead of print, Feb 4].

Paschal, B.M., and Vallee, R.B. (1987). Retrograde transport by the microtubule-associated protein MAP 1C. Nature *330*, 181-183.
Pasini, E.M., Kirkegaard, M., Salerno, D., Mortensen, P., Mann, M., and Thomas, A.W. (2008). Deep coverage mouse red blood cell proteome: a first comparison with the human red blood cell. Mol Cell Proteomics *7*, 1317-1330.
Passantino, L., Massaro, M.A., Jirillo, F., Di Modugno, D., Ribaud, M.R., Modugno, G.D., Passantino, G.F., and Jirillo, E. (2007). Antigenically activated avian erythrocytes release cytokine-like factors: a conserved phylogenetic function discovered in fish. Immunopharmacol Immunotoxicol *29*, 141-152.
Patel, S.R., Richardson, J.L., Schulze, H., Kahle, E., Galjart, N., Drabek, K., Shivdasani, R.A., Hartwig, J.H., and Italiano, J.E., Jr. (2005). Differential roles of microtubule assembly and sliding in proplatelet formation by megakaryocytes. Blood *106*, 4076-4085.
Patel, V.P., and Lodish, H.F. (1987). A fibronectin matrix is required for differentiation of murine erythroleukemia cells into reticulocytes. J Cell Biol *105*, 3105-3118.
Peters, D.T., and Musunuru, K. (2012). Functional evaluation of genetic variation in complex human traits. Hum Mol Genet *21*, R18-23.
Petrera, F., and Meroni, G. (2012). TRIM proteins in development. Adv Expt Med Biol *770*, 131-141.
Peyrard, T., Bardiaux, L., Krause, C., Kobari, L., Lapillonne, H., Andreu, G., and Douay, L. (2011). Banking of pluripotent adult stem cells as an unlimited source for red blood cell production: potential applications for alloimmunized patients and rare blood challenges. Transfusion Medicine Reviews *25*, 206-216.
Pickart, C.M. (2004). Back to the future with ubiquitin. Cell *116*, 181-190.
Poirier, K., Lebrun, N., Broix, L., Tian, G., Saillour, Y., Boscheron, C., Parrini, E., Valence, S., Pierre, B.S., Oger, M.*, et al.* (2013). Mutations in TUBG1, DYNC1H1, KIF5C and KIF2A cause malformations of cortical development and microcephaly. Nat Genet *45*, 639-647.
Pop, R., Shearstone, J.R., Shen, Q., Liu, Y., Hallstrom, K., Koulnis, M., Gribnau, J., and Socolovsky, M. (2010). A key commitment step in erythropoiesis is synchronized with the cell cycle clock through mutual inhibition between PU.1 and S-phase progression. PLoS Biol *8*, e1000484.

Popova, E.Y., Krauss, S.W., Short, S.A., Lee, G., Villalobos, J., Etzell, J., Koury, M.J., Ney, P.A., Chasis, J.A., and Grigoryev, S.A. (2009). Chromatin condensation in terminally differentiating mouse erythroblasts does not involve special architectural proteins but depends on histone deacetylation. Chromosome Res *17*, 47-64.

Puls, I., Jonnakuty, C., LaMonte, B.H., Holzbaur, E.L., Tokito, M., Mann, E., Floeter, M.K., Bidus, K., Drayna, D., Oh, S.J.*, et al.* (2003). Mutant dynactin in motor neuron disease. Nat Genet *33*, 455-456.

Quintyne, N.J., Gill, S.R., Eckley, D.M., Crego, C.L., Compton, D.A., and Schroer, T.A. (1999). Dynactin is required for microtubule anchoring at centrosomes. J Cell Biol *147*, 321-334.

Reiner, O., Carrozzo, R., Shen, Y., Wehnert, M., Faustinella, F., Dobyns, W.B., Caskey, C.T., and Ledbetter, D.H. (1993). Isolation of a Miller-Dieker lissencephaly gene containing G protein beta-subunit-like repeats. Nature *364*, 717-721.

Renella, R., and Wood, W.G. (2009). The congenital dyserythropoietic anemias. Hematol Oncol Clin North Am *23*, 283-306.

Repasky, E.A., and Eckert, B.S. (1981). A reevaluation of the process of enucleation in mammalian erythroid cells. Progress in clinical and biological research *55*, 679-692.

Reymond, A. (2001). The tripartite motif family identifies cell compartments. EMBO J *20*, 2140-2151.

Rhodes, D.A., de Bono, B., and Trowsdale, J. (2005). Relationship between SPRY and B30.2 protein domains. Evolution of a component of immune defence? Immunology *116*, 411-417.

Rhodes, D.A., and Trowsdale, J. (2007). TRIM21 is a trimeric protein that binds IgG Fc via the B30.2 domain. Nature *44*, 2406-2414.

Ribeil, J.A., Zermati, Y., Vandekerckhove, J., Cathelin, S., Kersual, J., Dussiot, M., Coulon, S., Moura, I.C., Zeuner, A., Kirkegaard-Sorensen, T.*, et al.* (2007). Hsp70 regulates erythropoiesis by preventing caspase-3-mediated cleavage of GATA-1. Nature *445*, 102-105.

Roberts, A.J., Malkova, B., Walker, M.L., Sakakibara, H., Numata, N., Kon, T., Ohkura, R., Edwards, T.A., Knight, P.J., Sutoh, K.*, et al.* (2012). ATP-driven remodeling of the linker domain in the dynein motor. Structure *20*, 1670-1680.

Roberts, A.J., Numata, N., Walker, M.L., Kato, Y.S., Malkova, B., Kon, T., Ohkura, R., Arisaka, F., Knight, P.J., Sutoh, K.*, et al.* (2009). AAA+ Ring and linker swing mechanism in the dynein motor. Cell *136*, 485-495.

Rosette, C., and Karin, M. (1995). Cytoskeletal control of gene expression: depolymerization of microtubules activates NF-kappa B. J Cell Biol *128*, 1111-1119.

Rothwell, S.W., and Calvert, V.S. (1997). Activation of human platelets causes post-translational modifications to cytoplasmic dynein. Thromb Haemost *78*, 910-918.

Roux-Dalvai, F., Gonzalez de Peredo, A., Simo, C., Guerrier, L., Bouyssie, D., Zanella, A., Citterio, A., Burlet-Schiltz, O., Boschetti, E., Righetti, P.G.*, et al.* (2008). Extensive analysis of the cytoplasmic proteome of human erythrocytes using the peptide ligand library technology and advanced mass spectrometry. Mol Cell Proteomics *7*, 2254-2269.

Ruud, J.T. (1954). Vertebrates without erythrocytes and blood pigment. Nature *173*, 848-850.

Sadahira, Y., Yoshino, T., and Monobe, Y. (1995). Very late activation antigen 4-vascular cell adhesion molecule 1 interaction is involved in the formation of erythroblastic islands. J Exp Med *181*, 411-415.

Salinas, S., Bilsland, L.G., and Schiavo, G. (2008). Molecular landmarks along the axonal route: axonal transport in health and disease. Curr Opin Cell Biol *20*, 445-453.

Samso, M., Radermacher, M., Frank, J., and Koonce, M.P. (1998). Structural characterization of a dynein motor domain. J Mol Biol *276*, 927-937.

Sankaran, V.G., Ludwig, L.S., Sicinska, E., Xu, J., Bauer, D.E., Eng, J.C., Patterson, H.C., Metcalf, R.A., Natkunam, Y., Orkin, S.H.*, et al.* (2012). Cyclin D3 coordinates the cell cycle during differentiation to regulate erythrocyte size and number. Genes Dev *26*, 2075-2087.

Sankaran, V.G., and Orkin, S.H. (2013). Genome-wide association studies of hematologic phenotypes: a window into human hematopoiesis. Curr Opin Genet Dev *23*, 339-344.

Sankaran, V.G., Orkin, S.H., and Walkley, C.R. (2008). Rb intrinsically promotes erythropoiesis by coupling cell cycle exit with mitochondrial biogenesis. Genes Dev *22*, 463-475.

Sasaki, S., Shionoya, A., Ishida, M., Gambello, M.J., Yingling, J., Wynshaw-Boris, A., and Hirotsune, S. (2000). A LIS1/NUDEL/cytoplasmic dynein heavy chain complex in the developing and adult nervous system. Neuron *28*, 681-696.
Sawada, K., Krantz, S.B., Dai, C.H., Koury, S.T., Horn, S.T., Glick, A.D., and Civin, C.I. (1990). Purification of human blood burst-forming units-erythroid and demonstration of the evolution of erythropoietin receptors. J Cell Physiol *142*, 219-230.
Schindelin, J., Arganda-Carreras, I., Frise, E., Kaynig, V., Longair, M., Pietzsch, T., Preibisch, S., Rueden, C., Saalfeld, S., Schmid, B.*, et al.* (2012). Fiji: an open-source platform for biological-image analysis. Nat Methods *9*, 676-682.
Schmidt, H., Gleave, E.S., and Carter, A.P. (2012). Insights into dynein motor domain function from a 3.3-A crystal structure. Nat Struct Mol Biol *19*, 492-497, S491.
Schnapp, B.J., and Reese, T.S. (1989). Dynein is the motor for retrograde axonal transport of organelles. Proc Natl Acad Sci U S A *86*, 1548-1552.
Schwartz, M. (2004). Rho signalling at a glance. J Cell Sci *117*, 5457-5458.
Schwarz, K., Iolascon, A., Verissimo, F., Trede, N.S., Horsley, W., Chen, W., Paw, B.H., Hopfner, K.P., Holzmann, K., Russo, R.*, et al.* (2009). Mutations affecting the secretory COPII coat component SEC23B cause congenital dyserythropoietic anemia type II. Nat Genet *41*, 936-940.
Schweers, R.L., Zhang, J., Randall, M.S., Loyd, M.R., Li, W., Dorsey, F.C., Kundu, M., Opferman, J.T., Cleveland, J.L., Miller, J.L.*, et al.* (2007). NIX is required for programmed mitochondrial clearance during reticulocyte maturation. Proc Natl Acad Sci U S A *104*, 19500-19505.
Schweiger, S., and Schneider, R. (2003). The MID1/PP2A complex: a key to the pathogenesis of Opitz BBB/G syndrome. Bioessays *25*, 356-366.
Shearstone, J.R., Pop, R., Bock, C., Boyle, P., Meissner, A., and Socolovsky, M. (2011). Global DNA demethylation during mouse erythropoiesis in vivo. Science *334*, 799-802.
Shen, Y., Li, N., Wu, S., Zhou, Y., Shan, Y., Zhang, Q., Ding, C., Yuan, Q., Zhao, F., Zeng, R.*, et al.* (2008). Nudel binds Cdc42GAP to modulate Cdc42 activity at the leading edge of migrating cells. Dev Cell *14*, 342-353.
Sherr, C.J., and Roberts, J.M. (2004). Living with or without cyclins and cyclin-dependent kinases. Genes Dev *18*, 2699-2711.

Shima, T., Kon, T., Imamula, K., Ohkura, R., and Sutoh, K. (2006). Two modes of microtubule sliding driven by cytoplasmic dynein. Proc Natl Acad Sci U S A *103*, 17736-17740.

Shohat, M., and Halpern, G.J. (2011). Familial Mediterranean fever--a review. Genet Med *13*, 487-498.

Short, K.M., Hopwood, B., Yi, Z., and Cox, T.C. (2002). MID1 and MID2 homo- and heterodimerise to tether the rapamycin-sensitive PP2A regulatory subunit, alpha 4, to microtubules: implications for the clinical variability of X-linked Opitz GBBB syndrome and other developmental disorders. BMC Cell Biol *3*, 1.

Shrum, C.K., Defrancisco, D., and Meffert, M.K. (2009). Stimulated nuclear translocation of NF-kappaB and shuttling differentially depend on dynein and the dynactin complex. Proc Natl Acad Sci U S A *106*, 2647-2652.

Shu, T., Ayala, R., Nguyen, M.D., Xie, Z., Gleeson, J.G., and Tsai, L.H. (2004). Ndel1 operates in a common pathway with LIS1 and cytoplasmic dynein to regulate cortical neuronal positioning. Neuron *44*, 263-277.

Siller, K.H., and Doe, C.Q. (2009). Spindle orientation during asymmetric cell division. Nat Cell Biol *11*, 365-374.

Siller, K.H., Serr, M., Steward, R., Hays, T.S., and Doe, C.Q. (2005). Live imaging of Drosophila brain neuroblasts reveals a role for Lis1/dynactin in spindle assembly and mitotic checkpoint control. Mol Biol Cell *16*, 5127-5140.

Simpson, C.F., and Kling, J.M. (1967). The mechanism of denucleation in circulating erythroblasts. J Cell Biol *35*, 237-245.

Sjogren, U., and Brandt, L. (1974). Erythroblastic islands and ineffective erythropoiesis in vitamin B12 deficiency. Acta Med Scand *196*, 369-372.

Skutelsky, E., and Danon, D. (1970). Comparative study of nuclear expulsion from the late erythroblast and cytokinesis. Exp Cell Res *60*, 427-436.

Smith, C.M., and Chircop, M. (2012). Clathrin-mediated endocytic proteins are involved in regulating mitotic progression and completion. Traffic *13*, 1628-1641.

Socolovsky, M. (2013). Exploring the erythroblastic island. Nature Medicine *19*, 399-401.

Soni, S., Bala, S., Gwynn, B., Sahr, K.E., Peters, L.L., and Hanspal, M. (2006). Absence of erythroblast macrophage protein (Emp) leads to failure of erythroblast nuclear extrusion. J Biol Chem *281*, 20181-20189.

Soranzo, N., Spector, T.D., Mangino, M., Kühnel, B., Rendon, A., Teumer, A., Willenborg, C., Wright, B., Chen, L., Li, M.*, et al.* (2009). A genome-wide meta-analysis identifies 22 loci associated with eight hematological parameters in the HaemGen consortium. Nat Geneti *41*, 1182-1190.
Spear, P.C., and Erickson, C.A. (2012a). Apical movement during interkinetic nuclear migration is a two-step process. Dev Biol *370*, 33-41.
Spear, P.C., and Erickson, C.A. (2012b). Interkinetic nuclear migration: a mysterious process in search of a function. Dev Growth Differ *54*, 306-316.
Splinter, D., Tanenbaum, M.E., Lindqvist, A., Jaarsma, D., Flotho, A., Yu, K.L., Grigoriev, I., Engelsma, D., Haasdijk, E.D., Keijzer, N.*, et al.* (2010). Bicaudal D2, dynein, and kinesin-1 associate with nuclear pore complexes and regulate centrosome and nuclear positioning during mitotic entry. PLoS Biol *8*, e1000350.
Stehman, S.A., Chen, Y., McKenney, R.J., and Vallee, R.B. (2007). NudE and NudEL are required for mitotic progression and are involved in dynein recruitment to kinetochores. J Cell Biol *178*, 583-594.
Straub, A.C., Lohman, A.W., Billaud, M., Johnstone, S.R., Dwyer, S.T., Lee, M.Y., Bortz, P.S., Best, A.K., Columbus, L., Gaston, B.*, et al.* (2012). Endothelial cell expression of haemoglobin alpha regulates nitric oxide signalling. Nature *491*, 473-477.
Streich, F.C., Jr., Ronchi, V.P., Connick, J.P., and Haas, A.L. (2013). Tripartite motif ligases catalyze polyubiquitin chain formation through a cooperative allosteric mechanism. J Biol Chem *288*, 8209-8221.
Stuchell-Brereton, M.D., Siglin, A., Li, J., Moore, J.K., Ahmed, S., Williams, J.C., and Cooper, J.A. (2011). Functional interaction between dynein light chain and intermediate chain is required for mitotic spindle positioning. Mol Biol Cell *22*, 2690-2701.
Sztiller-Sikorska, M., Jakubowska, J., Wozniak, M., Stasiak, M., and Czyz, M. (2009). A non-apoptotic function of caspase-3 in pharmacologically-induced differentiation of K562 cells. Br J Pharmacol *157*, 1451-1462.
Tamary, H., Shalev, H., Perez-Avraham, G., Zoldan, M., Levi, I., Swinkels, D.W., Tanno, T., and Miller, J.L. (2008). Elevated growth differentiation factor 15 expression in patients with congenital dyserythropoietic anemia type I. Blood *112*, 5241-5244.

Tanaka, Y., Kanai, Y., Okada, Y., Nonaka, S., Takeda, S., Harada, A., and Hirokawa, N. (1998). Targeted disruption of mouse conventional kinesin heavy chain, kif5B, results in abnormal perinuclear clustering of mitochondria. Cell *93*, 1147-1158.

Tanenbaum, M.E., Akhmanova, A., and Medema, R.H. (2010). Dynein at the nuclear envelope. Blood *11*, 649-649.

Tanenbaum, M.E., Akhmanova, A., and Medema, R.H. (2011). Bi-directional transport of the nucleus by dynein and kinesin-1. Commun Integr Biol *4*, 21-25.

Thom, C.S., Dickson, C.F., Gell, D.A., and Weiss, M.J. (2013). Hemoglobin variants: biochemical properties and clinical correlates. Cold Spring Harb Perspect Med *3*, a011858.

Traxler, E., and Weiss, M.J. (2013). Congenital dyserythropoietic anemias: III's a charm. Blood *121*, 4614-4615.

Trinczek, B., Marx, A., Mandelkow, E.M., Murphy, D.B., and Mandelkow, E. (1993). Dynamics of microtubules from erythrocyte marginal bands. Mol Biol Cell *4*, 323-335.

Trockenbacher, A., Suckow, V., Foerster, J., Winter, J., Krauss, S., Ropers, H.H., Schneider, R., and Schweiger, S. (2001). MID1, mutated in Opitz syndrome, encodes an ubiquitin ligase that targets phosphatase 2A for degradation. Nat Genet *29*, 287-294.

Tsai, J.-W., Bremner, K.H., and Vallee, R.B. (2007). Dual subcellular roles for LIS1 and dynein in radial neuronal migration in live brain tissue. Nat Neurosci *10*, 970-979.

Tsai, J.W., Chen, Y., Kriegstein, A.R., and Vallee, R.B. (2005). LIS1 RNA interference blocks neural stem cell division, morphogenesis, and motility at multiple stages. J Cell Biol *170*, 935-945.

Tsai, J.W., Lian, W.N., Kemal, S., Kriegstein, A.R., and Vallee, R.B. (2010). Kinesin 3 and cytoplasmic dynein mediate interkinetic nuclear migration in neural stem cells. Nat Neurosci *13*, 1463-1471.

Uehara, R., Tsukada, Y., Kamasaki, T., Poser, I., Yoda, K., Gerlich, D.W., and Goshima, G. (2013). Aurora B and Kif2A control microtubule length for assembly of a functional central spindle during anaphase. J Cell Biol *202*, 623-636.

Vale, R.D., and Milligan, R.A. (2000). The way things move: looking under the hood of molecular motor proteins. Science *288*, 88-95.

Vallee, R.B., McKenney, R.J., and Ori-McKenney, K.M. (2012). Multiple modes of cytoplasmic dynein regulation. Nat Cell Biol *14*, 224-230.

van der Harst, P., Zhang, W., Mateo Leach, I., Rendon, A., Verweij, N., Sehmi, J., Paul, D.S., Elling, U., Allayee, H., Li, X.*, et al.* (2012). Seventy-five genetic loci influencing the human red blood cell. Nature *492*, 369-375.

van Deurs, B., and Behnke, O. (1973). The microtubule marginal band of mammalian red blood cells. Z Anat Entwicklungsgesch *143*, 43-47.

Vaughan, K.T., and Vallee, R.B. (1995). Cytoplasmic dynein binds dynactin through a direct interaction between the intermediate chains and p150Glued. J Cell Biol *131*, 1507-1516.

Vergnolle, M.A., and Taylor, S.S. (2007). Cenp-F links kinetochores to Ndel1/Nde1/Lis1/dynein microtubule motor complexes. Curr Biol *17*, 1173-1179.

Verhey, K.J., Kaul, N., and Soppina, V. (2011). Kinesin assembly and movement in cells. Annu Rev Biophys *40*, 267-288.

Versteeg, G.A., Rajsbaum, R., Sanchez-Aparicio, M.T., Maestre, A.M., Valdiviezo, J., Shi, M., Inn, K.S., Fernandez-Sesma, A., Jung, J., and Garcia-Sastre, A. (2013). The E3-ligase TRIM family of proteins regulates signaling pathways triggered by innate immune pattern-recognition receptors. Immunity *38*, 384-398.

Wadia, J.S., and Dowdy, S.F. (2002). Protein transduction technology. Curr Opin Biotech *13*, 52-56.

Wadia, J.S., and Dowdy, S.F. (2005). Transmembrane delivery of protein and peptide drugs by TAT-mediated transduction in the treatment of cancer. Adv Drug Deliv Rev *57*, 579-596.

Wadsworth, P. (2005). Cytokinesis: Rho marks the spot. Curr Biol *15*, R871-874.

Walrafen, P., Verdier, F., Kadri, Z., Chretien, S., Lacombe, C., and Mayeux, P. (2005). Both proteasomes and lysosomes degrade the activated erythropoietin receptor. Blood *105*, 600-608.

Wang, J., Ramirez, T., Ji, P., Jayapal, S.R., Lodish, H.F., and Murata-Hori, M. (2012). Mammalian erythroblast enucleation requires PI3K-dependent cell polarization. J Cell Sci *125*, 340-349.

Wefes, I., Mastrandrea, L.D., Haldeman, M., Koury, S.T., Tamburlin, J., Pickart, C.M., and Finley, D. (1995). Induction of ubiquitin-conjugating enzymes during terminal erythroid differentiation. Proc Natl Acad Sci U S A *92*, 4982-4986.

Weiss, M.J., Yu, C., and Orkin, S.H. (1997). Erythroid-cell-specific properties of transcription factor GATA-1 revealed by phenotypic rescue of a gene-targeted cell line. Mol Cell Biol *17*, 1642-1651.

Welch, J.J., Watts, J.A., Vakoc, C.R., Yao, Y., Wang, H., Hardison, R.C., Blobel, G.A., Chodosh, L.A., and Weiss, M.J. (2004). Global regulation of erythroid gene expression by transcription factor GATA-1. Blood *104*, 3136-3147.

White, E.A., and Glotzer, M. (2012). Centralspindlin: At the heart of cytokinesis. Blood *69*, 882-892.

Wickrema, A., Koury, S.T., Dai, C.H., and Krantz, S.B. (1994). Changes in cytoskeletal proteins and their mRNAs during maturation of human erythroid progenitor cells. J Cell Physiol *160*, 417-426.

Wilson, M.H., and Holzbaur, E.L. (2012). Opposing microtubule motors drive robust nuclear dynamics in developing muscle cells. J Cell Sci *125*, 4158-4169.

Woo, J.-S., Imm, J.-H., Min, C.-K., Kim, K.-J., Cha, S.-S., and Oh, B.-H. (2006a). Structural and functional insights into the B30.2/SPRY domain. EMBO J *25*, 1353-1363.

Woo, J.S., Suh, H.Y., Park, S.Y., and Oh, B.H. (2006b). Structural basis for protein recognition by B30.2/SPRY domains. Mol Cell *24*, 967-976.

Wu, C., Orozco, C., Boyer, J., Leglise, M., Goodale, J., Batalov, S., Hodge, C.L., Haase, J., Janes, J., Huss, J.W., 3rd*, et al.* (2009). BioGPS: an extensible and customizable portal for querying and organizing gene annotation resources. Genome Biol *10*, R130.

Wu, H., Liu, X., Jaenisch, R., and Lodish, H.F. (1995). Generation of committed erythroid BFU-E and CFU-E progenitors does not require erythropoietin or the erythropoietin receptor. Cell *83*, 59-67.

Xia, C., Rahman, A., Yang, Z., and Goldstein, L.S. (1998). Chromosomal localization reveals three kinesin heavy chain genes in mouse. Genomics *52*, 209-213.

Xie, Z., Sanada, K., Samuels, B.A., Shih, H., and Tsai, L.-H. (2003). Serine 732 Phosphorylation of FAK by Cdk5 Is Important for Microtubule Organization, Nuclear Movement, and Neuronal Migration. Cell *114*, 469-482.

Xu, P., Wen, Z., Shi, X., Li, Y., Fan, L., Xiang, M., Li, A., Scott, M.J., Xiao, G., Li, S.*, et al.* (2013a). Hemorrhagic shock augments Nlrp3 inflammasome activation in the lung through impaired pyrin induction. J Immunol *190*, 5247-5255.

Xu, Y., Swartz, K.L., Siu, K.T., Bhattacharyya, M., and Minella, A.C. (2013b). Fbw7-dependent cyclin E regulation ensures terminal maturation of bone marrow erythroid cells by restraining oxidative metabolism. Oncogene (in press)
Xue, S.P., Zhang, S.F., Du, Q., Sun, H., Xin, J., Liu, S.Q., and Ma, J. (1997). The role of cytoskeletal elements in the two-phase denucleation process of mammalian erythroblasts in vitro observed by laser confocal scanning microscope. Cell Mol Biol *43*, 851-860.
Yoshida, H., Kawane, K., Koike, M., Mori, Y., Uchiyama, Y., and Nagata, S. (2005). Phosphatidylserine-dependent engulfment by macrophages of nuclei from erythroid precursor cells. Nat Cell Biol *437*, 754-758.
Yu, D., dos Santos, C.O., Zhao, G., Jiang, J., Amigo, J.D., Khandros, E., Dore, L.C., Yao, Y., D'Souza, J., Zhang, Z.*, et al.* (2010). miR-451 protects against erythroid oxidant stress by repressing 14-3-3zeta. Genes Dev *24*, 1620-1633.
Yoshida, Y. (1996). Physician Education: Myelodysplastic Syndrome. Oncologist *1*, 284-287.

Yu, Y., and Feng, Y.M. (2010). The role of kinesin family proteins in tumorigenesis and progression: potential biomarkers and molecular targets for cancer therapy. Cancer *116*, 5150-5160.
Zeuner, A., Eramo, A., Testa, U., Felli, N., Pelosi, E., Mariani, G., Srinivasula, S.M., Alnemri, E.S., Condorelli, G., Peschle, C.*, et al.* (2003). Control of erythroid cell production via caspase-mediated cleavage of transcription factor SCL/Tal-1. Cell Death Differ *10*, 905-913.
Zhang, J., Socolovsky, M., Gross, A.W., and Lodish, H.F. (2003). Role of Ras signaling in erythroid differentiation of mouse fetal liver cells: functional analysis by a flow cytometry-based novel culture system. Blood *102*, 3938-3946.
Zhang, L., Flygare, J., Wong, P., Lim, B., and Lodish, H.F. (2011). miR-191 regulates mouse erythroblast enucleation by down-regulating Riok3 and Mxi1. Genes Dev *25*, 119-124.
Zhang, L., Huang, N.J., Chen, C., Tang, W., and Kornbluth, S. (2012a). Ubiquitylation of p53 by the APC/C inhibitor Trim39. Proc Natl Acad Sci U S A *109*, 20931-20936.

Zhang, L., Mei, Y., Fu, N.Y., Guan, L., Xie, W., Liu, H.H., Yu, C.D., Yin, Z., Yu, V.C., and You, H. (2012b). TRIM39 regulates cell cycle progression and DNA damage responses via stabilizing p21. Proc Natl Acad Sci U S A *109*, 20937-20942.

Zhao, W., Wang, L., Zhang, M., Yuan, C., and Gao, C. (2012). E3 ubiquitin ligase tripartite motif 38 negatively regulates TLR-mediated immune responses by proteasomal degradation of TNF receptor-associated factor 6 in macrophages. J Immunol *188*, 2567-2574.

Zhu, L., and Skoultchi, A.I. (2001). Coordinating cell proliferation and differentiation. Curr Opin Genet Dev *11*, 91-97.

Zimmet, J., and Ravid, K. (2000). Polyploidy: occurrence in nature, mechanisms, and significance for the megakaryocyte-platelet system. Exp Hematol *28*, 3-16.

Manuscript in revision: Note that manuscript from the Weiss lab by Maxim Pimkin *et al* is currently in revision for publication.